

A huge, undescribed soil ciliate (Protozoa: Ciliophora) diversity in natural forest stands of Central Europe

WILHELM FOISSNER^{1,*}, H. BERGER², K. XU¹
and S. ZECHMEISTER-BOLTENSTERN³

¹Institut für Zoologie, Universität Salzburg, Hellbrunnerstrasse 34, A-5020 Salzburg, Austria; ²Consulting Engineering Office for Ecology, Radetzkystrasse 10, A-5020 Salzburg, Austria; ³Federal Office and Research Centre for Forests (BFW), Seckendorff-Gudent Weg 8, A-1131 Wien, Austria; *Author for correspondence (e-mail: eva.herzog@sbg.ac.at; fax: +43-662-8044-5698)

Received 15 July 2003; accepted in revised form 11 November 2003

Key words: Biodiversity, Community structure, Deciduous forests, Intermediate disturbance hypothesis, New species, *Pinus nigra* forests, Soil protozoa, Undisturbed temperate forests

Abstract. We investigated 12 natural forest stands in eastern Austria for soil ciliate diversity, viz., eight beech forests and two lowland and *Pinus nigra* forests each. The stands span a wide range of climatic (e.g., 543–1759 mm precipitation, 160–1035 m above sea-level) and abiotic (e.g., pH 4–7.4) factors. Samples were taken twice in autumn and late spring and analysed with the non-flooded Petri dish method. Species were identified *in vivo*, in silver preparations, and in the scanning electron microscope. A total of 233 species were found, of which 30 were undescribed, a surprising number showing our ignorance of soil ciliate diversity, even in Central Europe. Species number varied highly from 45 (acidic beech on silicate) to 120 (floodplain forest) and was strongly correlated with pH and overall habitat quality, as measured by climate, the C/P quotient (ratio of r-selected colpodean and k-selected polyhymenophorean ciliates), and the proportion of mycophagous ciliate species; multivariate analysis showed further important variables, viz., the general nutrient status (glucose, nitrogen, C/N ratio) and microbial (urease) activity. The highest species number occurred in one of the two floodplain soils, supporting the intermediate disturbance hypothesis. The three main forest types could be clearly distinguished by their ciliate communities, using similarity indices and multidimensional scaling. Individual numbers varied highly from 135⁻¹ (lowland forest) to 10,925 ml⁻¹ (beech on silicate) soil percolate and showed, interestingly, a weak correlation with soil protozoan phospholipid fatty acids. Eight of the 30 new species found and a forgotten species, *Arcuospathidium coemeterii* (Kahl 1943) nov. comb., are described in detail, as examples of how species were recognized and soil protozoan diversity should be analyzed: *Latispathidium truncatum bimicronucleatum*, *Protospathidium fusioplites*, *Erimophrya sylvatica*, *E. quadrinucleata*, *Paragonostomum simplex*, *Periholosticha paucicirrata*, *P. sylvatica*, and *Australocirrus zechmeisterae*.

Introduction

Sustainable forest management has become a significant guiding principle in managing the remaining forest worldwide (Mendoza and Prabhu 2001), but is hampered by the lack of widely accepted concepts and methods (Zeide 2001). However, there is general agreement that soil contains a large proportion of the Earth's biodiversity: 1 m² of forest soil harbors more than 1000 species of animals (Anderson and Healey 1972) and, possibly, over half a million species of prokaryotes, mainly bacteria (Torsvik et al. 1996; Dykhuizen 1998). Much of this

diversity is still unknown, and description of the many new species and exploring their functional role is an important task for coming generations of soil biologists and biodiversity researchers. This applies also to the soil protozoa: 70–80% of their estimated global diversity of 1600–2000 species have not yet been discovered (Foissner 1997b), which is supported not only by a recent study on Namibian soil ciliates (Foissner et al. 2002), where 128 new species were discovered in 73 samples, but also by the present investigation, where 30 new species were found at 12 sites.

There is convincing evidence that soil protozoa respire about 10% of the total carbon input, mineralize 20–40% of the net nitrogen, and significantly enhance the growth of plants and earthworms (Foissner 1987a, 2004; Alphei et al. 1996; Bonkowski and Schaefer 1997; Darbyshire 1994). Thus, studies on their dynamics and community structures should provide powerful means for assessing and monitoring changes in the biotic and abiotic soil conditions (Foissner 1994, 2004). Unfortunately, most of this new knowledge is still widely ignored by forest researchers and general soil ecologists, possibly because methodological and taxonomical problems are still considerable, the organisms are too minute to be easily recognized and studied, and few specialists are available for their identification.

The present study is part of a larger project with the main objectives to select a combination of bioindicators for forest soil biodiversity, to single out forest types harboring rich decomposer communities, and to define relationships between bio-coenoses at different trophic levels (Zechmeister et al. 2003). The protozoan pilot project should investigate and elucidate (i) biodiversity of ciliates in major natural forest types of eastern Austria, (ii) the main variables determining ciliate species richness, (iii) the capacity of ciliates to discriminate these forests, and (iv) in the long run, provide a reference basis for studies of degraded and damaged forests. Ciliates were used as indicators because their diversity surpasses that of any other soil protozoan group, such as testate amoebae and flagellates.

Material and methods

This study is part of a larger project. Thus, site characteristics (Table 1) and analytical data (Table 4) could be taken from previous publications, where methods are described and referenced in detail (Hackl et al. 2000a, b, 2004, 2005).

Study sites and sampling design

Six forest types, each represented by two stands, were studied. They comprise the zonale vegetation types found in eastern Austria (i.e., oak and beech forests) and two azonale vegetation types typical of dry and wet sites (i.e., pine and floodplain forests). The zonale vegetation types are distributed along a thermal gradient: oak–hornbeam forests are favored by warm and dry conditions and are succeeded by beech forests and further by spruce–fir–beech forests towards colder and wetter

Table 1. Site characteristics of the forest stands under investigation. Climate data include mean annual temperature (Temp) and total annual precipitation (Ppt) from long-term averages. From Hackl (2001) and Hackl et al. (2005).

Forest type	Site ^a	Location (Lat. N, Long. E)	Elevation (m a.s.l.)	Annual climate data		Soil type	Humus type	Geology
				Temp (°C)	Ppt (mm)			
Oak-hornbeam	JE	48°11'N, 16°13'E	325	8.8	643	Dystric Planosol	Typical mull	Laab formation
	K	47°58'N, 16°41'E	270	8.7	593	Calcaric Planosol	Mull-like moder	Micashist/limestone
Woodruff-beech	JB	48°11'N, 16°13'E	320	8.8	643	Dystric Planosol	Moder-like mull	Laab formation
	KL	48°07'N, 16°03'E	510	7.6	768	Dystric Cambisol	Moder-like mull	Laab formation
Acidophilous beech	D	48°24'N, 15°32'E	500	7.6	613	Dystric Cambisol	Acidic moder	Gföhl gneiss
	S	48°32'N, 15°33'E	550	7.4	631	Dystric Cambisol	Acidic moder	Gföhl gneiss
Spruce-fir-beech	R	47°46'N, 15°07'E	1035	5.5	1759	Chromic Cambisol	Moder-like mull	Dolomite
	N	47°46'N, 15°32'E	995	5.8	1262	Stagnic Luvisol	Mild moder	Sandstone
Floodplain	M	48°00'N, 16°42'E	160	9.7	582	Calcaric Fluvisol	Typical mull	Recent clay
	B	48°08'N, 16°33'E	160	9.7	534	Calcaric Fluvisol	Typical mull	Recent clay
Austrian pine	ST	47°53'N, 16°02'E	640	7.0	668	Rendzic Leptosol	Calcareous moder	Dolomite
	ME	47°59'N, 16°10'E	475	8.2	554	Rendzic Leptosol	Xeromorphic mull	Dolomite

^aJE – Johammer Kogel (plant community: *Carpinion*), K – Kolnberg (*Carpinion*), JB – Johammer Kogel (*Eti-Fagetum*), KL – Klausen-Leopoldsdorf (*Hordeleyo-Fagetum*), D – Dürnstein (*Luzulo-Fagetum*), S – Saubrunn (*Luzulo-Fagetum*), R – Rothwald (*Adenostylo glabrae-Fagetum*), N – Neuwald (*Cardamino trifoliate-Fagetum*), M – Müllerboden (*Pruno-Fraxinetum*), B – Beugenau (*Fraxino-Populetum*), ST – Stampftal (*Euphorbio saxatilis-Pinetum nigrae*), ME – Merkenstein (*Euphorbio saxatilis-Pinetum nigrae*).

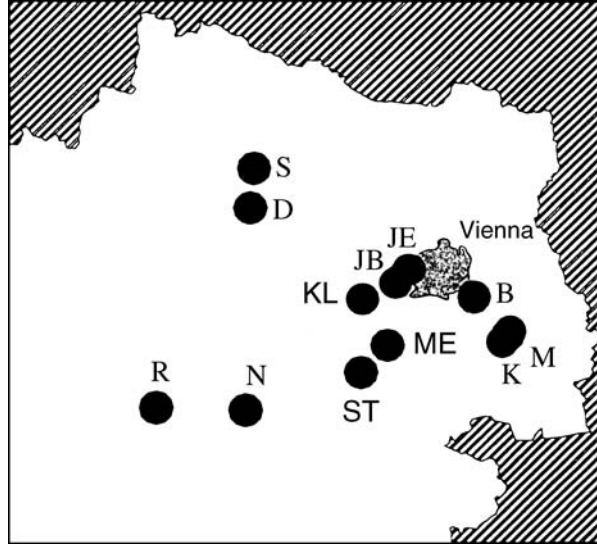


Figure 1. Location of the study sites in eastern Austria (modified from Hackl 2001). For site details, see Table 1. B – Beugenau, D – Dürnstein, JB – Johannser Kogel Beech, JE – Johannser Kogel Oak, K – Kolmberg, KL – Klausen-Leopoldsdorf, M – Müllerboden, ME – Merkenstein, N – Neuwald, R – Rothwald, S – Saubrunn, ST – Stampftal.

climates. At all sites, the composition of the plant community is considered to be natural, that is, has not been influenced by human activities. The sites Rothwald and Neuwald are forests not disturbed for at least 100 years. Site locations and characteristics are summarized in Figure 1 and Table 1.

Two ‘reference sites’ were included in data analysis and discussion, viz., the soil ciliate communities of a beech forest in the surroundings of the town of Salzburg (Foissner, unpublished) and of spruce forests from Austria and Germany (Aescht and Foissner 1993; Foissner 2000b). These sites were studied extensively, that is, each was investigated more than 10 times over a year or more, until species number did not further increase significantly. Thus, they can serve as a reference for the present study, where sites were investigated only twice.

Samples were taken with a small, sharp garden shovel twice at each site, viz., in September and November 2001 and in May/June 2002, at 5 m intervals along an established 50 m transect and in 0–10 cm soil depth, including the litter layer. Thus, ten 5 cm × 5 cm × 10 cm soil blocs were obtained at each site and thoroughly mixed to a composite sample. After removing larger pieces of gravel (≥ 1 cm) and roots, about 2 kg of the litter–soil mixture was transported to Salzburg, where it was air-dried for a month and then mixed thoroughly again. If necessary, soil was manually crushed, but not sieved, to pieces of under about 1 cm in size. Then, the samples were stored in sterile plastic bags until investigation, which occurred 1–3 months after air-drying because it was impossible to handle all samples concomitantly.

Sample processing and qualitative investigation

All samples were analyzed with the non-flooded Petri dish method as described by Foissner (1987a, 1992) and Foissner et al. (2002) using, however, a larger amount of soil (150–600 g, see below) because this increases the number of species found and the amount of material available for preparations (Foissner et al. 2002). The higher amount of soil required to use Petri dishes 18 cm in diameter and 4 cm high. They were filled to a height of 3 cm with the dry soil/litter mixture and slightly over-saturated (110%) with distilled water to obtain ‘non-flooded Petri dish cultures’; saturation was determined by the method of Buitkamp (1979). We preferred this volumetric method, not a fixed amount of soil, because the soil/litter mixture from the individual sites had very different weight (mass), depending on soil type and amount of litter contained. For instance, the Petri dish was full with 150 g of the voluminous, light soil/litter mixture from the Rothwald site, while 600 g were needed to fill the Petri dish with the heavy, loamy floodplain soil from Müllerboden.

The non-flooded Petri dish cultures were investigated for ciliate species by inspecting about 2 ml of the run-off on days 2, 7, 14, 21, and 28. During this time occurs a succession, which basically ends about 1 month after rewetting (for further details, see Foissner 1987a; Foissner et al. 2002). The non-flooded Petri dish method cannot reactivate all cysts and species present, and undescribed species or species with specialized demands are very likely undersampled (Foissner 1997a, b). Thus, the real number of species in the samples investigated is very likely considerably higher. This is sustained by the high species numbers in the reference sites mentioned above (Table 2). Unfortunately, a better method is not available for soil ciliate diversity assessment at large.

Quantitative investigations

Soil ciliate abundance is best determined by direct counting of fresh samples and requires several samples distributed over a year because numbers fluctuate highly (Berthold and Palzenberger 1995; Foissner 1987a, 1994). Such detailed investigations were impossible within the narrow financial frame of the present pilot project. Thus, we used a simple culture method to estimate potential ciliate abundance at water saturation in the samples of the second campaign; it is similar to that used by Buitkamp (1979).

The dry soil/litter mixture was sieved to 2 mm, 30 g each put into a Petri dish (5 cm across), and slightly over-saturated (110%) with distilled water, as described above. Then, samples were stored at room temperature for 9 days, where ciliates usually reach maximum diversity and abundance (Buitkamp 1979; Foissner 1987a). At day 10, Petri dishes were tilted (45°) for 5 min and the percolating liquid (‘soil water’), about 2–5 ml each, collected with a pipette. The ciliates contained in the percolate were preserved with osmium acid solution (2%), that is, one drop (~0.1 ml) per ml percolate. For counting and identification, a 0.1 ml percolate drop was placed on a microscope slide, covered with a 18 mm × 18 mm cover glass

supported by minute vaseline feet at the corners, and investigated with an ordinary microscope at a magnification of $\times 250$ (objective 25:1, ocular 10:1). Depending on numbers, 2–5 drops each were counted and values transformed to 1 ml soil percolate. Species were pre-identified *in vivo*.

Community analysis

Data were analyzed with PRIMER v 5, as distributed and described by Clarke and Gorley (2001) and Clarke and Warwick (2001). This modern computer program uses multidimensional scaling (MDS; Figure 4), which preserves the original data matrix better than the widely used principal component analysis (PCA). The program offers a variety of similarity coefficients and cluster methods. We tried most of them. Results were rather consistent, but best-fitting clusters were obtained with Euclidian distance and group average clustering (Figure 2) as well as with the Sørensen similarity index and complete linkage clustering (Figure 3).

Species identification and taxonomic methods

Identification, nomenclature and terminology of species followed the literature cited in this paper, in Foissner (1998) and in Foissner et al. (2002). Determinations were done mainly on live specimens using a high-power ($\times 100$, N.A. 1.32) oil immersion objective and bright field, phase contrast, or differential interference contrast microscopy. However, all 'difficult', new, or supposedly new species were investigated with the techniques described by Foissner (1991). The descriptions of the new taxa were based on material obtained with the non-flooded Petri dish method described above.

Counts and measurements on silvered specimens were performed at a magnification of $\times 1000$. *In vivo* measurements were made at magnifications of $\times 40$ – 1000 . While the later measurements provide only rough estimates, it is worth giving such data as specimens usually shrink in preparations or contract during fixation. Standard deviation and coefficient of variation were calculated according to statistics textbooks. Illustrations of live specimens were based on freehand sketches and micrographs; those of impregnated cells were made with a camera lucida. All figures were oriented with the anterior end of the organism directed to the top of the page.

Results and discussion

Diversity

The knowledge that soil harbours a diverse and specific ciliate community is only 20 years old (for a review, see Foissner 1987a). The total number of ciliate species reliably reported from terrestrial habitats globally presently stands at about 800

species (Foissner 1998; Foissner et al. 2002). However, most of these were discovered during anecdotal investigations. As concerns forests, reliable, systematic data on soil ciliate diversity are available only from acidified coniferous stands (Aescht and Foissner 1993; Lehle 1994), some deciduous forests of lower Austria (Foissner et al. 1985), and the reference sites reported in this study (Table 2). Thus, few data are available for comparison.

As many protozoans are likely dormant (encysted) most of their life, total species numbers are difficult to obtain. The few long-term data available show that 5–10 samples distributed over 1 year are necessary to find >80% of the carrying capacity, which is about 60, respectively, 150 species in small areas of coniferous and deciduous forests (Table 2; Foissner et al. 1985; Foissner 1987a, 1998, 1999b; Aescht and Foissner 1993; Lehle 1994). Single samples, in contrast, provide only 20–40 (coniferous forests) or 30–80 (deciduous forests) species (Foissner 1987a, d, 1995, 1997a; Blatterer and Foissner 1988; Table 6). Such dependence on sampling effort and forest type is to be expected from the life strategy (cysts) and the general knowledge that deciduous forests with circumneutral mull or mull/moder humus have more diverse soil life than coniferous forests with acidic raw humus (Franz 1975; Kuntze et al. 1983; Meyer et al. 1989).

At the 12 sites investigated, a total of 233 species were identified (note that 276 species are listed in Table 2 because it contains species found only at the comparison sites), of which 30 were undescribed (Table 2). Both figures are remarkable! The total number amounts for almost one third of the known global diversity (see above), while the average of 2.7 new species/site surpasses most values from soils globally, except of Africa, where 2.6 new species/site (sample) occur (Foissner 1997b; Foissner et al. 2002). This shows convincingly that soil ciliate diversity is still poorly known, even in Central Europe, and Foissner's (1997b) estimation of 1400–2000 species global soil ciliate diversity is likely to be an under-estimation. This is sustained by a recent study on Namibian soil ciliates, where 365 species were found, of which 128 (34%) were undescribed, in 73 samples from a variety of habitats (Foissner et al. 2002). Accordingly, the 3060 global, free-living (soil, freshwater, marine) ciliate diversity suggested by Finlay (2001) must be a gross under-estimation (Foissner 1999b; Foissner et al. 2002).

Several of the species found are remarkable either because our record is the first since the original description many years ago (*Amphisiella raptans*; *Colpoda distincta*; *Dileptus costaricanus*, previously known only from Costa Rica; *Dileptus falciformis*; *Phialinides muscicola*, a 'forgotten' species; *Tachysoma terricola*, previously known only from South America); the first reliable terrestrial record of a typical freshwater species (*Enchelys gasterosteus* from floodplain soil Beugenaue); or because it significantly extends the geographical range of species described recently: *Amphisiella namibiensis* (previously known only from the Etosha Pan in Namibia); *Diplites telmatobius* (previously known only from Namibia); *Enchelyodon armatides* (previously known only from Namibia and Australia); *Idiocolpoda pelobia* (previously known only from Hawaii and Namibia); *Paraenchelys brachyarmatus* (previously known only from Venezuela and Namibia); *Platyophrya paoletti* (previously known only from Venezuela);

Table 2. (continued)

Species ^a	Sites ^b																
	JE	K	K	JB	KL	D	S	R	N	M	B	ST	ME	F	SA		
<i>Enchelyodon lagenula</i> (Kahl)												+				+	
<i>Enchelyodon terrenus</i> Foissner																	
<i>Enchelys gasterosteus</i> Kahl											+						+
<i>Enchelys gelei</i> (Foissner)	+			+													
<i>Enchelys polymucleata</i> (Foissner)										+							
<i>Engelmanniella mobilis</i> (Engelmann)										+							
<i>Epispalthidium amphoriforme</i> (Greeff)	+			+						+							
<i>Epispalthidium ascendens</i> (Wenzel)										+							
<i>Epispalthidium papilliferum</i> (Kahl)	+			+						+							
<i>Epispalthidium polymucleatum</i> Foissner, Agatha & Berger										+							
<i>Epispalthidium regium</i> Foissner	+			+						+							
<i>Epispalthidium terricola</i> Foissner	+			+						+							
<i>Erimophrya quadrinucleata</i> n.sp.																	
<i>Erimophrya syhvatika</i> n.sp.																	
<i>Euplotopsis muscicola</i> (Kahl)										+							
<i>Frontonia depressa</i> (Stokes)										+							
<i>Frontonia terricola</i> Foissner										+							
<i>Fuscheria terricola</i> Berger, Foissner & Adam																	
<i>Gastronauta derouxi</i> Blatterer & Foissner																	
<i>Gastrostyla bavariensis</i> Foissner, Agatha & Berger																	
<i>Gastrostyla mystacea mystacea</i> (Stein)																	
<i>Gonostomum affine</i> (Stein)	+			+						+							
<i>Gonostomum atgicola</i> Gellért										+							
<i>Gonostomum kuehnelti</i> Foissner										+							
<i>Grossglockneria acuta</i> Foissner	+			+						+							
<i>Grossglockneria hyalina</i> Foissner	+			+						+							
<i>Halteria grandinella</i> (Müller)	+			+						+							
<i>Haplocaulus terrenus</i> Foissner	+			+						+							

Table 2. (continued)

Species ^a	Sites ^b														
	JE	K	K	JB	KL	D	S	R	N	M	B	ST	ME	F	SA
<i>Lagynophrya trichocystis</i> Foissner	+	+		+								+	+		
<i>Lamostyla edaphoni</i> Berger & Foissner												+		+	
<i>Lamostyla hyalina</i> (Berger, Foissner & Adam)				+								+			
<i>Lamostyla islandica</i> Berger & Foissner												+			+
<i>Latispathidium truncatum bimicronucleatum</i> n.g. n.ssp.												+			
<i>Leptopharynx costatus</i> Mermod	+	+		+								+			+
<i>Litonotus muscorum</i> (Kahl)	+	+		+								+			+
<i>Maryna ovata</i> (Gelei)												+			+
<i>Metopus hassei</i> Sondheim												+			+
<i>Microdiaphanosoma arcuatum</i> (Grandori & Grandori)	+											+			+
<i>Microthorax simulans</i> (Kahl)	+	+		+								+			+
<i>Mykophagophrys terricola</i> (Foissner)	+	+		+								+			+
<i>Nivaliella plana</i> Foissner	+	+		+								+			+
<i>Notohymena antarctica</i> Foissner				+								+			+
<i>Notoxoma parabryophryides</i> Foissner												+			+
<i>Odontochlamys alpestris alpestris</i> Foissner				+								+			+
<i>Odontochlamys alpestris biciliata</i> Foissner, Agatha & Berger												+			+
<i>Odontochlamys gouraudi</i> Certes	+			+								+			+
<i>Opercularia curvicaule</i> (Penard)				+								+			+
<i>Orthoamphisiella stramenticola</i> Eigner & Foissner												+			+
<i>Orthokreyella schiffmanni</i> Foissner												+			+
<i>Ottowphrya dragescoi</i> (Foissner)				+								+			+
<i>Oxytricha elegans</i> Foissner												+			+
<i>Oxytricha granulifera</i> Foissner & Adam	+	+										+			+
<i>Oxytricha islandica</i> Berger & Foissner		+										+			+
<i>Oxytricha lanceolata</i> Shibuya		+										+			+
<i>Oxytricha longa</i> Gelei & Szabados												+			+
<i>Oxytricha longigramulosa</i> Berger & Foissner	+	+										+			+

Table 2. (continued)

Species ^a	Sites ^b													
	JE	K	JB	KL	D	S	R	N	M	B	ST	ME	F	SA
<i>Pleuroplites australis</i> Foissner									+			+		
<i>Podophrya tristriata</i> Foissner, Agatha & Berger	+	+			+				+				+	
<i>Protocyclidium muscicola</i> (Kahl)	+	+	+	+	+			+	+	+		+	+	+
<i>Protocyclidium terricola</i> (Kahl)											+			
<i>Protospathidium fusioplites</i> n.sp.	+		+											
<i>Protospathidium serpens</i> (Kahl)									+					+
<i>Pseudochilodonopsis mutabilis</i> Foissner	+			+	+			+	+	+		+		+
<i>Pseudochilodonopsis polyvacuolata</i> Foissner & Didier	+		+	+	+		+	+	+	+			+	+
<i>Pseudocohilembus putrinus</i> (Kahl)	+			+	+			+	+	+		+		+
<i>Pseudocytolophosis alpestris</i> Foissner	+	+	+	+	+			+	+	+		+	+	+
<i>Pseudoholophrya terricola</i> Berger, Foissner & Adam	+	+	+	+	+			+	+	+		+	+	+
<i>Pseudoplatyphrya nana</i> (Kahl)	+	+	+	+	+			+	+	+		+	+	+
<i>Pseudoplatyphrya saltans</i> Foissner	+	+	+	+	+			+	+	+		+	+	+
<i>Pseudoureleptus buitkampii</i> (Foissner)									+					
<i>Rostrophryides africana</i> Foissner												+		
<i>Rostrophryides australis</i> Blatterer & Foissner													+	
<i>Sathrophilus muscorum</i> (Kahl)	+	+	+	+	+			+	+	+		+	+	+
<i>Spathidium claviforme</i> Kahl														
<i>Spathidium muscicola</i> Kahl									+	+		+	+	+
<i>Spathidium procerum</i> Kahl									+	+		+	+	+
<i>Spathidium seppelti etoschense</i> Foissner, Agatha & Berger														
<i>Spathidium spathula</i> (Müller)	+	+								+			+	+
<i>Sphaerophrya terricola</i> Foissner														
<i>Stammeridium kahli</i> (Wenzel)	+	+	+		+				+	+				+
<i>Sterkiella cavicola</i> (Kahl)	+	+	+											+
<i>Sterkiella histriomuscorum</i> (Foissner et al.)	+	+	+					+	+	+		+	+	+
<i>Stichotricha aculeata</i> Wrzesniowski														
<i>Tachysoma humicola humicola</i> Gellert										+			+	+

Table 2. (continued)

Species ^a	Sites ^b													
	JE	K	JB	KL	D	S	R	N	M	B	ST	ME	F	SA
<i>Colpoda</i> n.sp.														+
<i>Dileptus</i> n.sp.														+
<i>Dileptus</i> n.sp. 1	+													
<i>Dileptus</i> n.sp. 2					+									
<i>Drepanomonas</i> n.sp.							+							+
<i>Epispathidium</i> n.sp.														+
<i>Euploes</i> n.sp.														+
<i>Holosticha</i> n.sp.	+													
<i>Kuehneliella</i> n.sp.														
<i>Kuehneliella</i> n.sp.														
<i>Lamiosyla</i> n.sp.														
<i>Lamiosyla</i> n.sp.														
<i>Opercularia</i> n.sp.														
<i>Oxytrichides</i> n.g. n.sp.														
<i>Paragonostomum</i> n.sp.														
<i>Paragonostomum</i> n.sp.														
<i>Plagiocampa</i> n.sp. 1														
<i>Plagiocampa</i> n.sp. 2														
<i>Protospathidium</i> n.sp.														
<i>Pseudoplatyophrya</i> n.sp.														
<i>Pseudoplatyophrya</i> n.sp.														
<i>Rhabdosyla</i> n.sp.														
<i>Rhabdosyla</i> n.sp.														
<i>Sigmocolpoda</i> n.g. n.sp.														
<i>Sigmocolpoda</i> n.g. n.sp.														
<i>Spathidium</i> n.sp. 1														
<i>Spathidium</i> n.sp. 2														
<i>Spathidium</i> n.sp. 3														
<i>Spathidium</i> n.sp. 4														

Table 2. (continued)

Species ^a	Sites ^b													
	JE	K	JB	KL	D	S	R	N	M	B	ST	ME	F	SA
<i>Semibryophyllum</i> n.g., n.sp.									+					
<i>Urosoma</i> cf. <i>cienkowski</i> n.sp.									+					
<i>Urosomoida</i> n.sp.														
Total number of species	92	87	83	52	90	45	69	54	120	86	99	81	95	+
New species	5	5	3	3	4	1	3	1	10	4	11	9	— ^d	14

^aSee Foissner (1998) and Foissner et al. (2002) for nomenclature, that is, date of description and combining authors.

^bSee Table 1.

^cMost of these species will be described in other publications; some are described here.

^dSeveral, but all have been described meanwhile.

Platyophrya spumacola hexasticha (previously known only from Namibia); *Podophrya tristriata* (previously known only from Australia and Japan); *Urosomoida antarctica* (previously known only from Antarctica and Namibia); and *Urosomoida granulifera* (previously known only from Antarctica). These records seemingly support Finlay's hypothesis of a cosmopolitan distribution of all ciliate species, an idea with which we only partially agree because there are several 'flagship species' which doubtlessly have a restricted geographic range (Foissner 1999b; Foissner et al. 2002). Certainly, the present investigation extends the geographical range of several species, but on the other hand, it adds 30 new species all found, as yet, only in Austria or Europe; how many of them, if any at all, are really restricted to these areas cannot be charged at the present state of knowledge. However, *Erimophrya sylvatica* and *E. quadrinucleata*, two new species described here, are impressive examples for the need of very accurate investigations before cosmopolitanism is stated for a certain species. The genus *Erimophrya* was established by Foissner et al. (2002) for two new species discovered in the Namib Desert. On superficial investigation, the Austrian species would be probably confused with the Namibian species because the overall appearance is very similar!

The species numbers found at the individual sites span a wide range from 45 to 120. This matches the very different forest types investigated and shows the high bioindicative potential (discriminating power) of ciliate species number. At first glance, however, the pine forests, which grow on 'poor', protorendzic leptosols and belong to the species-poor coniferous forest type, appear as a remarkable exception because they have numbers as high as those found in the deciduous forests, including many undescribed species (Tables 1 and 6). However, these open forests have a dense grass cover, high organic C content, and circumneutral (mild), mull/moder humus (Tables 1 and 4). Thus, they are in several respects more similar to deciduous forests than to the strongly acidic (pH 3–5), raw humus *Picea* and *Abies* forests investigated in the studies cited above. A rich soil life is also indicated by the low C/P quotient (see functional groups discussed below) and the high contents of amino acids and bacterial and fungal PLFAs (Table 4; Hackl et al. 2000b, 2004).

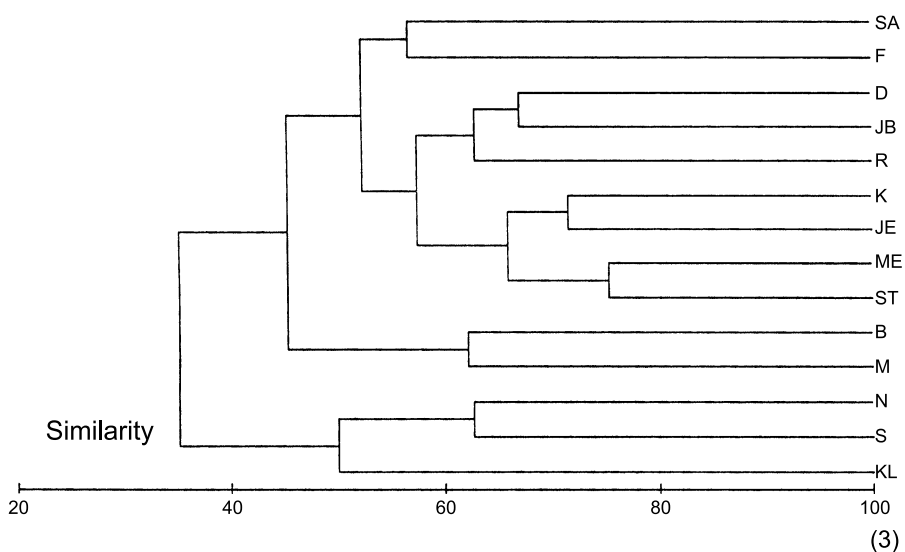
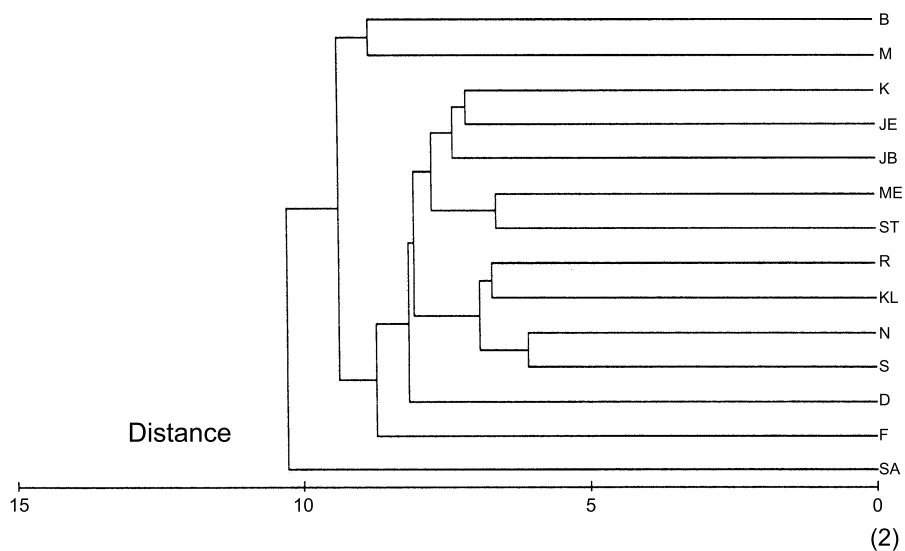
The highest number of ciliate species (120) occurs in one of the two floodplain forest soils; and the second site with 86 species is also in the upper range. Partially, these high numbers are caused by an increased proportion of freshwater species in the soil ciliate community (Table 6). Both, the high ciliate diversity and the increased proportion of freshwater species in floodplain forest soils is in accordance with (i) previous investigations on floodplain forest soils globally (Foissner et al. 2002) and (ii) the intermediate disturbance hypothesis that slightly disturbed habitats usually have higher organism diversities than stable ones (Townsend et al. 1997). Several soil and microbial key values (C/N ratio, N_{mic} , C_{mic} , urease activity) match the ciliate data (Table 4; Hackl et al. 2000b, 2004). Genus diversity, however, is lower in the floodplain than virgin forests, where several highly specialized genera occur, for instance, a new epizoic peritrich ciliate on a terrestrial crustacean belonging to the family *Canthacampyidae* (Table 6).

All other ciliate diversities, though varying from 45 to 92 species, are in the range to be expected from only two samples taken at each site (see above);

however, a more fine-tuned explanation is possible and provided in the chapter on functional groups. Likewise, the nutrient and microbial parameters show a rather varying pattern, except in the spruce-fir-beech forest soils, whose high nutrient pool and microbial and fungal biomass does not match the rather low ciliate diversity of 54–69 species (Tables 1, 4 and 6; Hackl et al. 2000a, b, 2004, 2005). On the other hand, pH is rather low (4–5) and elevation near 1000 m, which already delays decomposition rather distinctly, as evident from the thick litter layer and the composition of the ciliate community, where r-selected species dominate (see discussion of functional groups below).

Community structures

Of the 233 species found, only 16 occurred at all stands and also at the reference sites, showing a strong differentiation of the ciliate communities (Table 2): *Blepharisma hyalinum*, *Colpoda cucullus*, *C. inflata*, *C. steinii*, *Cyrtolophosis mucicola*, *Drepanomonas pauciciliata*, *Epispathidium terricola*, *Frontonia depressa*, *Gonostomum affine*, *Leptopharynx costatus*, *Nivaliella plana*, *Platyophrya vorax*, *Protocyclidium muscicola*, *Pseudocyrtolophosis alpestris*, *Pseudoplatyophrya nana*, and *Sathrophilus muscorum*. Thirteen of the 16 species occurring at all sites furnish 11 but 3 most frequent and abundant species in Table 3. Except for *Frontonia depressa*, all these and several other species have been found with high frequency and abundance (Table 3) in certain soils/areas globally (for a review, see Foissner et al. 2002), suggesting that they represent the core of the soil ciliate community, composed mainly of bacterivores and omnivores, except for some predators (here, *Epispathidium terricola*) and some fungivores (here, *Nivaliella plana* and *Pseudoplatyophrya nana*), using the high bacterial abundance and diversity typically present in natural forest soils. However, the most characteristic members of the core are the mycophagous ciliates, which are restricted to terrestrial habitats and evolved a special feeding tube penetrating the fungal cell wall (Foissner 1987a, 1998). *Frontonia depressa*, the sole new core species, is indeed a highly characteristic moss and forest soil ciliate in Central Europe, but rare in many other regions of the world, occurring, for instance, in Namibia only at 1 out of 73 sites investigated (Foissner et al. 2002). Foissner (1987a) classified *F. depressa* as an indicator for acidic moder and raw humus, which is only partially supported by the present investigations, where mull/moder humus, though often rather acidic, prevailed. Another remarkable species is *Territricha stramenticola*, as yet found only in beech forests of Austria and Germany. In the eastern Austrian forests, it was also restricted to such habitats, occurred, however, only in three out of the eight beech forests investigated. *Metopus hasei*, an obligately anaerobic ciliate, occurred in the two floodplain forest soils, showing that they are occasionally anaerobic, likely when flooded. The lack of such ciliates at all other sites show that they are well aerated. The occurrence of species of the hypotrich ciliate genus *Urosoma* is highly characteristic for floodplain forest soils and was observed not only during the present investigation (Table 2), but also by Foissner et al. (1985) and in floodplain soils globally (Foissner et al. 2002; Foissner, unpublished).



Figures 2 and 3. Similarity clusters of the 12 study and the 2 reference sites (F, SA) based on ciliate species diversity. **2:** Euclidian distance and group average clustering. **3:** Sørensen similarity index and complete linkage clustering. For methods, see Clarke and Gorley (2001) and Clarke and Warwick (2001).

The functional relationships and particularities of the ciliate communities discussed above and in the next section make sites rather sharply discriminated by a variety of similarity coefficients and cluster methods and, especially, multidimensional scaling (MDS). The MDS pattern is very stable (Figure 4), as indicated by the low stress value (0.08), and is repeated in the similarity clusters (Figures 2 and 3).

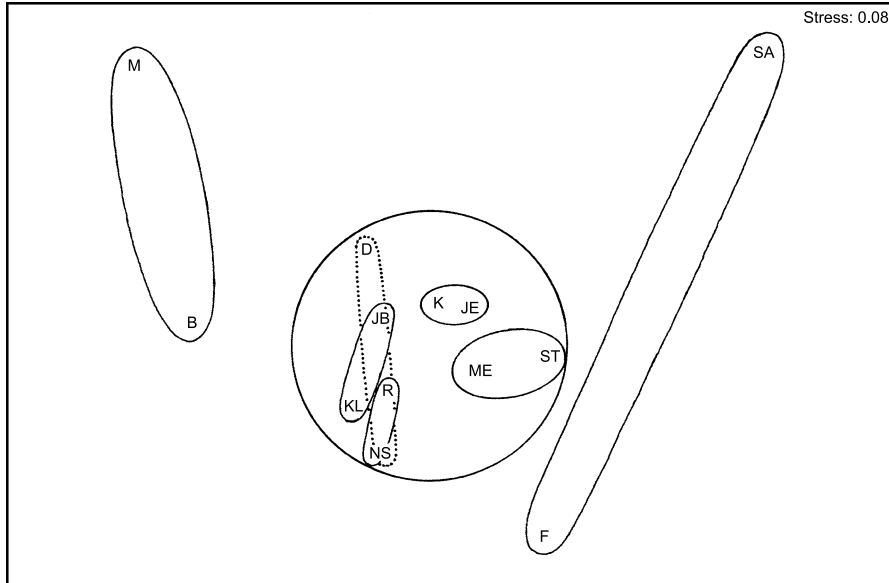


Figure 4. Multidimensional scaling using Euclidian distances between the ciliate communities of the 12 study and the 2 reference sites (F, SA). For methods, see Clarke and Gorley (2001) and Clarke and Warwick (2001).

Thus, only the MDS outcomes will be discussed in detail. The close similarity between protozoan communities within sites of the same vegetation type and plant community is evident for the two pine forests and the two floodplain forests. These two forest types are also most distinct in terms of their microbial communities (Hackl et al. 2005). In addition all forests containing beech trees are clustered together, which is also in accordance with the microbial data. Here too, oak hornbeam forests are separated from different types of beech forests. Both MDS and similarity clusters show convincingly that groupings are not caused by simple spatial relationships (the nearer the sites are together the more similar are the ciliate communities; Figure 1), but by distinct similarities in the species composition of the individual site pairs. This is in accordance with previous data from natural and human-influenced habitats (Foissner 1987a; Aescht and Foissner 1993) and shows that ciliates are useful bioindicators in the soil environment.

Abundance

As explained in the material and method section, the quantitative data are very incomplete and preliminary (Table 3). Actually, they are presented because (i) they basically agree with literature data (e.g., Foissner 1987a; Petz and Foissner 1988; Aescht and Foissner 1993; Berthold and Palzenberger 1995) and (ii) show an

Table 3. Abundance (ml⁻¹ soil percolate) of ciliates in soils from the second sampling campaign.

Species	Sites												
	JE	K	JB	KL	D	S	R	N	M	B	ST	ME	
<i>Arcuospathidium namibiense</i>	50												
<i>Australocirrus octonucleatus</i>			100	8	100		20						
<i>Blepharisma hyalinum</i>	50						60						140
<i>Colpoda aspera</i>							40	160					
<i>Colpoda cucullus</i>							80						
<i>Colpoda henneguyi</i>				10		1850	2480	790		10	20		
<i>Colpoda inflata</i>				6			140	60					
<i>Colpoda lucida</i>	50		3600		750		300	170		100			40
<i>Colpoda maupasi</i>						475							
<i>Colpoda steinii</i>	1800	175	1100	210	200								
<i>Cyrtolophosis mucicola</i>									95				
<i>Diplites telmatobius</i>	50	1275	25	10	475	3425	180	2730					
<i>Drepanomonas pauciciliata</i>					75								
<i>Drepanomonas revoluta</i>													
<i>Euplotopsis muscicola</i>			200			625	40	40	10	20	30		10
<i>Gonostomum affine</i>										110			50
<i>Gonostomum algicola</i>			450										
<i>Gonostomum kuehnelti</i>													
<i>Grossglockneria acuta</i>						25		30					
<i>Halteria grandinella</i>	200												
<i>Holosticha tetracirrata</i>				10									
<i>Homalogastra setosa</i>	50				1650					720	320		270
<i>Lagnophyra trichocystis</i>	400												
<i>Lamostyla hyalina</i>						75							
<i>Leptopharynx costatus</i>	450	600	100	10	1375	1350	400	3110	25		40		30
<i>Mycophagophrys terricola</i>		25						60			10		
<i>Nivaliella plana</i>						2700	80	10					
<i>Opercularia curvicaule</i>			50			25							

Table 3. (continued)

Species	Sites												
	JE	K	JB	KL	D	S	R	N	M	B	ST	ME	
<i>Oxytricha setigera</i>					25								
<i>Paracineteta lauterborni</i>					25							40	
<i>Paragonostomum simplex</i>											10		
<i>Plesiocaryon elongatum</i>											50	70	
<i>Protocyclidium muscicola</i>	6300	3075	500		6050		340	120		10			
<i>Pseudochilodonopsis mutabilis</i>													
<i>Pseudochilodonopsis polyvacuolata</i>				10									
<i>Pseudocytolophosis alpestris</i>	150			30				330					
<i>Pseudoplatyophrya nana</i>				10		25		20					
<i>Pseudoplatyophrya saltans</i>							80						
<i>Sathrophihilus muscorum</i>	150	1000	150		50	50	300	150		20	280		
<i>Sterkiella histriomuscorum</i>								10		10		10	
<i>Urosomoida agilisformis</i>							40	30		20	140	10	
<i>Vorticella astyliformis</i>	100	250									20	10	
Undetermined	300	50	350	40	150	0	220	370	5	10	60	30	
Σ ml ⁻¹ soil percolate	10100	6475	6550	354	10925	10625	4800	8220	135	1030	980	710	

interesting, though weak, positive correlation (Spearman $R = 0.48$) with the protozoan phospholipid fatty acids (Table 4), an important aspect because a reliable overall measure of soil protozoan abundance is still lacking (Darbyshire 1994) and PLFAs are increasingly used to characterize soil microbiological communities at large (Frostegård et al. 1997; Hill et al. 2000; Fierer 2003). Most species found in the quantitative investigations are common and ubiquitous and were also reported in the investigations cited above. Further there is no correlation between abundance and species number, which is much lower in the quantitative than qualitative cultures because the former were investigated only once (vs. 5) and set up with a much smaller quantity of soil (30 g vs. 150–600 g) which, additionally, was sieved (vs. unsieved).

Functional groups and relationships between species numbers and biotic and abiotic factors

The variables determining and structuring organism communities are not easily recognized and quantified, and few concrete data are available for soil ciliates, all reviewed in Foissner (1987a, 1994, 1997c, 2004). The present investigations show the capacity of ciliates to discriminate different forests (Figures 2–4) and provide some new insights, based on functional groups and the large set of biotic and abiotic factors measured (Tables 1, 4 and 6). Two of the four independent functional groups distinguished in the present investigation have been discussed above, viz., the increased proportions of freshwater and anaerobic species in the floodplain soils, which cause, inter alia, their pronounced distinctness in the similarity analyses (Figures 2–4). Two further functional groups remain to be discussed, viz., the C/P quotient and the proportion of obligate fungivores.

The C/P quotient is the proportion of the usually r-selected colpodid and the usually k-selected polyhymenophoran ciliate species and an important measure of habitat conditions (Lüftenegger et al. 1985; Foissner 1987a). It is ≤ 1 in 'ordinary', predictable habitats and > 1 in more harsh, unpredictable habitats. This is confirmed by the present investigations, where the quotient shows a significant correlation (Spearman $R = -0.83$) with species number, that is, species diversity decreases with increasing habitat severity and elevation (Spearman $R = -0.5$). Thus, the undisturbed forests at 1000 m above sea-level and the strongly acidic (pH ~ 4) beech forests at Saubrunn (S) and Klausen-Leopoldsdorf (KL) all have C/P quotients well above 1, suggesting that they are already rather extreme habitats, at least for ciliates. This is sustained by the positive correlation between species number and pH (Spearman $R = 0.575$) and the negative correlation between species number and the percentage of mycophagous ciliates (Spearman $R = -0.75$), that is, species number decreases with decreasing pH and an increasing proportion of mycophagous ciliates. More detailed quantitative data (Table 3) would likely further refine the discrimination and characterization of the habitats. For instance, *Colpoda* spp. and *Cyrtolophosis mucicola* furnish large numbers in the eight hornbeam/beech forests (pH ≤ 5.1 , C/P ≥ 1 except for one site), while they are rare or absent in the floodplain/Austrian pine forests (pH 7.2–7.4, C/P 0.5–1).

Table 4. Abiotic and biotic soil parameters of the 12 sites investigated. Values are means from two sampling occasions each in spring and autumn 1997 and 1998 ($n=4$). Each sample consists of 10 individually analyzed subsamples taken at 0–10 cm soil depth (litter removed) and 5 m intervals on a 50 m transect. For details on sampling and the analytic methods, see Hackl et al. (2000a, b, 2004, 2005).

Parameters ^a	Sites											
	JE	K	KB	KL	D	S	R	N	M	B	ST	ME
Soil moisture (%)	34.2	29.8	35.4	34.3	40.9	32.0	57.9	43.3	38.7	29.4	35.4	22.7
pH	4.5	5.4	5.1	4.1	4.6	4.0	4.9	4.0	7.2	7.4	7.4	7.4
NH ₄ -N ($\mu\text{g g}^{-1}$ dw)	17.6	10.5	26.0	15.4	68.8	296.6	127.4	56.1	1.5	0.9	14.4	3.4
NO ₃ -N ($\mu\text{g g}^{-1}$ dw)	55.6	53.8	58.4	54.5	11.1	0.3	150.9	96.0	109.5	89.1	2.0	1.0
Total soil N (%)	0.22	0.20	0.19	0.33	0.35	0.30	0.94	0.38	0.47	0.23	0.61	0.26
Organic C (%)	5.04	4.23	4.38	4.36	9.45	7.03	16.0	6.46	5.46	3.92	16.99	9.64
C/N	23.4	21.0	22.5	13.1	26.9	23.5	17.1	16.9	11.7	17.2	28.0	37.0
N _{mic} ($\mu\text{g biomass-N g}^{-1}$ dw)	59.8	70.0	100.9	118.7	103.9	61.0	297.6	102.4	159.4	84.6	97.9	49.0
C _{mic} ($\mu\text{g biomass-C g}^{-1}$ dw)	529	859	484	451	678	511	1,897	802	1,593	1,167	1,084	625
Total sugar ($\mu\text{g g}^{-1}$ dw)	106.3	113.5	66.6	63.8	159.5	130.6	239.1	90.3	104.1	52.7	182.2	147.5
Glucose ($\mu\text{g g}^{-1}$ dw)	83.2	72.0	41.5	35.1	98.3	45.5	168.9	28.9	48.8	26.8	93.6	59.2
Total amino acids ($\mu\text{g g}^{-1}$ dw)	5.80	9.23	7.31	5.79	19.43	11.51	26.80	5.59	30.04	14.17	56.67	37.57
Urease activity ($\mu\text{g NH}_4\text{-N g}^{-1}$ dw h ⁻¹)	54.5	51.5	62.5	76.5	55.0	26.0	110.5	46.5	95.5	56.3	74.0	55.5
Phosphatase activity ($\mu\text{g phenol g}^{-1}$ dw h ⁻¹)	530	536	690	654	712	654	1,030	732	520	514	800	776
PLFA total (nmol g ⁻¹ dw)	274.1	243.9	158.7	204.8	304.1	252.1	865.7	459.1	191.6	238.3	323.7	252.9
PLFA protozoa	2.34	1.64	0.54	2.02	4.94	3.35	8.15	8.93	0.62	0.70	2.47	2.33
PLFA total bacteria	230.4	204.5	133.7	175.9	250.6	209.7	733.5	386.5	165.4	203.9	262.4	198.1
PLFA fungi	41.3	37.7	24.4	26.9	48.6	39.1	124.0	63.7	25.6	33.7	58.8	52.4

^aC – carbon, dw – dry mass, mic – microbial, N – nitrogen, PLFA – phospholipid fatty acids.

Table 5. Combinations of the 18 environmental variables from Table 4 yielding the best matches with ciliate species numbers as measured by weighted Spearman rank correlation (BIO-ENV procedure of PRIMER v 5; Clarke and Gorley 2001).

	Variables ^a	Correlation coefficients (<i>pw</i>)	Correlation selections (best results) with variables listed in left column
1	Water	0.508	2, 5, 7, 8, 12, 17
2	pH	0.491	2, 7, 8, 12, 17
3	N _{mic}	0.484	2, 5, 8, 12, 17
4	C _{mic}	0.483	2, 8, 12, 17
5	Glucose	0.480	2, 5, 7, 8, 17
6	PLFA total	0.469	2, 5, 8, 17
7	PLFA protozoa	0.467	2, 5, 7–9, 12, 17
8	NH ₄ -N	0.466	2, 5, 7, 8, 12
9	NO ₃ -N	0.464	2, 5, 7–9, 17
10	Total soil N	0.460	2, 8, 12
11	Organic C	0.460	2, 7–9, 12, 17
12	C/N	0.458	2, 5, 8, 12
13	Total sugar	0.457	2, 5, 7, 17
14	Total amino acids	0.456	2, 5, 7–9, 12
15	PLFA total bacteria	0.456	2, 5, 7–9
16	PLFA fungi	0.456	2, 5, 7, 12, 17
17	Urease activity	0.455	2, 7, 8, 12
18	Phosphatase activity	0.447	2, 5, 7, 8

^aFor explanation of abbreviations of variables, see Table 4.

Table 6. Main characteristics and some functional groups of the ciliate communities in 12 Austrian forest stands.

Forest type	Site ^a	Ciliate species numbers ^b	New species	Genus diversity	C/P quotient ^c	Strict mycophages (%) ^d	Freshwater species (%) ^d
Oak–hornbeam	JE	68/75/92	5	1.56	1	6.5	27
	K	73/58/87	5	1.61	0.8	5.7	29
Woodruff–beech	JB	65/64/83	3	1.53	1	6.0	23
	KL	39/34/52	3	1.16	1.2	8.0	30
Acidophilus beech	D	67/61/90	4	1.43	1	6.7	27
	S	36/33/45	1	1.36	1.9	8.9	27
Spruce–fir–beech	R	38/55/69	3	1.47	1.6	7.2	30
	N	28/49/54	1	1.35	1.6	7.4	26
Floodplain	M	72/101/120	10	1.64	0.5	3.3	25
	B	55/60/86	4	1.56	0.8	5.8	36
Austrian pine	ST	75/77/99	11	1.48	0.8	5.1	19
	ME	60/63/81	9	1.36	1	5.0	26

^aFor abbreviations, see Table 1.

^bThe three numbers refer to the first and second sampling campaign and to the total (cumulated) number found in both samples.

^cQuotient of colpodid and polyhymenophoran (hypotrichs, heterotrichs, oligotrichs) ciliate species. For classification, see Foissner (1998).

^dMarked with a single asterisk in the compilations of Foissner (1998) and Foissner et al. (2002).

All these correlations match well the general knowledge that, in Central Europe, diversity of soil animals decreases at 1000 m above sea-level and/or in habitats with a pH around and lower than 4, while fungal diversity and abundance increase (Franz 1975; Kuntze et al. 1983). For soil ciliates, such relationships are known to occur at large scales, viz., that diversity decreases in high mountains above the timberline, in Antarctica, and deserts (Foissner 1987a, 1997b; Bamforth 2001). Our study is the first to show such relationships at small scales, viz., in a single vegetation (forest) and climate (temperate) type.

Except for pH, all variables listed in Table 4 lack significant correlations with ciliate species numbers, supporting the key role of general habitat quality (\pm climate and elevation) and pH discussed above. However, multivariate analysis (Table 5) suggests, not surprisingly, some role for a combination of variables, viz., the general nutrient status (glucose, nitrogen, C/N ratio) and microbial activity, as measured by the urease content.

Description of new and insufficiently known species

Morphometric data shown in Tables 7–12 are repeated in this section only as needed for clarity. All observations are from field material, that is, not from clonal cultures. Thus, it cannot be excluded that similar, but different species are mixed, although this is unlikely because we exclude specimens which deviate in at least one prominent character. Certainly, this can generate some bias in the data if used too uncritically. However, we usually exclude only such specimens which have, for instance, a different nuclear structure (very likely often postconjugates), a distinctly deviating ciliary pattern (often very likely injured, regenerating or malformed specimens), or an unusually small size (often very likely degenerating, just excysted or divided specimens). The inclusion of such individuals, which might sometimes belong to another species, would artificially increase variability. For further details on recognition of species and subspecies, see Foissner et al. (2002).

***Latispathidium* nov. gen.**

Diagnosis: Spathidiidae with dorsal brush on left side of cell and ciliature in Spathidium pattern.

Type species: *Latispathidium lanceoplites* (Foissner, Agatha and Berger 2002) nov. comb. (basonym: *Spathidium lanceoplites* Foissner, Agatha and Berger 2002).

Etymology: Composite of the Latin noun *latus* (lateral side) and the generic name *Spathidium* (small spatula), referring to both, the laterally located dorsal brush and the *Spathidium*-like general organization. Neuter gender.

Comparison with related genera: *Latispathidium* is established for the reasons discussed by Foissner (2003), when he founded the genus *Cultellothrix*. As yet, it comprises only two species, viz., *Latispathidium lanceoplites*, discovered by Foissner et al. (2002) in Namibia, and *L. truncatum bimicronucleatum* described

below. Both, *Latispathidium* and *Cultellothrix* have the dorsal brush on the left side of the cell, while the basic ciliary pattern is as in *Spathidium* and *Arcuospathidium*, which have the brush located dorsally or dorsolaterally. A slight dorsolateral location of the dorsal brush is also recognizable in some specimens of *Latispathidium truncatum bimicronucleatum* (Figures 5l, m) and in *L. lanceoplites* (Foissner, Agatha and Berger 2002), as shown by a reinvestigation of the type population (Figure 5n). Thus, the distinction from *Spathidium* is not very sharp, but helpful for recognizing evolutionary lines and species in this highly diverse group.

At first glance, the lateral location of the dorsal brush appears to be caused by spatial constraints, viz., the narrowness of the anterior body half and/or the small number of ciliary rows, especially in *Latispathidium lanceoplites*. However, an evolutionary interpretation is more likely because there are quite a number of similarly sized and shaped *Spathidium* and *Arcuospathidium* species, which have the brush exactly on the dorsal side, for instance, *Spathidium claviforme*, *S. turgitorum*, *S. etoschense* (Figure 5o), *Arcuospathidium vlassaki*, and *A. namibiense* (Foissner 1987a, 2000a; Foissner et al. 2002).

***Latispathidium truncatum* (Stokes 1885) nov. comb.**

1885 *Lacrymaria truncata* Stokes, Ann. Mag. nat. Hist., 15: 442.

1930 *Spathidium (Lacrymaria) truncatum* Stokes, 1885 – Kahl, Tierwelt Dtl., 18: 159.

Extended diagnosis (to include subspecies *bimicronucleatum*): Length 70–125 µm. Obclavate to slenderly bursiform with slanted, short oral bulge distinctly narrower than widest trunk region. Macronucleus tortuous and almost extending whole body length or spiralized in middle third of body. Several micronuclei distributed along macronuclear strand or one each near to ends of macronucleus.

Remarks: We split this species into two subspecies, differing mainly in the micronucleus pattern. The diagnosis is incomplete because Stokes' species has not yet been redescribed.

***Latispathidium truncatum truncatum* (Stokes 1885)
nov. comb., nov. stat. (Figure 5h)**

Diagnosis: Length about 125 µm. Several micronuclei along macronuclear strand.

Type location: Standing water with dead leaves from shallow ponds in central New Jersey, USA.

Description: See Stokes (1885).

***Latispathidium truncatum bimicronucleatum* nov. sspec.
(Figures 5a–g, i–m, p, q, 6a–g; Table 7)**

Diagnosis: Size about 100 µm × 15 µm *in vivo*. Obclavate with oblique oral bulge about two thirds as long as widest trunk region. Macronucleus in middle third of

body, spiralized. Invariably two micronuclei, one each near or attached to ends of macronucleus. Extrusomes finely acicular, about $7\ \mu\text{m} \times 0.5\ \mu\text{m}$. On average 14 ciliary rows, 3 anteriorly differentiated to dorsal brush occupying 19% of body length; brush row 3 distinctly shortened.

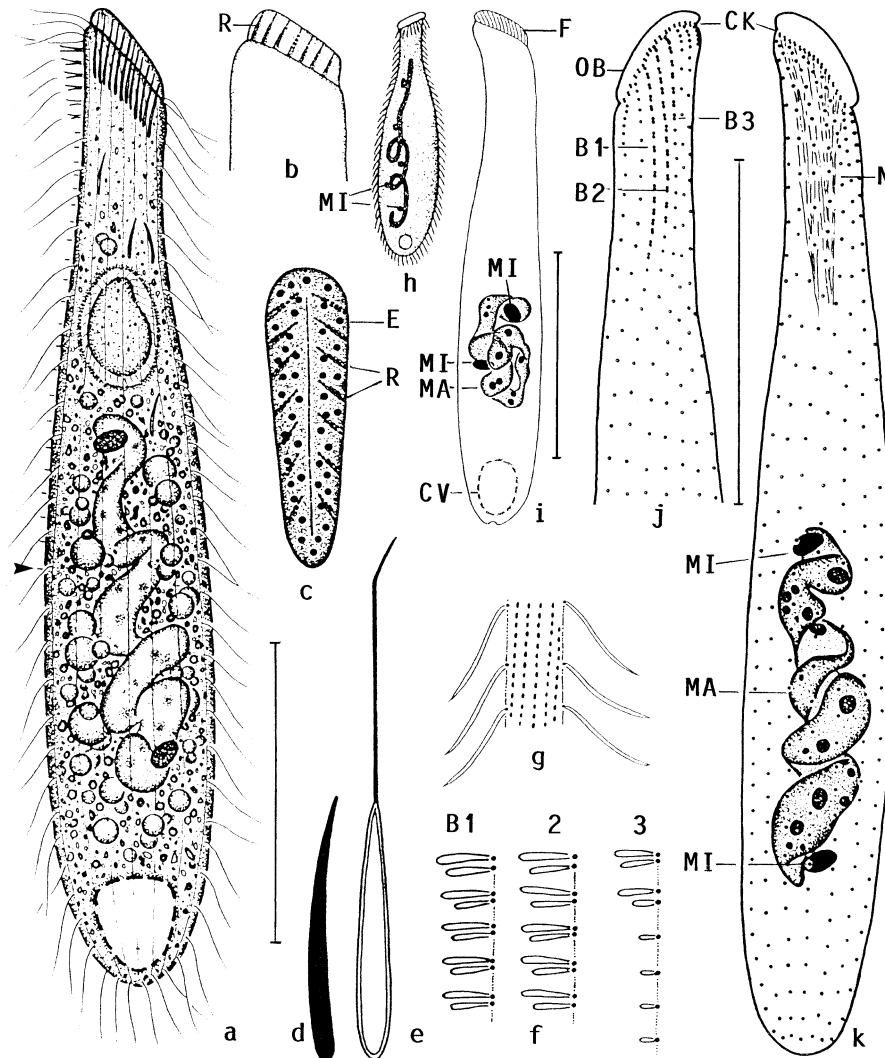
Type location: *Pinus nigra* forest soil in the Stampftal near Vienna, Austria, E16°02' N47°53'.

Etymology: The Latin adjective *bimicronucleatum* (two micronuclei) refers to the characteristic micronuclear pattern.

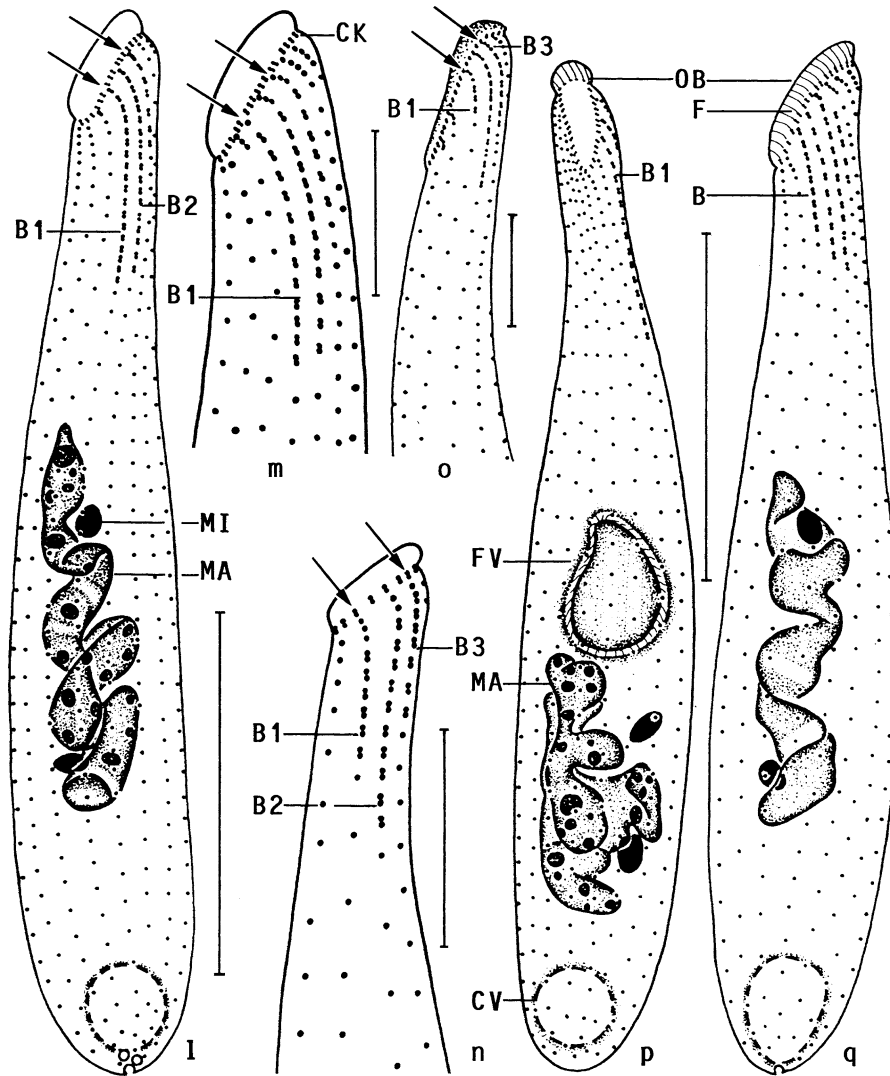
Type material: One holotype slide and two paratype slides with protargol-impregnated specimens (Foissner's method) have been deposited in the Biology Center of the Oberösterreichische Landesmuseum in Linz (LI), Austria. All specimens illustrated and some other well-impregnated cells are individually marked by a black ink circle on the cover glass.

Description: Size 70–110 $\mu\text{m} \times 10$ –20 μm *in vivo*, usually near 100 $\mu\text{m} \times 15\ \mu\text{m}$, as calculated from some *in vivo* measurements and the morphometric data (Table 7); length:width ratio 4.2–7.6:1, on average near 6:1 both *in vivo* and in protargol preparations. Size and shape similar to *Epispathidium terricola* Foissner 1987, but smaller and more slender, frequently almost cylindroidal or obclavate because oral bulge hardly widened and on average shorter by 1/3 than widest trunk region; neck *in vivo* typically more pronounced ventrally than dorsally; anterior (oral) body end obliquely truncate, posterior narrowly rounded; flattened only in oral region (Figures 5a, i, k, l, q, 6a–c); very flexible but non-contractile. Macronucleus in middle third of body, in most specimens rather distinctly spiralized and, interestingly, distinctly flattened, in some specimens even ribbon-like (>3:1); rarely highly tortuous or lobate, about 50 μm long when despiralized; contains several large and small nucleoli. Invariably two ellipsoidal to broadly ellipsoidal micronuclei (on average $3\ \mu\text{m} \times 2\ \mu\text{m}$ in protargol preparations), one each near or attached to ends of macronucleus, an unusual feature in spathidiids (Figures 5a, i, k, l, p, q, 6a–c, f). Contractile vacuole in rear body end, several excretory pores in pole area. Extrusomes accumulated in oral bulge and scattered in cytoplasm, inconspicuous *in vivo* because finely acicular and about $7\ \mu\text{m} \times 0.5\ \mu\text{m}$ in size (Figures 5a, d); those attached to oral bulge never impregnate with the protargol method used, while a certain, acicular, 4 – $4.5\ \mu\text{m} \times 0.7$ – $0.8\ \mu\text{m}$ -sized cytoplasmic developmental stage impregnates faintly. Released extrusomes of typical toxicyst structure, about 15 μm long (Figure 5e). Cortex very flexible, contains about five granule rows between each two kineties; granules minute, that is, approximately $0.4\ \mu\text{m} \times 0.2\ \mu\text{m}$, but rather refractive and thus distinct *in vivo*. Cytoplasm colourless, usually contains many lipid droplets 1–5 μm across; specimens with a large food vacuole containing ciliate prey were occasionally observed. Swims rapidly by rotation about main body axis.

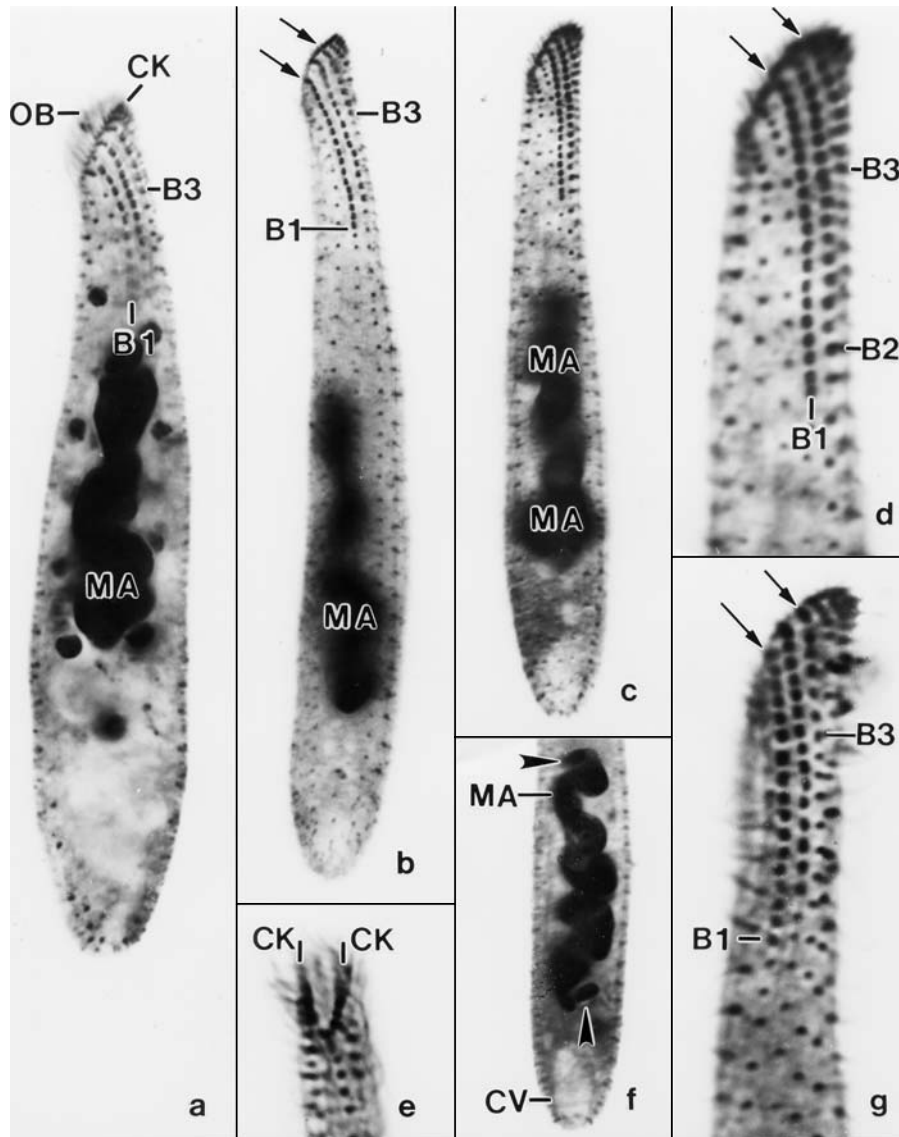
Cilia 8–9 μm long *in vivo*, arranged in an average of 14 equidistant, bipolar, ordinarily spaced but rather loosely ciliated rows abutting on circumoral kinety at an acute (on right side) or almost right angle (on left), as typical for *Spathidium* (Foissner 1984). Dorsal brush entirely on left side of cell, rarely it is located slightly dorsolaterally (Figures 5j, l, m, p, q, 6a–d, g); dikinetidal and three-rowed,



Figures 5a–k. *Latispathidium truncatum bimiconucleatum* (a–g, i–k) and *L. truncatum truncatum* (h; from Stokes 1885) from life (a–h) and after protargol impregnation (i–k). **a**: Right lateral view of a representative specimen. Arrowhead marks last bristle of tail of brush row 3. **b**, **c**: Lateral and frontal view of oral bulge. **d**: Oral bulge extrusome, length 7 μ m. **e**: Exploded toxicyst, length 15 μ m. **f**: Middle portion of dorsal brush. **g**: Surface view showing cortical granulation. **h**: *L. truncatum truncatum*, length about 125 μ m, differs from the European population by the micronuclear pattern. **i**: Specimen with tortuous macronucleus. **j**, **k**: Ciliary pattern of left and right side of holotype specimen. B1–3 – dorsal brush rows, CK – circumoral kinety, CV – contractile vacuole, E – extrusome, F – fibres, MA – macronucleus, MI – micronuclei, N – nematodesmata, OB – oral bulge, R – granule ridge. Scale bars 30 μ m.



Figures 5l–q. *Latispathidium truncatum bimicronucleatum* (l, m, p, q), *L. lanceoplites* (n; new figure from type population) and *Spathidium etoschense* (o; from Foissner et al. 2002) after protargol impregnation. Arrows mark dorsal brush in centre of left side in *L. truncatum bimicronucleatum* and *L. lanceoplites*, while dorsolaterally in *S. etoschense*. **l, m**: Ciliary pattern of left side. **n, o**: Left anterior region of *L. lanceoplites* and dorsolateral view of *S. etoschense*. For details, see discussion. **p**: A specimen with lobate macronucleus. **q**: A specimen with four brush rows and strongly flattened macronucleus. B(1–3) – dorsal brush (rows), CK – circumoral kinety, CV – contractile vacuole, F – fibres, FV – food vacuole, MA – macronucleus, MI – micronucleus, OB – oral bulge. Scale bars 30 μm (l, p, q) and 10 μm (m–o).



Figures 6a–g. *Latispathidium truncatum bimicronucleatum*, ciliary and nuclear pattern after protargol impregnation. Note cylindrical to obclavate body shape and macronucleus in middle body third. Arrows denote the genus-specific dorsal brush location in centre of left side, while the arrowheads in figure (f) mark the main subspecies-specific feature, viz., a micronucleus each at the ends of the macronucleus (several micronuclei distributed along macronuclear strand in *L. truncatum truncatum*; Figure 5h). The dorsal brush consists of three rows of paired bristles (dikinetics) at the anterior end of three left lateral ciliary rows; row 3 is strongly shortened. B1–3 – dorsal brush rows, CK – circumoral kinety, CV – contractile vacuole, MA – macronucleus, OB – oral bulge.

occupying 19% of body length on average, a fourth row occurs in one out of more than 50 specimens analyzed (Figure 5q); all rows with one or few ordinary cilia anteriorly, continue as somatic kineties posteriorly; bristles up to 4–5 μm long *in vivo*, length gradually decreases posteriorly, anterior bristles longer than posterior. Brush rows 1 and 2 of similar length, each composed of 15 dikinetids on average; row 3 invariably distinctly shorter than rows 1 and 2, comprises an average of only six dikinetids, but has a monokinetidal tail of 1 μm long bristles extending to mid-body, occasionally to near body end (Figures 5a, f, j, l, m, 6a–d, g; Table 7).

Oral bulge obliquely slanted by about 45° , conspicuously short, that is, about two thirds as long as widest trunk region; slightly cuneate in frontal view; about 3 μm high and 3 μm wide *in vivo*, dorsally slightly higher than ventrally; contains rows of very densely spaced cortical granules, forming conspicuous, ridge-like accumulations (Figures 5b, c). Circumoral kinety at base of oral bulge and also slightly cuneate, composed of ordinarily spaced dikinetids (two to three, on average 2.4 between two kineties each) forming continuous row; each dikinetid associated with a cilium, a fiber extending into oral bulge, and a basket rod. Oral basket hardly recognizable *in vivo* and also inconspicuous in protargol preparations (Figures 5i–m, p, q).

Occurrence and ecology: As yet found only at type location, where it was moderately abundant. This species is well adapted to the soil habitat by its slender body.

Comparison with related species: This population is fairly similar to *Latispathidium truncatum* (Stokes 1885), a poorly known, not yet redescribed species from North America. The main difference concerns the micronucleus pattern, viz., several micronuclei distributed along the macronucleus strand, as definitely stated and shown (Figure 5h) by Stokes (1885) versus one each at ends of macronucleus (Figures 5k, l, p, q). Certainly, this is a rather sophisticated feature, but sufficient to separate our population at subspecies level, considering that the pattern is highly constant and unusual. Possibly, there is a second main difference, viz., the extrusomes, which Stokes (1885), unfortunately, did not mention, but likely misinterpreted as a long (about one third of body length), conical pharyngeal basket. This interpretation, which we apply in the following species comparison, is reasonable because the oral basket of small and middle-sized spathidiids is very fine and thus hardly recognizable in the light microscope, even with interference contrast optics, while long, rod-shaped extrusomes, for instance, those of *Epispathidium terricola*, are easily recognized with an ordinary bright field microscope. Indeed, *Latispathidium truncatum bimicronucleatum* looks, at first glance, like a small *Epispathidium terricola* Foissner 1987b, which, however, differs clearly by the location of the dorsal brush (dorsally vs. laterally), the number of ciliary rows (39 vs. 14 on average), the extrusomes (40 μm long rods vs. short and acicular), and the arrangement of the ciliary rows (*Epispathidium* vs. *Spathidium* pattern).

Latispathidium truncatum bimicronucleatum is easily distinguished from its sole congener, *L. lanceoplites*, in most main features, especially the nuclear pattern (spiralized strand vs. ellipsoidal) and the shape of the extrusomes (finely acicular vs. lanceolate). It differs distinctly from similar *Spathidium* species, especially from

Table 7. Morphometric data on *Arcuospathidium coemeterii* (upper line) and *Latispathidium truncatum bimicronucleatum* (lower line).

Characteristics ^a	\bar{x}	<i>M</i>	SD	SE	CV	Min	Max	<i>n</i>
Body, length	87.2	86.0	11.2	2.4	12.8	67.0	103.0	21
	82.9	83.0	10.4	2.3	12.6	66.0	101.0	21
Body, width	20.8	20.0	3.7	0.8	17.8	16.0	28.0	21
	13.7	14.0	1.7	0.4	12.4	11.0	17.0	21
Body length:width, ratio	4.3	4.3	0.7	0.2	16.1	3.0	5.4	21
	6.1	6.2	0.9	0.2	14.9	4.2	7.6	21
Oral bulge, length (measured as length of cord of circumoral kinety)	21.8	22.0	2.5	0.5	11.5	18.0	28.0	21
	9.3	9.0	0.6	0.1	6.7	8.0	10.0	21
Oral bulge, height	4.4	4.3	0.6	0.2	14.4	3.5	5.0	10
	3.1	3.0	–	–	–	3.0	3.5	8
Dorsal brush row 1, length (distance circumoral kinety to last dikinetid)	17.1	17.0	2.3	0.5	13.2	14.0	21.0	21
	15.7	16.0	2.1	0.5	13.6	12.0	20.0	19
Dorsal brush row 2, length (distance circumoral kinety to last dikinetid)	20.4	19.0	3.8	0.8	18.6	15.0	30.0	21
	15.2	15.0	1.5	0.3	9.9	12.0	18.0	19
Dorsal brush row 3, length (distance circumoral kinety to last dikinetid)	6.7	6.0	1.4	0.3	20.6	5.0	10.0	21
	7.5	7.0	1.0	0.2	12.9	6.0	10.0	19
Anterior body end to macronucleus, distance	45.0	45.0	8.2	1.8	18.1	33.0	67.0	21
	33.7	34.0	9.3	2.0	27.5	17.0	52.0	21
Macronuclear figure, length	21.9	22.0	3.0	0.7	13.8	16.0	26.0	21
	31.8	32.0	7.9	1.7	24.9	20.0	48.0	21
Macronucleus, width	6.1	6.0	0.9	0.2	13.9	5.0	7.0	21
	5.1	5.0	0.6	0.1	12.3	4.0	6.0	21
Macronucleus, number	1.0	1.0	0.0	0.0	0.0	1.0	1.0	21
	1.0	1.0	0.0	0.0	0.0	1.0	1.0	21
Micronucleus, largest diameter	3.0	3.0	0.4	0.1	14.9	2.0	4.0	21
	3.0	3.0	0.6	0.1	18.5	2.5	4.5	21
Micronucleus, number	1.0	1.0	0.0	0.0	0.0	1.0	1.0	21
	2.0	2.0	0.0	0.0	0.0	2.0	2.0	21
Somatic kineties, number	11.6	12.0	1.2	0.3	10.4	9.0	14.0	21
	14.5	14.0	1.0	0.2	6.8	13.0	16.0	21
Ciliated kinetids in a right side kinety, number	29.3	30.0	4.6	1.0	15.8	22.0	36.0	21
	30.4	32.0	7.9	1.7	26.0	18.0	43.0	21
Dorsal brush rows, number	3.0	3.0	0.0	0.0	0.0	3.0	3.0	21
	3.0	3.0	0.0	0.0	0.0	3.0	3.0	21
Dikinetids in brush row 1, number	12.0	12.0	1.6	0.4	13.4	9.0	15.0	21
	14.8	15.0	2.8	0.6	18.6	10.0	19.0	19
Dikinetids in brush row 2, number	14.6	14.0	2.6	0.6	17.6	11.0	19.0	21
	14.4	15.0	1.7	0.4	11.9	12.0	18.0	19
Dikinetids in brush row 3, number	5.6	5.0	1.1	0.2	19.1	4.0	7.0	21
	6.4	6.0	0.7	0.2	10.7	5.0	8.0	19

^aData based on mounted, protargol-impregnated (Foissner 1991, protocol A), and randomly selected specimens from a non-flooded Petri dish culture. Measurements in μm . CV – coefficient of variation in %, *M* – median, Max – maximum, Min – minimum, *n* – number of individuals investigated, SD – standard deviation, SE – standard error of arithmetic mean, \bar{x} – arithmetic mean.

S. aciculare and *S. etoschense* (Figure 5o), both described in Foissner et al. (2002), by the special location of the dorsal brush. Furthermore, these species differ also in several main morphometrics, especially the length of the oral bulge and of dorsal

brush rows 1 and 2, and the number of circumoral dikinetids between each two somatic kineties (on average 2.4 vs. 5). Nonetheless, several main features of *Spathidium aciculare*, for instance, body shape, size, and nuclear pattern match well those of *Latispathidium truncatum truncatum*, suggesting that *Spathidium aciculare* might be a junior synonym, especially, if further investigations disprove our suggestion that Stokes' species has long, rod-shaped extrusomes, as explained above; unfortunately, Foissner et al. (2002) did not include *Latispathidium truncatum truncatum* in the species comparison.

***Arcuospathidium coemeterii* (Kahl 1943) nov. comb
(Figures 7a–r, 8a–t; Table 7)**

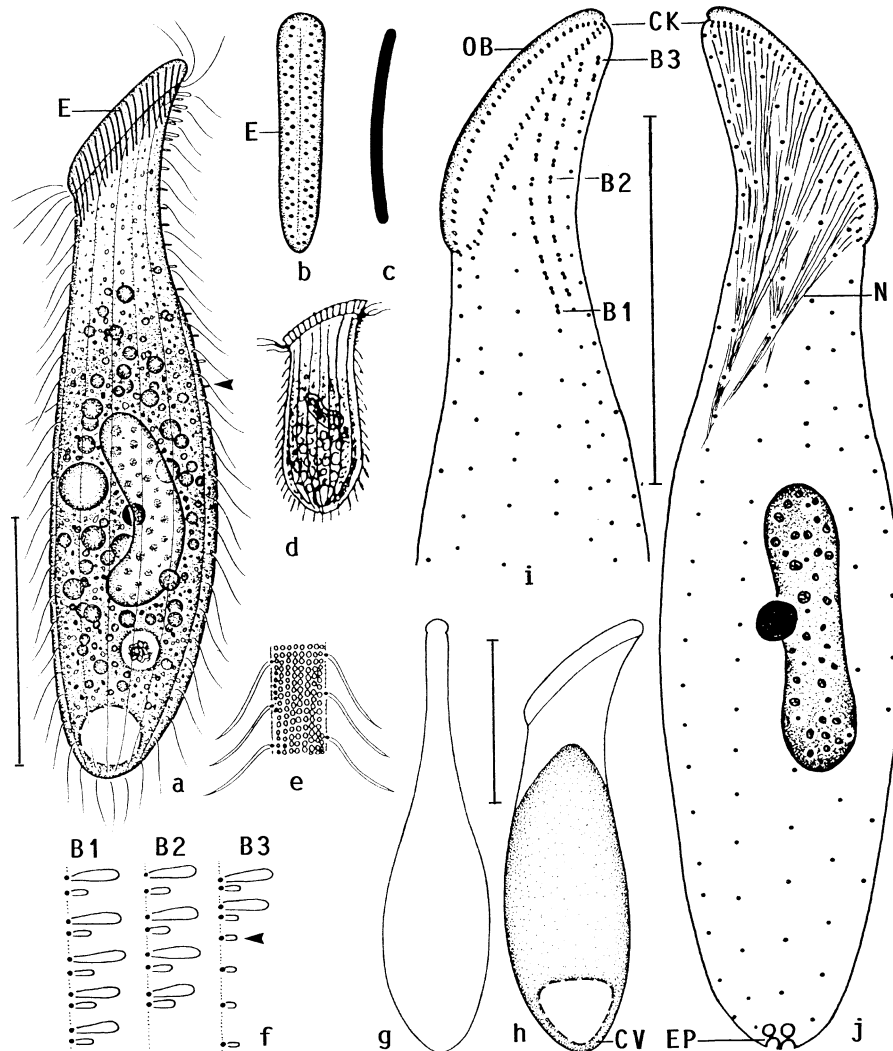
1943 *Spathidium coemeterii* Kahl, Infusorien: 26.

Improved diagnosis: Size about $95\ \mu\text{m} \times 23\ \mu\text{m}$ *in vivo*. Basically spatulate, but distinctly asymmetrical due to the pronounced neck dorsally and the strongly slanted, slenderly elliptical oral bulge about as long as widest trunk region. Macronucleus slenderly reniform. Extrusomes slightly curved, about $6\ \mu\text{m} \times 0.5\ \mu\text{m}$ sized rods. On average 12 ciliary rows, 3 anteriorly differentiated to dorsal brush occupying about 23% of body length; brush row 3 distinctly shortened.

Neotype location: *Pinus nigra* forest soil in the Stampftal near Vienna, Austria, E16°02'N47°53'.

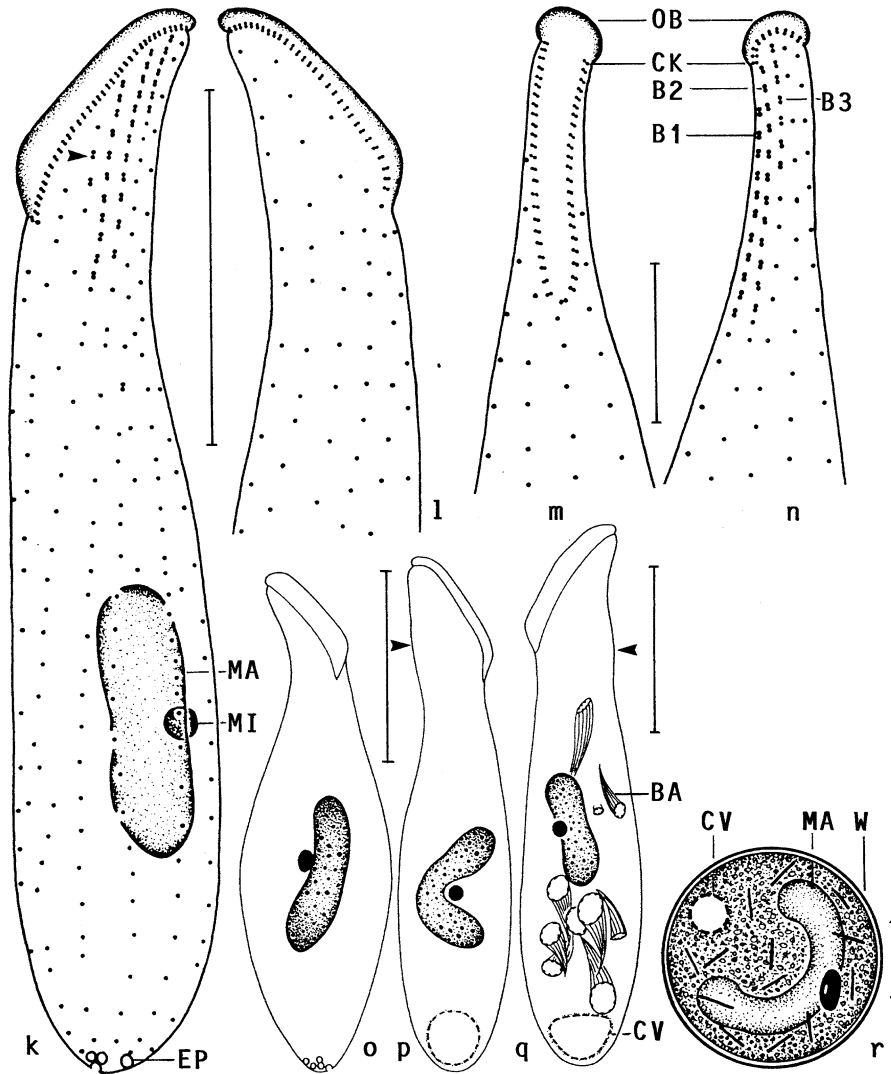
Neotype material: One neotype slide and two additional slides ('paraneotypes') with protargol-impregnated specimens (Foissner's method) have been deposited in the Biology Center of the Oberösterreichische Landesmuseum in Linz (LI), Austria. All specimens illustrated and some other well-impregnated cells are individually marked by a black ink circle on the cover glass.

Description (of Austrian neotype): Size $70\text{--}110\ \mu\text{m} \times 15\text{--}30\ \mu\text{m}$ *in vivo*, usually near $95\ \mu\text{m} \times 23\ \mu\text{m}$, as calculated from some *in vivo* measurements and the morphometric data; length:width ratio 3–4:1 *in vivo* and about 4.3:1 in protargol preparations (Table 7); oral and neck area flattened laterally up to 3:1, well-fed specimens thicker and less flattened than starved ones, as usual. Shape conspicuously asymmetrical, that is, dorsal side distinctly longer and more sigmoidal than ventral side due to the narrowed neck and strongly ($\sim 50^\circ$) slanted oral bulge about as long as widest trunk region; neck hyaline and rather pronounced dorsally, in protargol preparations often slightly inflated in brush area; widest usually near unflattened mid-region of body, posterior end moderately broadly rounded (Figures 7a, g, h, j, o–q, 8a, c, d, h, i, k, l, n, p). Macronucleus usually beneath mid-body, basically slenderly reniform, occasionally horseshoe-shaped or elongate ellipsoidal; contains numerous small nucleoli. Micronucleus globular, very near or attached to mid-macronucleus (Figures 7a, j, k, o–q, 8b–d; Table 7). Contractile vacuole in rear body end, four to five excretory pores in pole area. Oral extrusomes rod-shaped, slightly curved, about $5.5\text{--}6.5\ \mu\text{m} \times 0.5\ \mu\text{m}$ in size and thus longer than oral bulge height, never impregnate with the protargol method used (Figures 7a–c, 8b, f, j, m). Cortex flexible and often distinctly furrowed in SEM preparations, likely due to



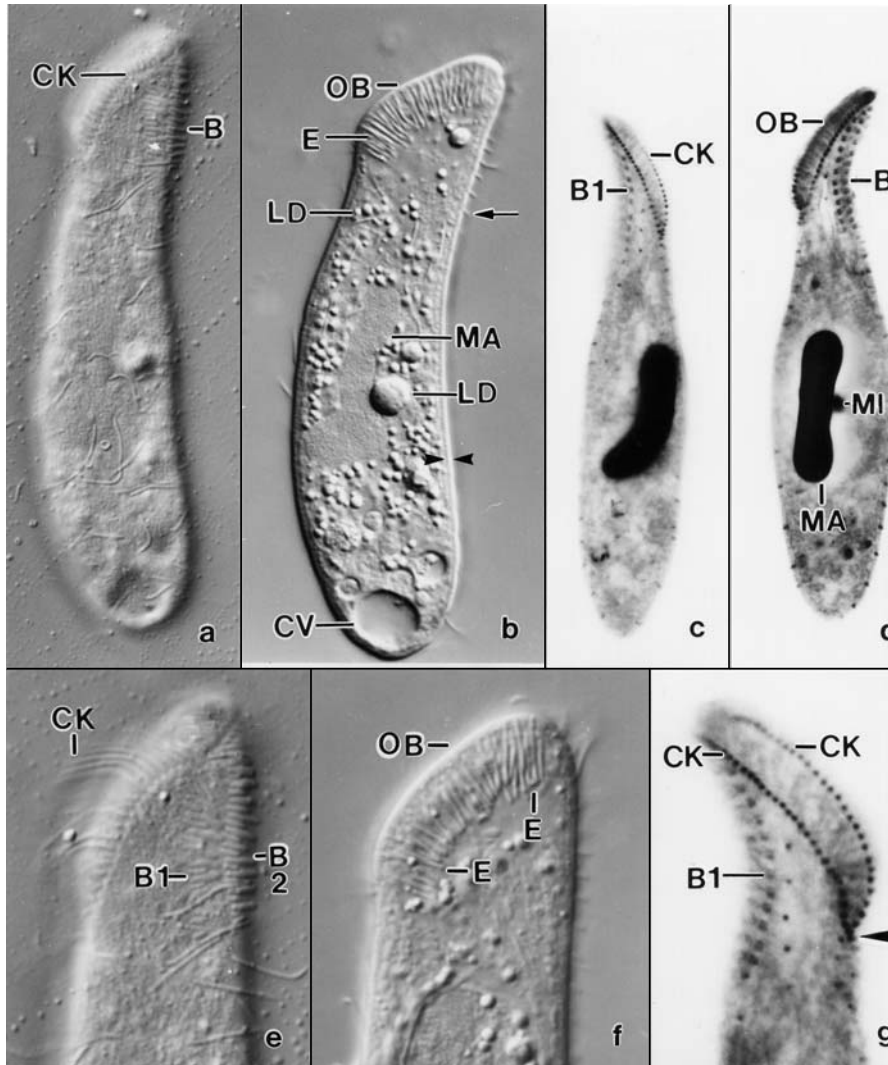
Figures 7a-j. *Arcuospithidium coemeterii* from life (a-h) and after protargol impregnation (i, j). **a**: Left lateral view of a representative specimen. Arrowhead marks bristle tail of row 3. **b**: Frontal view of oral bulge. **c**: Oral bulge extrusome, length 6 μm . **d**: Original figure by Kahl (1943), length 100 μm . **e**: Surface view showing the very narrowly spaced cortical granules. **f**: Middle portion of dorsal brush. Arrowhead marks monokinetid bristle tail of row 3. **g**, **h**: Dorsal and lateral view of a well-nourished specimen. **i**, **j**: Ciliary pattern of left and right side and nuclear apparatus of holotype specimen. B1-3 - dorsal brush rows, CK - circumoral kinety, CV - contractile vacuole, E - extrusomes, EP - excretory pores, N - nematodesmata, OB - oral bulge. Scale bars 30 μm .

postciliary microtubule bundles, as indicated by the oblique arrangement of the furrows; also conspicuous *in vivo* because about 1 μm thick due to the plate-like packed cortical granules; individual granules <1 μm across and hardly recognizable



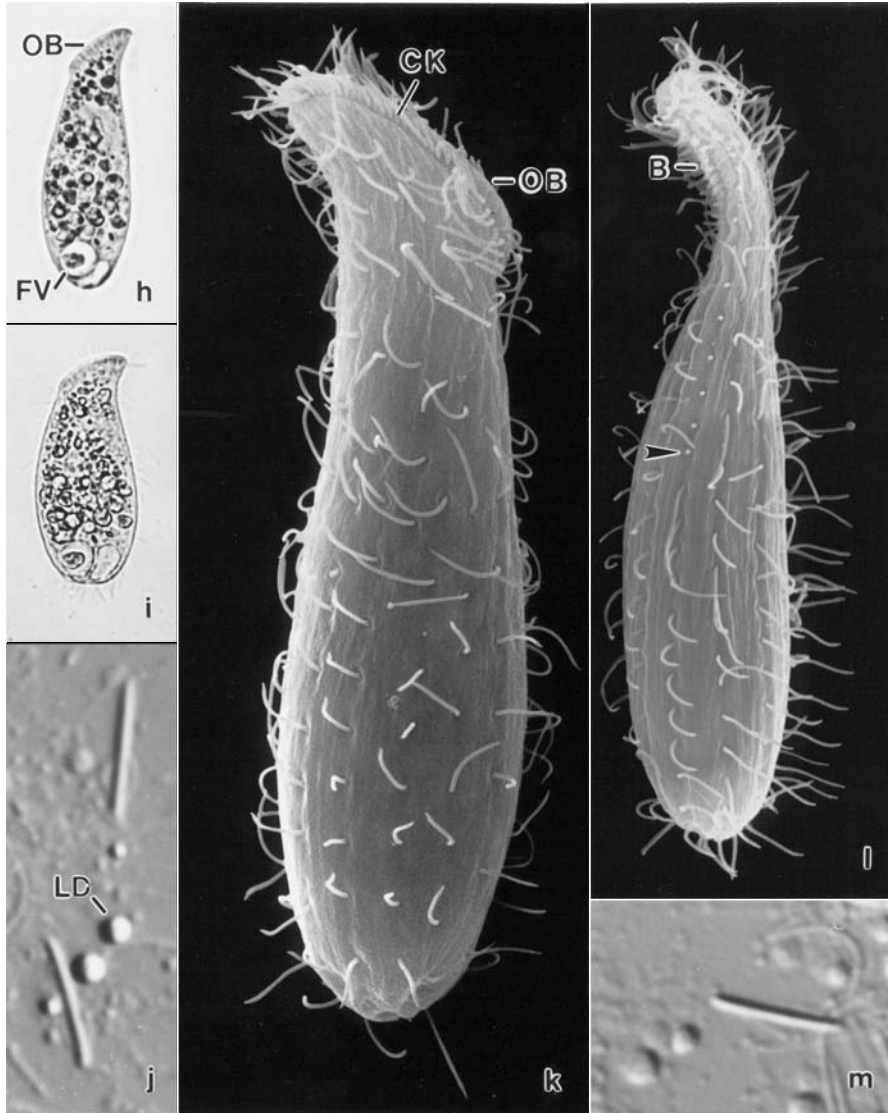
Figures 7k-r. *Arcuospathidium coemeterii* after protargol impregnation. **k, l**: Ciliary pattern of left and right side of a specimen with two dikinetids right of brush row 1 (arrowhead). **m, n**: Ventral and dorsal anterior body portion, showing the slightly cuneate circumoral kinety and the dorsal brush. **o-q**: Variations of body outline and nuclear pattern. One specimen (q) contains oral baskets of microthoracid ciliate prey. Arrowheads mark neck region slightly inflated due to the preparation procedures. **r**: Resting cyst. B1-3 - dorsal brush rows, BA - oral basket of prey, CK - circumoral kinety, CV - contractile vacuole, EP - excretory pores, MA - macronucleus, MI - micronucleus, OB - oral bulge, W - cyst wall. Scale bars 30 μm (k, l, o-q) and 10 μm (m, n, r).

because pale, colourless, and very closely arranged (Figures 7e, 8b, n, o). Cytoplasm colourless, contains few to many lipid droplets 1-6 μm across and few to many 3-12 μm -sized food vacuoles with heterotrophic flagellates (*Polytomella*) and



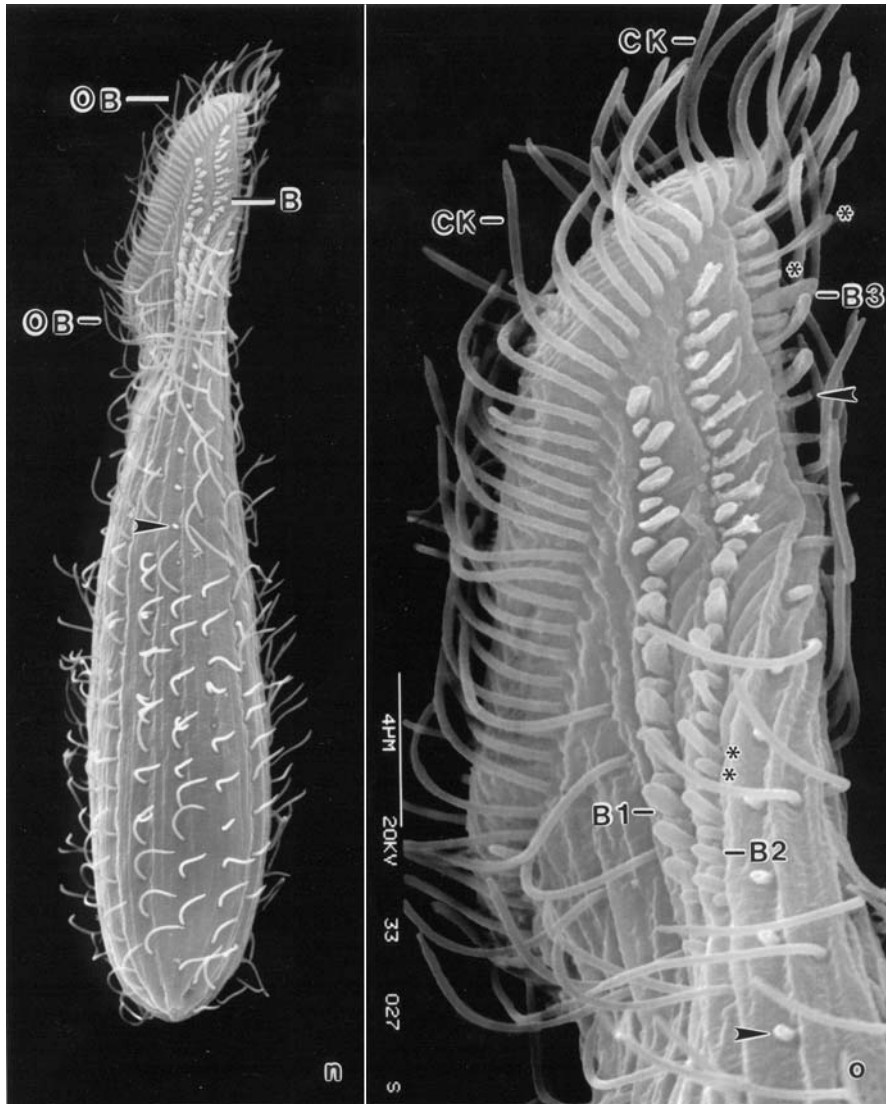
Figures 8a–g. *Arcuospathidium coemeterii* from life (a, b, e, f) and after protargol impregnation (c, d, g). **a, b, e:** Left side views of same specimen at several focal planes to show, inter alia, body shape, loose ciliation (a, e), and the widely spaced cilia of the circumoral kinety (e). Arrow marks bristles of tail of brush row 3. Opposed arrowheads denote the cortex which is comparatively thick due to the narrowly spaced cortical granules. **f:** The oral bulge is studded with rod-shaped, about 6 μm long extrusomes. **c, d, g:** Left side views of ciliary pattern and nuclear apparatus. Arrowhead marks narrowed ventral end of circumoral kinety. B(1, 2) – dorsal brush (rows), CK – circumoral kinety, CV – contractile vacuole, E – extrusomes, LD – lipid droplets, MA – macronucleus, MI – micronucleus, OB – oral bulge.

microthoracid ciliates, whose oral baskets can be seen in protargol-impregnated specimens (Figures 7q, 8b, h, i, j). Glides slowly on microscope slide and swims by rotation about main body axis.



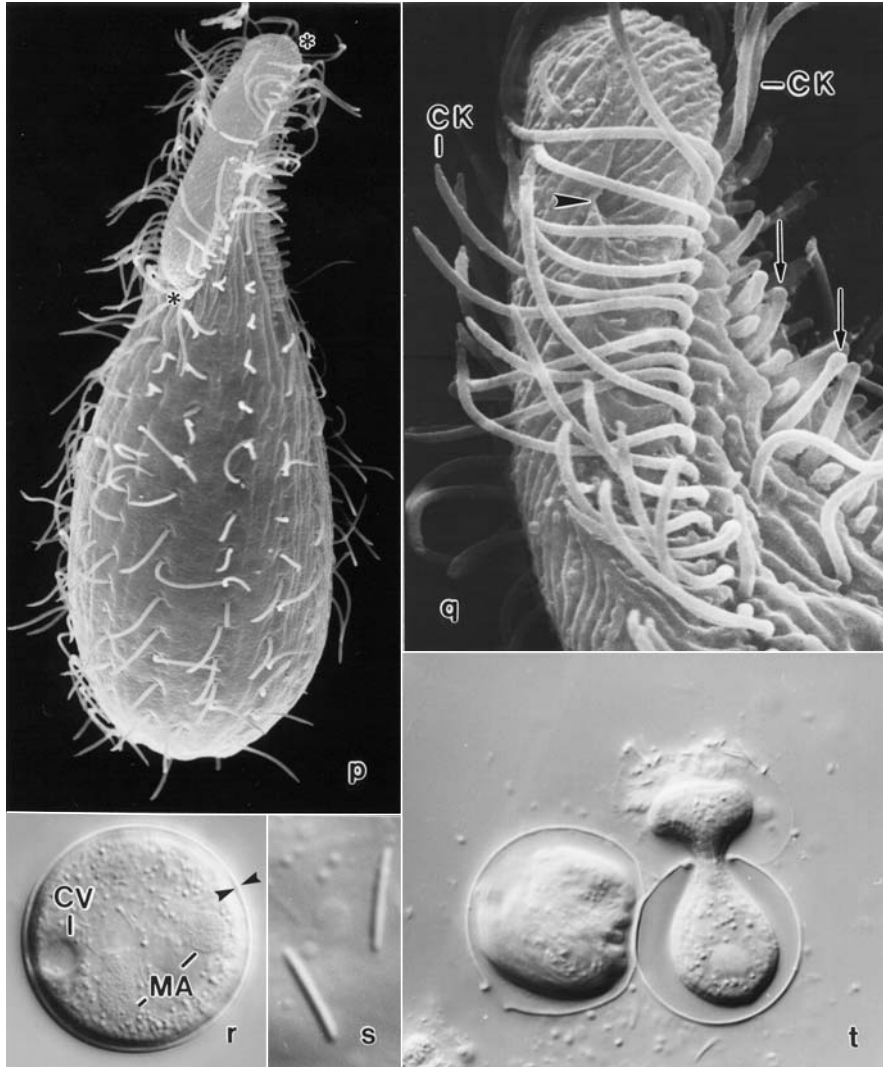
Figures 8h–m. *Arcuospathidium coemeterii* from life (h–j, m) and in the SEM (k, l). **h, i:** Left side overviews of a well-nourished specimen with many lipid (dark) droplets in freely motile (h) and slightly squeezed (i) condition, where shape changes considerably. **j, m:** Extrusomes are about 6 μm long. **k, l:** Right side and dorsal view showing loose ciliation and last bristle (arrowhead) of monokinetid tail of brush row 3. B – dorsal brush, CK – circumoral kinety, FV – food vacuole, LD – lipid droplet, OB – oral bulge.

Somatic cilia about 7 μm long *in vivo*, fairly widely spaced, arranged in pronounced *Arcuospathidium*-pattern, that is, in an average of 12 longitudinal rows anteriorly curved dorsally and distinctly separate from circumoral kinety at both



Figures 8n, o. *Arcuospithidium coemeterii*, left side views in the SEM. This well-preserved specimen shows the spatulate body with the steep oral bulge, the loose ciliature, and the comparatively widely spaced cilia of the circumoral kinety. The dorsal brush consists of three rows of paired, distally inflated bristles with the anterior bristle longer than the posterior one (asterisk pairs), especially in anterior portion of row 3, which has a monokinetidal bristle tail (arrowheads). B(1-3) – dorsal brush (rows), CK – circumoral kinety, OB – oral bulge.

sides (Figures 7a, i-l, 8a, c, d, k, n, o; Table 7). Dorsal brush dikinetidal and three-rowed, in some specimens a few bristles right of row 1, all rows continue as ordinary somatic kineties posteriorly and lack ordinary cilia anteriorly; *in vivo* rather



Figures 8p–t. *Arcuospathidium coemeterii* in the SEM (p, q) and from life (r–t). **p**: Ventral view showing the elongate-elliptical, strongly flattened oral bulge with ends marked by asterisks. **q**: The oral bulge has a minute, conical indentation ('second mouth') near the dorsal end (arrowhead). Arrows mark distally inflated dorsal brush bristles. **r, t**. Resting cysts are about 30 μm across and have a smooth, thin ($\leq 1 \mu\text{m}$) wall (opposed arrowheads), which becomes distinct in squashed cysts (t). **s**: Resting cyst extrusomes, length 6 μm . CK – cilia of circumoral kinety, CV – contractile vacuole, MA – macronucleus.

conspicuous, although occupying only 23% of body length, because bristles 2–3 times as thick as ordinary somatic cilia, most bristles, however, collapse in SEM preparations assuming a more or less wrinkled shape (Figures 8o, q). Anterior bristle of pairs about 3 μm long and slightly fusiform, posterior approximately 1 μm long

and rod-shaped. Brush row 1 slightly shorter than row 2, both extend somewhat beyond oral bulge region; row 3 distinctly shorter than rows 1 and 2, composed of an average of only five dikinetids, but followed by a monokinetidal tail of 1 μm long bristles extending to mid-body (Figures 7a, f, i, k, n, 8a–e, g, l, n, o; Table 7).

Oral bulge occupies anterior body end slanted by 40° – 50° , on average as long as widest trunk region, rather indistinct because hardly separate from body proper and only about 3 μm high; outline indistinctly convex or sigmoidal, rarely flat; in frontal view elongate elliptical to indistinctly cuneate, rarely rather distinctly cuneate because slightly narrowed ventrally. Bulge surface with arrowhead-like pattern of crests and furrows forming small whirl near dorsal bulge end; whirl not recognizable *in vivo* and in protargol preparations, but likely corresponds to a temporary cytosome, as described in *A. multinucleatum* Foissner 1999 and *Spathidium seppelti* Petz and Foissner 1997 (Figures 7a, b, i–n, o–q; 8a–h, k, n–q; Table 7). Circumoral kinety of same shape as oral bulge, continuous, composed of comparatively widely spaced dikinetids, viz., about five to six between two somatic kineties each; individual dikinetids associated with an about 10 μm long cilium and a basket rod. Nematodesmata (oral basket rods) fairly distinct and bundled, forming rather conspicuous basket in protargol-impregnated specimens (Figure 7j).

Resting cysts spherical (\bar{x} 30.9 μm , M 31, SD 2.5, SE 0.5, CV 8, Min 26, Max 35 μm ; n 23), colourless; nuclear apparatus, contractile vacuole, and extrusomes maintained; cytoplasm densely granulated by lipid droplets $\leq 2 \mu\text{m}$ across (Figures 7r, 8r–t). Cyst wall smooth, thin ($\leq 1 \mu\text{m}$).

Occurrence and ecology: Kahl (1943) mentioned that he discovered *A. coemeterii* in moss, but did not indicate the site. We found this species in 9 of the 12 sites investigated, both in deciduous and coniferous forest soils, showing that it is common and has a wide ecological range. Abundances were low to moderate. Likely, we did not identify *A. coemeterii* in our previous studies or misidentified it as a ‘small variety’ of *Spathidium spathula*, which is occasionally rather similar (see below). Further, there is at least one other similar, not yet described *Spathidium* species (Foissner, unpublished).

Identification: Kahl’s (1943) description is extremely brief: “Size 100 μm , similar to *Spathidium muscicola*, but with shorter toxicysts”. However, the figure provided (Figure 7d) suggests that our population belongs to that species; at least, it would be difficult to find a significantly different feature, except of body shape, which is considerably stouter in Kahl’s specimen (2.75 vs. 3–4:1 *in vivo*), providing our population with a rather different general appearance (Figures 7a, d, h, i, k, o–q, 8b–d, k, n); further, the oral bulge, which is slightly convex in Kahl’s figure, is frequently indistinctly sigmoidal in our specimens, that is, slightly depressed in or near the center (cp. Figures 7d, k, 8b, n). These differences appear inconspicuous when compared with the matching features, viz., body size ($\sim 100 \mu\text{m}$), the number of ciliary rows (about 10–12, according to Kahl’s figure) and, especially, the reniform macronucleus. Thus, and because Kahl’s description is very brief, we suggest neotypification of *S. coemeterii* with the Austrian population.

Generic allocation and comparison with related species: Kahl (1943) classified his population in *Spathidium*. However, silver impregnation shows that the ciliary rows are

directed dorsally on both sides of the oral bulge and distinctly separate from the continuous circumoral kinety. Thus, the species belongs to *Arcuospathidium* Foissner 1984.

There are several species with a close resemblance to *A. coemeterii*, viz., *A. muscorum* (Dragesco and Dragesco-Kernéis 1979) Foissner 1984; *A. atypicum* Wenzel 1953, as redescribed by Foissner (1988, 1998); *A. japonicum* Foissner 1988; and *Spathidium spathula* (O. F. Müller 1786), as redescribed by Foissner (1981). At first glance, *A. coemeterii* is indistinguishable from *A. muscorum*, especially from the Austrian and Venezuelan populations studied by Foissner (1981, 2000c), because most obvious features are rather similar. However, a more detailed comparison reveals significant differences, viz., the shape of the macronucleus (reniform vs. a long, tortuous strand), the ratio of oral bulge to body length (25% vs. 41–49%), and the ratio of oral bulge to the longest brush row (about 1:1 vs. about 1:0.3). Thus, the oral bulge is much longer and the brush distinctly shorter in *A. muscorum* than in *A. coemeterii*. *Arcuospathidium coemeterii* differs from *A. atypicum* and *A. japonicum* mainly by the reniform macronucleus (vs. two ellipsoidal nodules); from *A. japonicum*, additionally, by the rod-shaped (vs. acicular) extrusomes.

Certain populations of *Spathidium spathula*, as redescribed by Foissner (1981, 1984), are *in vivo* also rather similar to *Arcuospathidium coemeterii*. However, the ciliary pattern is different (*Spathidium* pattern), the number of kineties distinctly higher (18–30 vs. 9–14), and the oral bulge is more massive and less slanted.

***Protospathidium fusioplites* nov. spec. (Figures 9a–x, 10a–l; Table 8)**

We studied three populations of this species, but only the Austrian population was fully investigated. The North American specimens were also studied rather carefully (Table 8), while the South African population was routinely identified *in vivo* by the main features, viz., size and shape of body, oral bulge and extrusomes; the macronucleus pattern; and the number of somatic kineties. Although conspecificity is beyond reasonable doubt, the observations are kept separate, and the diagnosis and description contain only data from the Austrian population.

Diagnosis: Size about $110\ \mu\text{m} \times 10\ \mu\text{m}$ *in vivo*. Cylindroidal to slightly fusiform with oblique, obovate, minute oral bulge about $2/3$ as long as widest trunk region. Approximately 13 macronuclear nodules scattered in middle body third. Extrusomes fusiform, about $1.5\text{--}2\ \mu\text{m} \times 0.8\ \mu\text{m}$ in size. On average eight ciliary rows, three anteriorly differentiated to dorsal brush occupying 17% of body length; brush row 1 minute, dikinetids of row 3 widely spaced. Circumoral kinetofragments each composed of 1–2 dikinetids.

Type location: *Pinus nigra* forest soil in the Stampftal near Vienna, Austria, E16°02' N47°53'.

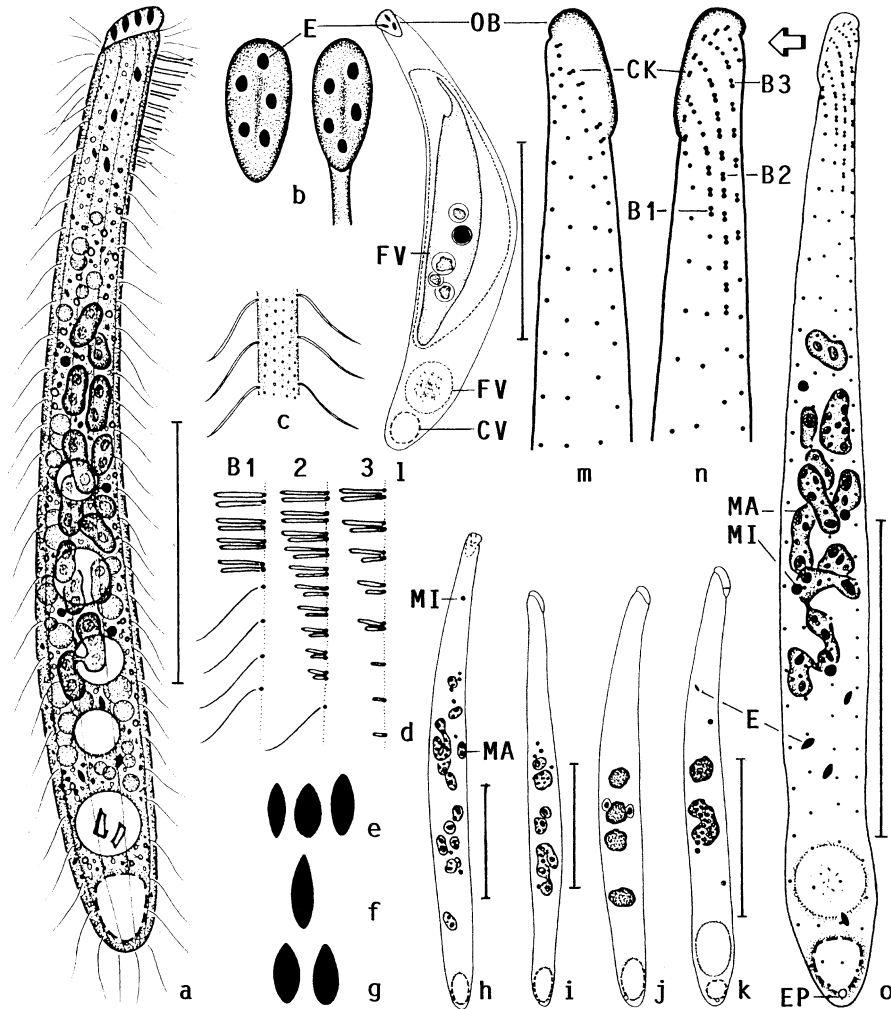
Etymology: Composite of the Latin noun *fuscus* (spindle) and the Greek noun *hoplites* (soldier ~ extrusome), referring to the fusiform extrusomes.

Type material: One holotype and two paratype slides with protargol-impregnated specimens (Foissner's method) have been deposited in the Biology Center of the Oberösterreichische Landesmuseum in Linz (LI), Austria. Two voucher slides with

Table 8. Morphometric data on *Protospathidium fusioplites* from Stampftal, Austria (upper line) and the USA (lower line).

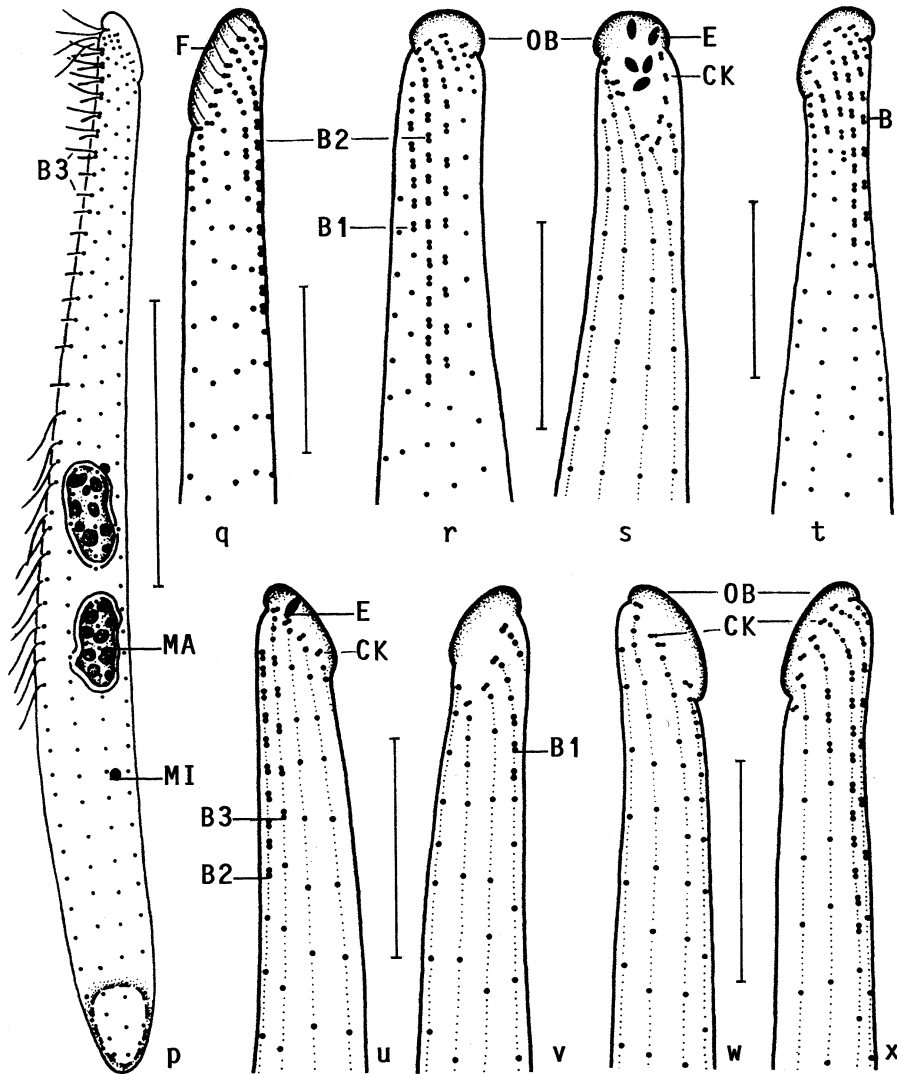
Characteristics ^a	\bar{x}	<i>M</i>	SD	SE	CV	Min	Max	<i>n</i>
Body, length	97.6	96.0	14.2	3.1	14.5	75.0	130.0	21
	74.1	71.5	13.2	4.2	17.9	53.0	103.0	10
Body, width	9.1	9.0	1.3	0.3	13.9	7.0	12.0	21
	10.0	10.0	1.6	0.5	16.1	6.0	12.0	10
Body length:width, ratio	10.8	10.8	1.1	0.2	10.5	8.8	12.5	21
	7.6	7.3	1.8	0.6	24.1	4.8	11.5	10
Oral bulge, length	6.9	7.0	0.8	0.2	12.0	5.0	8.0	21
	5.7	5.8	0.8	0.3	14.4	4.0	7.0	10
Oral bulge, width	3.3	3.0	0.4	0.1	11.1	3.0	4.0	9
	2.8	3.0	0.3	0.2	10.2	2.5	3.0	3
Circumoral kinety to last dikinetid of brush row 1, distance	7.5	8.0	1.1	0.2	14.4	6.0	10.0	21
	8.7	8.0	0.9	0.3	10.0	8.0	10.0	9
Circumoral kinety to last dikinetid of brush row 2, distance	15.9	16.0	2.3	0.5	14.7	12.0	20.0	21
	12.1	12.0	1.9	0.6	15.7	10.0	16.0	9
Circumoral kinety to last dikinetid of brush row 3, distance	13.5	13.0	2.1	0.5	15.3	10.0	18.0	21
	10.0	10.0	1.2	0.4	12.0	8.0	12.0	8
Anterior body end to first macronuclear nodule, distance	29.2	30.0	6.2	1.4	21.4	15.0	39.0	21
	17.3	17.0	4.4	1.4	25.6	12.0	25.0	10
Nuclear figure, length	45.4	40.0	15.8	3.4	34.8	24.0	92.0	21
	40.5	37.5	14.6	4.6	36.0	21.0	68.0	10
Macronuclear nodules, length	5.4	5.0	1.4	0.3	24.9	4.0	9.0	21
	5.4	5.5	1.6	0.5	30.5	3.5	9.0	10
Macronuclear nodules, width	2.9	2.5	0.8	0.2	27.2	2.0	4.0	21
	3.4	3.0	0.8	0.3	23.8	2.5	5.0	10
Macronuclear nodules, number	11.6	13.0	3.4	0.7	29.5	5.0	15.0	21
	10.9	11.0	4.7	1.6	43.4	4.0	20.0	9
Micronuclei, across	1.1	1.0	0.2	0.0	14.5	1.0	1.5	21
	1.1	1.0	0.2	0.1	20.6	1.0	1.5	8
Micronuclei, number	4.5	4.0	1.4	0.3	31.7	2.0	9.0	21
	3.6	4.0	1.1	0.5	31.7	2.0	5.0	5
Circumoral dikinetids, number	12.4	13.0	1.2	0.3	9.4	8.0	13.0	21
	–	–	–	–	–	–	–	–
Somatic kineties, number	8.4	8.0	0.6	0.1	7.0	8.0	10.0	21
	10.3	10.0	0.7	0.2	6.6	9.0	11.0	10
Ciliated kinetids in a right side kinety, number	34.0	33.0	8.2	1.8	24.1	20.0	55.0	21
	44.3	42.0	9.2	3.1	20.7	32.0	60.0	9
Dorsal brush rows, number	3.0	3.0	0.0	0.0	0.0	3.0	3.0	21
	3.0	3.0	0.0	0.0	0.0	3.0	3.0	9
Dikinetids in brush row 1, number	4.2	4.0	1.1	0.2	26.8	3.0	7.0	21
	6.6	7.0	0.5	0.2	8.0	6.0	7.0	9
Dikinetids in brush row 2, number	12.2	12.0	2.1	0.5	17.1	10.0	17.0	21
	12.1	12.0	1.4	0.5	11.3	10.0	15.0	9
Dikinetids in brush row 3, number	7.0	7.0	1.4	0.3	20.7	5.0	11.0	21
	7.9	8.0	1.3	0.5	17.1	6.0	9.0	7

^aData based on mounted, protargol-impregnated (Foissner 1991, protocol A), and randomly selected specimens from non-flooded Petri dish cultures. Measurements in μm . CV – coefficient of variation in %, M – median, Max – maximum, Min – minimum, *n* – number of individuals investigated, SD – standard deviation, SE – standard error of arithmetic mean, \bar{x} – arithmetic mean.

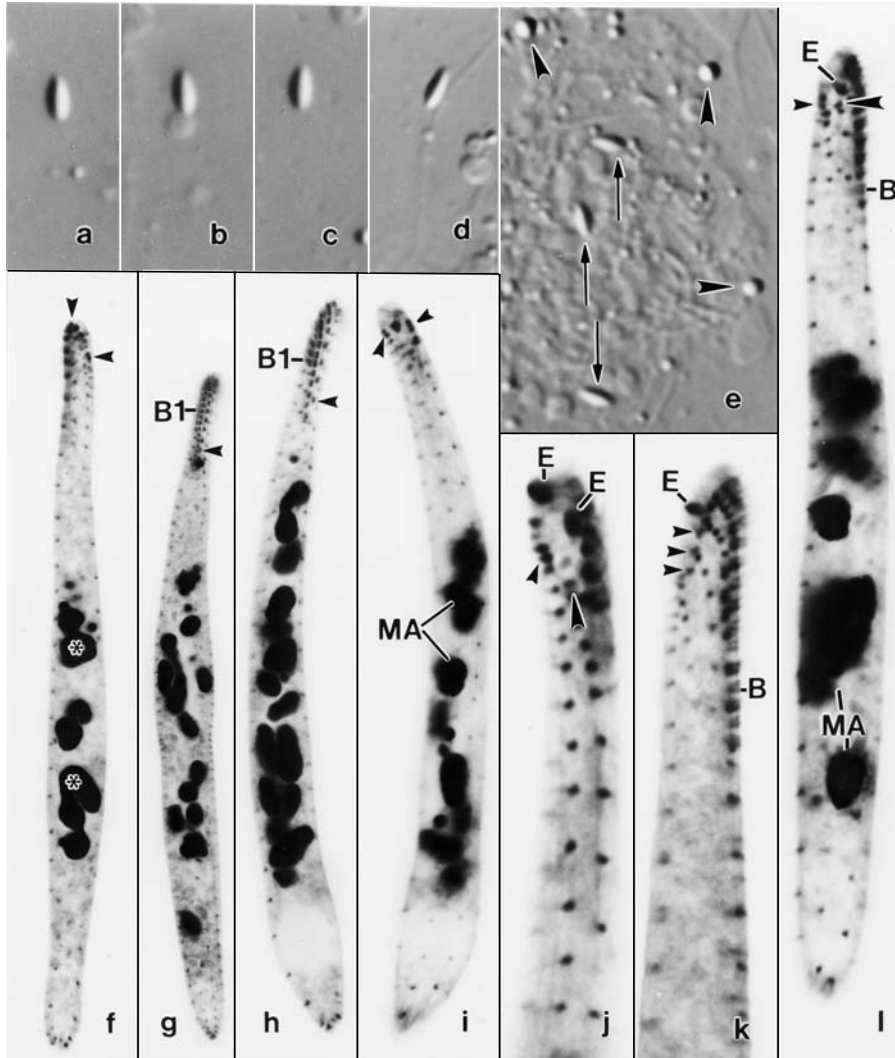


Figures 9a–o. *Protospathidium fusioplites* from life (a–g) and after protargol impregnation (h–o). **a**: Left side view of a representative specimen. **b**: Frontal views of oral bulge containing few, thick extrusomes. **c**: Surface view showing cortical granulation. **d**: Posterior portion of dorsal brush, bristles up to 5 μm long. **e–g**: Oral bulge extrusomes of specimens from Austria (1.5–2 $\mu\text{m} \times 0.8 \mu\text{m}$ in size), USA (2.5 $\mu\text{m} \times 0.8 \mu\text{m}$), and the Republic of South Africa (2 $\mu\text{m} \times 1 \mu\text{m}$). **h–k**: Variations of body shape and nuclear pattern. **l**: A specimen with a very large food vacuole containing amoeboid prey. **m–o**: Ciliary pattern of holotype specimen orientated slightly dorsolaterally. Note individual circumoral kinetofragments composed of only one or two dikinetids. B1–3 – dorsal brush rows, CK – circumoral kinety, CV – contractile vacuole, E – extrusomes, EP – excretory pores, FV – food vacuole, MA – macronuclear nodules, MI – micronuclei, OB – oral bulge. Scale bars 30 μm .

protargol-impregnated specimens from the North American population have also been deposited. All specimens illustrated and some other well-impregnated cells are individually marked by a black ink circle on the cover glass.



Figures 9p-x. *Protospathidium fusioplites* after protargol impregnation. **p, q**: Ciliary pattern of right side and left anterior body portion of same specimen. Note monokinetidal tail of brush row 3 extending to mid-body. **r, s**: Ciliary pattern of dorsal and ventral anterior body portion of a specimen where the oral bulge extrusomes impregnated with protargol. **t**: A specimen with four dorsal brush rows. **u, v**: Ciliary pattern of right and left anterior body portion of a specimen with one circumoral dikinetid at anterior end of each somatic kinety. **w, x**: Ciliary pattern of right and left anterior body region of a specimen with circumoral kinetofragments composed of one or two dikinetids. B – dorsal brush, B1–3 – dorsal brush rows, CK – circumoral kinety, E – extrusomes, F – fibre, MA – macronuclear nodule, MI – micronucleus, OB – oral bulge. Scale bars 30 μ m (p) and 10 μ m (q-x).



Figures 10a–l. *Protospathidium fusioplites* from life (a–e) and after protargol impregnation (f–l). **a–d**: Oral bulge extrusomes are fusiform to indistinctly ovate and 1.5–2 μm long. **e**: Oral bulge extrusomes in lateral (arrows) and transverse (arrowheads) view. **f**: Right side overview showing the minute oral bulge (arrowheads) and eight macronuclear nodules (asterisks). **g, h**: Dorsal views of specimens with many scattered macronuclear nodules. Dorsal brush row 1 consists of only three dikanetids, while dikanetids of row 3 are very widely spaced (arrowheads). **i–l**: Ventral (i, j) and left side (k, l) views showing the circumoral kinetofragments (arrowheads) composed of only one to two dikanetids. Note dorsal location of brush. B(1) – dorsal brush (row1), E – extrusomes, MA – macronuclear nodules.

Description: Size 90 μm –140 \times 10–15 μm *in vivo*, usually near 110 μm \times 12 μm , as calculated from some *in vivo* measurements and the morphometric data (Table 8); length:width ratio 8.8–12.5:1, on average about 11:1 both *in vivo* and in protargol

preparations. Shape cylindroidal to slenderly fusiform, frequently somewhat curved; anterior (oral) body end obliquely slanted, posterior narrowly rounded, occasionally bluntly pointed, but never tail-like, widest in or slightly underneath mid-body (Figures 9a, h–k, o, p, 10f–i, l). Macronucleus pattern difficult to recognize *in vivo*, basically nodular with individual nodules scattered in middle body third; however, in about 40% of specimens occur a mixture of nodules and short, moniliform pieces; furthermore, 9% of specimens have four nodules and 6% only two (Figures 9a, h–k, o, p, 10f–i; Table 8), similar as in *Spathidium turgitorum*, where Foissner et al. (2002) stated that they could not follow the origin of this pattern. Individual nodules globular to elongate ellipsoidal, on average $5\ \mu\text{m} \times 2.5\ \mu\text{m}$ in protargol preparations, each usually contains 1–3 nucleoli. Micronuclei globular, most scattered among macronuclear nodules, some rather distant near anterior or posterior body end. Contractile vacuole in posterior body end, some excretory pores in pole area, several empty, acontractile (food?) vacuoles occur in posterior body half. Extrusomes studied in oral bulge and scattered in cytoplasm, fusiform to indistinctly ovate, that is, both ends pointed or one end rather distinctly rounded; minute, that is, about $1.5\text{--}2\ \mu\text{m} \times 0.8\ \mu\text{m}$ in size, but rather compact and thus distinct *in vivo*, where they appear as conspicuous, bright dots when the oral bulge is viewed frontally; both, oral bulge and cytoplasmic extrusomes frequently impregnate rather intensely with protargol (Figures 9a, b, e, k, o, s, u, 10a–e, j–l). Cortex very flexible, contains several rows of colourless, approximately $0.2\ \mu\text{m}$ sized, loosely arranged granules between each two kineties. Cytoplasm colourless, contains few to many lipid droplets $1\text{--}5\ \mu\text{m}$ across and, frequently, a subterminal vacuole with crystals and granular remnants causing a rather distinct subterminal inflation in protargol-prepared cells; occasionally occur specimens with a massive, large food vacuole containing amoeboid prey (Figures 9a, l, o, 10h, i). Movement without peculiarities.

Cilia about $7\ \mu\text{m}$ long *in vivo*, arranged in an average of eight equidistant, bipolar, rather loosely ciliated rows connected with inconspicuous oral kinetofragments (Figures 9a, m–x, 10f–l; Table 8). Dorsal brush dikinetidal and three-rowed occupying 17% of body length on average, a fourth row occurs in one out of 40 specimens analyzed; all rows have several ordinary cilia anteriorly and continue as somatic kineties posteriorly. Brush rows of same structure anteriorly, that is, bristles conspicuously rod-shaped and of nearly same length ($5\ \mu\text{m}$) *in vivo*; posteriorly, bristle length decreases gradually with anterior bristles longer than posterior. Brush row 1 shorter than rows 2 and 3 comprising an average of only four dikinetids; middle row 2 longer than row 3, composed of 12 dikinetids on average; row 3 composed of an average of seven dikinetids much more widely spaced than those of rows 1 and 2, followed by a monokinetidal tail of $1\ \mu\text{m}$ long bristles extending to mid-body (Figures 9a, n–r, t–x; Table 8).

Oral bulge rather distinct both in protargol preparations and *in vivo* due to the refractive extrusomes contained, basically, however, fairly inconspicuous because only about $3\ \mu\text{m}$ high, hardly set off from body proper ventrally, and shorter by about $1/3$ than widest trunk region; slanted by about 45° and slightly convex in lateral view, while obovate when seen frontally (Figures 9a, b). Individual circumoral kinetofragments inconspicuous because composed of only one to two

dikinetids, forming a “circumoral kinety” comprising an average of only 13 dikinetids; in an extreme specimen, even only 8, that is, one each at end of kineties. Kinetofragments almost equidistantly spaced and thus inconspicuous on left side of cell, while separated from each other by gaps one to three dikinetids wide on right side. Each dikinetid associated with a single cilium and a fibre extending into oral bulge (Figures 9m–x, 10i–k; Table 8). Oral basket rods (nematodesmata) not recognizable *in vivo*, also indistinct in over-impregnated cells; no oralized somatic monokinetids, as typical for the Fuschertiidae and Acropisthiidae (Foissner et al. 2002).

Observations on the North American and South African populations: The North American population matches the European specimens in all main features, for instance, body and extrusome shape, nuclear pattern, number and arrangement of somatic kineties, and the structure of the circumoral kinety and dorsal brush (Table 8). There are only a few minor differences: (i) slightly smaller and stouter (length:width ratio 7.6:1 on average), likely because broad specimens with numerous food inclusions are more frequent; (ii) extrusomes slightly longer, viz., $2.5\ \mu\text{m} \times 0.8\ \mu\text{m}$ (Figure 9f); (iii) dikinetids of dorsal brush rather widely spaced not only in row 3 but also in row 1; (iv) dorsal bristles generally shorter, that is, only about $2\ \mu\text{m}$ long *in vivo*.

The South African specimens were identified *in vivo*, where they showed the same features as those of the other two populations. The extrusomes are even more conspicuous because they are slightly thicker ($2\ \mu\text{m} \times 1\ \mu\text{m}$; Figure 9g). The cortical granules are also minute, but more refractive and thus distinct *in vivo*. The dorsal brush is as in the American specimens.

Occurrence and ecology: As yet found at type location (Pine forest soil from Austria, where it was moderately abundant), in the United States of America (rare in a grassland soil of Arizona between the towns of San Lucas and Caolinga; pH 6.2), and in South Africa (rare in soil from the bank of the Skeleton River in the Botanical Gardens of Kirstenbosch near Cape Town; pH 6.7). These records indicate that *P. fusioplites* is a cosmopolitan, possibly preferring acidic or circumneutral conditions. It is well adapted to soil life by the slender body.

Generic assignment and comparison with related species: The populations described above can be considered as a *Spathidium* with unusually widely spaced circumoral dikinetids or as a *Protospathidium* with unusually small circumoral kinetofragments. We prefer the later interpretation because (i) the body is as slender and the oral bulge as small as in some other *Protospathidium* species; and (ii) *Spathidium* and *Arcuospathidium* species have closely spaced circumoral dikinetids (usually \geq five between two kineties each), while *Protospathidium* circumoral kinetofragments are usually composed of \leq five dikinetids. Thus, our population is likely a *Protospathidium* with a reduced number of dikinetids composing the individual circumoral kinetofragments.

Five *Protospathidium* species have been described (Foissner 1998; Foissner et al. 2002). *In vivo*, *P. fusioplites* differs from the congeners by the fusiform (vs. rod-shaped) extrusomes. In protargol preparations, *P. fusioplites* differs from the other species by its minute circumoral kinetofragments (composed of one to two vs.

three to six dikinetids). Other features, like body and nucleus shape are also different, but not to an extent that would make identification easy.

At first glance, the populations also strongly resemble *Sikorops* in the arrangement of the circumoral ciliature and the fusiform extrusomes (Foissner 1999a; Foissner et al. 2002). However, *Sikorops* has nematodesmata (oral basket rods) originating from both the circumoral dikinetids and the anterior somatic monokinetids, and thus belongs to the family Acropisthiidae (Foissner et al. 2002).

***Erimophrya sylvatica* nov. spec. (Figures 11a–f, 13a, d; Table 9)**

Diagnosis: Size about $95\ \mu\text{m} \times 15\ \mu\text{m}$ *in vivo*; slenderly pisciform and slightly twisted about main body axis. On average 2 almost abutting, very elongate ellipsoidal (4.8:1) macronuclear nodules, 14 adoral membranelles, 19 cirri in right and 17 in left marginal row, 2 postoral cirri, 2 transverse cirri, 2 caudal cirri, and 3 dorsal kineties with kinety 1 composed of 3 bristles.

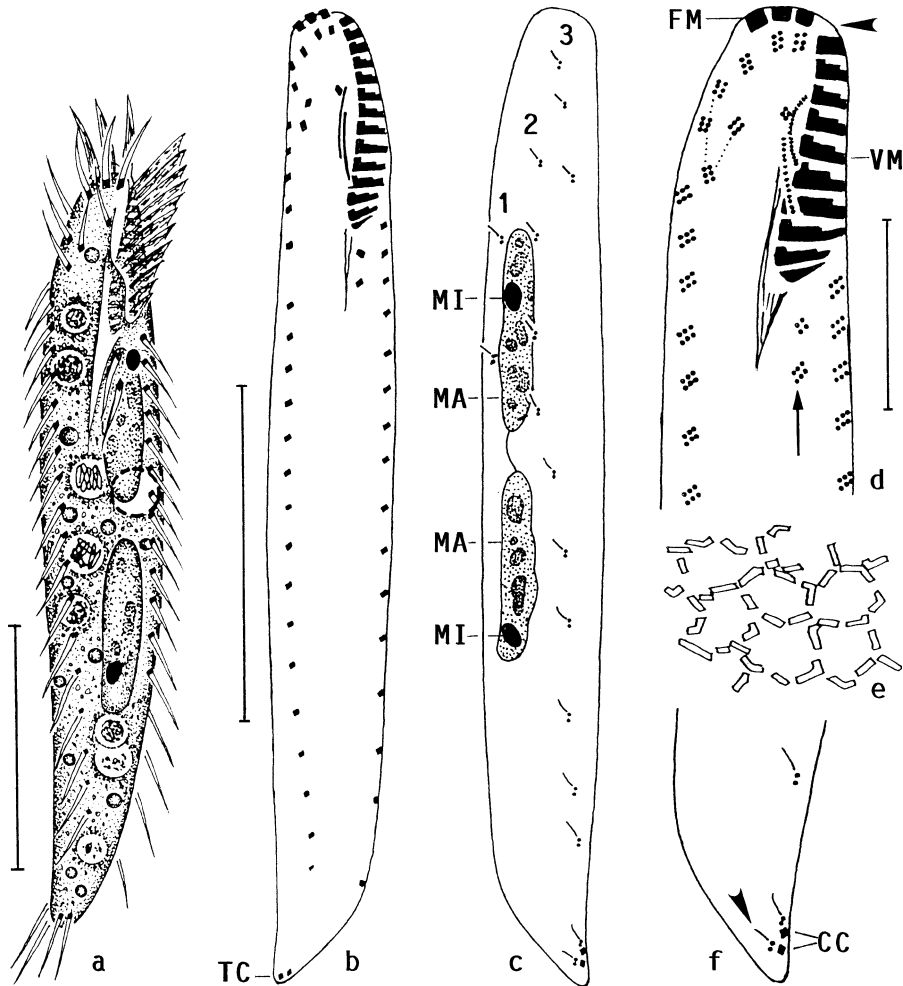
Type location: *Pinus nigra* forest soil in the Stampftal near Vienna, Austria, E16°02' N47°53'.

Type material: One holotype and two paratype slides with protargol-impregnated specimens (Foissner's method) have been deposited in the Biology Center of the Oberösterreichische Landesmuseum in Linz (LI), Austria. The slides contain many specimens, with relevant cells marked by black ink circles on the cover glass.

Etymology: The Latin adjective *sylvatica* (belonging to forests) refers to the habitat the species was discovered.

Description: Size $80\text{--}115\ \mu\text{m} \times 10\text{--}20\ \mu\text{m}$ *in vivo*, length:width ratio about 7:1 on average both *in vivo* and protargol preparations (Table 9); acontractile. Shape moderately variable, usually slenderly pisciform or lanceolate with narrowly rounded anterior end and curved, bluntly pointed posterior; occasionally almost parallel-sided; invariably slightly twisted about main body axis and up to 2:1 flattened dorsoventrally (Figures 11a, b, 13a). Macronuclear nodules in middle body third left of midline, usually close together and connected by a fine thread, ellipsoidal (2:1) to cylindroidal (7:1), on average very elongate ellipsoidal (4.8:1; Table 9); nucleoli rather large, globular to ellipsoidal. Two ellipsoidal, inconspicuous micronuclei, one attached to each macronuclear nodule in variable position. Contractile vacuole above mid-body at left cell margin, surrounded by small vacuoles during diastole. Cortex very flexible, yellowish due to a reticular pattern of $0.5\text{--}2\ \mu\text{m}$ sized crystals conspicuously sparkling under interference contrast illumination (Figures 11e, 13a, d). Cytoplasm colourless, contains some lipid droplets up to $3\ \mu\text{m}$ across and crystals like those found in the cortex. Feeds on bacteria digested in vacuoles about $5\ \mu\text{m}$ across. Glides rapidly on microscope slide and soil particles showing great flexibility.

Cirral pattern very constant, number of cirri of usual variability (Figures 11b, d; Table 9). Cirri about $8\ \mu\text{m}$ long *in vivo*, most composed of only six cilia, in posterior third of even only four cilia. Marginal cirral rows extend slightly obliquely backwards due to body torsion, both distinctly shortened posteriorly; right row commences far off anterior body end at level of last frontoventral cirrus, left



Figures 11a-f. *Erimophrya sylvatica* from life (a, e) and after protargol impregnation (b-d, f). **a**: Ventral view of a representative specimen slightly twisted about main body axis. **b, c, f**: Infraciliature of ventral and dorsal side and nuclear apparatus of holotype specimen. Arrowhead marks posterior bristle of dorsal kinety 1 close to the posterior caudal cirrus. Note the very slender macronuclear nodules, a specific feature of this species. **d**: Infraciliature of oral region at high magnification. Frontoventral cirri connected by dotted line. Note the two postoral cirri (arrow) and the gap (arrowhead) between frontal and ventral adoral membranelles. **e**: Surface view showing cortical crystal pattern in mid-body (cp. Figures 13a, d). CC – caudal cirri, FM – frontal adoral membranelles, MA – macronuclear nodules, MI – micronuclei, TC – transverse cirri, VM – ventral adoral membranelles, 1, 2, 3 – dorsal bristle rows. Scale bars 30 μm (a-c) and 10 μm (d).

extends onto dorsolateral surface posteriorly. Frontal cirri of same size as other cirri. Buccal cirrus right of anterior end of paroral membrane, consists of only four cilia. Four frontoventral cirri, uppermost cirrus in, or almost in line with frontal cirri, distance slightly increased between penultimate and last frontoventral cirrus,

gap occupied by frontoventral cirrus III/2 slightly displaced leftwards. One to two, usually two postoral cirri distinctly left of midline and one after the other. Transverse and caudal cirri difficult to observe because very near to narrowed posterior body end: transverse cirri side by side; caudal cirri one after the other at right margin of dorsal side, each accompanied by a dorsal bristle, producing highly characteristic pattern similar to that found in *E. arenicola* (Figures 11a–c, f; Table 9).

Dorsal bristles 2.5–3 μm long *in vivo*, arranged in three rows (Figures 11c, f; Table 9): row 1 composed of only three bristles on average, that is, two in anterior half and, separated by a wide distance, one very near to the corresponding caudal cirrus; row 2 slightly shortened anteriorly and somewhat sigmoidal, last bristle very near to the corresponding caudal cirrus; row 3 at right margin of oral body portion, composed of only three bristles on average.

Adoral zone occupies 18–25%, on average 20% of body length, extends along left margin of cell, composed of an average of 14 membranelles, of which the frontal three are separated by a minute gap, as in congeners. Buccal cavity narrow and flat; buccal lip angularly projecting covering posterior third of adoral zone. Both undulating membranes slightly curved and side by side, endoral about 6 μm long, paroral 8 μm on average commencing approximately 3 μm in front of endoral at level of buccal cirrus; exact structure (dikinetid?) of membranes not recognizable. Pharyngeal fibers inconspicuous *in vivo* and protargol preparations, of ordinary length and structure (Figures 11b, d; Table 9).

Occurrence and ecology: To date found only at the two Pine forest sites (Table 2), indicating some preference for this type of habitat. *Erimophrya sylvatica* was numerous already 2 days after rewetting the sample, suggesting an r-selected life strategy, while most hypotrichs are more k- than r-selected (Foissner 1987a). A preference for dry, ephemeral habitats is emphasized by *E. quadrinucleata*, which occurs at the same site (see below), and the African congeners, which were discovered in the Namib Desert (Foissner et al. 2002).

Comparison with related species: The genus *Erimophrya* was recently established by Foissner et al. (2002) for two species discovered in the Namib Desert, Southwest Africa, viz., *Erimophrya glatzeli* and *E. arenicola*. Thus, it was a great surprise to discover two further species in Austrian Pine forest soils. Although the four species look quite similar, especially *in vivo* and at superficial observation, they can be easily distinguished in protargol preparations, mainly by morphometric features, such as the number of macronuclear nodules and dorsal kineties.

Erimophrya sylvatica is most similar to *E. arenicola*, differing, however, by two main features, viz., the number of postoral (2 vs. 1) and transverse (2 vs. 1) cirri. Minor differences are the more slender macronuclear nodules (4.8:1 vs. 3.6:1) and the cortical crystal reticulum (present vs. absent). Differences to *E. glatzeli* and *E. quadrinucleata* are more conspicuous. From the former, *E. sylvatica* differs by the more slender body (7:1 vs. 4.8:1), the slender (4.8:1 vs. 2.6:1) and narrowly spaced (3.3 μm vs. 14.2 μm) macronuclear nodules, and the number of adoral membranelles (14 vs. 20), dorsal kineties (3 vs. 4), and bristles in dorsal kinety 1 (3 vs. 9). *Erimophrya quadrinucleata* has four macronuclear nodules (vs. two in all other species) and three postoral cirri (vs. one or two in all other species).

Table 9. Morphometric data on *Erimophrya sylvatica* (upper line) and *Erimophrya quadrinucleata* (lower line).

Characteristics ^a	\bar{x}	<i>M</i>	SD	SE	CV	Min	Max	<i>n</i>
Body, length	83.0	83.0	8.4	1.8	10.1	72.0	101.0	21
	92.7	96.0	11.1	2.6	12.0	68.0	110.0	19
Body, width	11.7	12.0	1.0	0.2	8.6	10.0	14.0	21
	13.0	13.0	2.4	0.5	18.3	9.0	17.0	19
Body length:width, ratio	7.1	7.4	0.9	0.2	12.0	5.2	8.7	21
	7.4	7.1	1.7	0.4	22.4	4.7	10.3	19
Anterior body end to proximal end of adoral zone, distance	17.1	17.0	1.2	0.3	7.0	15.0	20.0	21
	20.5	21.0	1.9	0.4	9.3	16.0	23.0	19
Body length:length of adoral zone, ratio	4.9	4.8	0.5	0.1	9.4	4.0	5.6	21
	4.6	4.4	0.6	0.1	13.7	3.4	5.6	19
Anterior body end to paroral membrane, distance	5.6	5.0	1.0	0.2	17.3	4.0	8.0	21
	7.5	8.0	1.2	0.3	16.2	5.0	9.0	19
Paroral membrane, length	5.6	6.0	–	–	–	5.0	6.0	21
	5.5	5.0	0.9	0.2	16.4	4.0	7.0	19
Anterior body end to endoral membrane, distance	8.4	8.0	0.9	0.2	11.2	7.0	11.0	20
	9.6	10.0	1.2	0.3	12.6	7.0	11.0	19
Endoral membrane, length	6.2	6.0	0.9	0.2	15.4	5.0	9.0	20
	6.6	7.0	0.2	0.2	13.7	5.0	8.0	19
Anterior body end to first frontoventral cirrus, distance	4.8	5.0	0.6	0.1	12.5	4.0	6.0	21
	5.2	5.0	0.5	0.1	9.7	5.0	7.0	19
Anterior body end to last frontoventral cirrus, distance	9.8	10.0	0.9	0.2	9.1	8.0	11.0	21
	10.7	11.0	0.8	0.2	7.0	10.0	12.0	19
Anterior body end to buccal cirrus, distance	6.0	6.0	0.6	0.1	10.5	5.0	7.0	21
	8.0	8.0	1.2	0.3	14.4	6.0	10.0	19
Anterior body end to right marginal row, distance	9.7	10.0	1.9	0.4	19.0	5.0	12.0	21
	9.7	10.0	1.6	0.4	16.7	7.0	13.0	19
Anterior body end to first postoral cirrus, distance	19.3	19.0	1.5	0.3	7.7	16.0	23.0	21
	21.5	22.0	1.8	0.4	8.6	18.0	24.0	19
Anterior body end to last postoral cirrus, distance	23.0	23.0	2.2	0.5	9.7	19.0	30.0	21
	27.6	28.0	1.8	0.4	6.5	24.0	30.0	19
Anterior body end to dorsal kinety 1, distance	18.1	17.0	2.2	0.5	13.4	15.0	23.0	21
	23.0	22.0	3.9	0.9	17.0	16.0	31.0	19
Anterior body end to dorsal kinety 2, distance	15.0	15.0	2.3	0.5	15.5	11.0	21.0	21
	18.7	19.0	3.1	0.7	16.5	13.0	24.0	19
Anterior body end to dorsal kinety 3, distance	5.3	5.0	0.7	0.1	12.3	4.0	6.0	21
	5.1	5.0	0.8	0.2	15.4	4.0	7.0	19
Anterior body end to first macronuclear nodule, distance	18.8	18.0	2.4	0.5	12.8	16.0	26.0	21
	20.4	20.0	2.4	0.5	11.6	15.0	24.0	19
Nuclear figure, length	35.7	34.0	5.9	1.3	16.4	28.0	47.0	21
	46.6	46.0	6.6	1.5	14.3	37.0	61.0	19
Macronuclear nodules, distance in between (between central nodules in <i>E. quadrinucleata</i>)	3.3	3.0	1.9	0.4	57.1	1.0	9.0	21
	0.8	0.0	–	–	–	0.0	2.0	19
Anterior macronuclear nodule, length	16.9	17.0	3.1	0.7	18.4	10.0	22.0	21
	12.3	12.0	2.7	0.6	22.1	9.0	20.0	19
Anterior macronuclear nodule, width	3.5	3.0	0.8	0.2	21.3	3.0	5.0	21
	4.0	4.0	0.6	0.1	14.4	3.0	5.0	19
Macronuclear nodules, number	2.0	2.0	0.0	0.0	0.0	2.0	2.0	21
	4.1	4.0	0.5	0.1	11.2	3.0	5.0	19

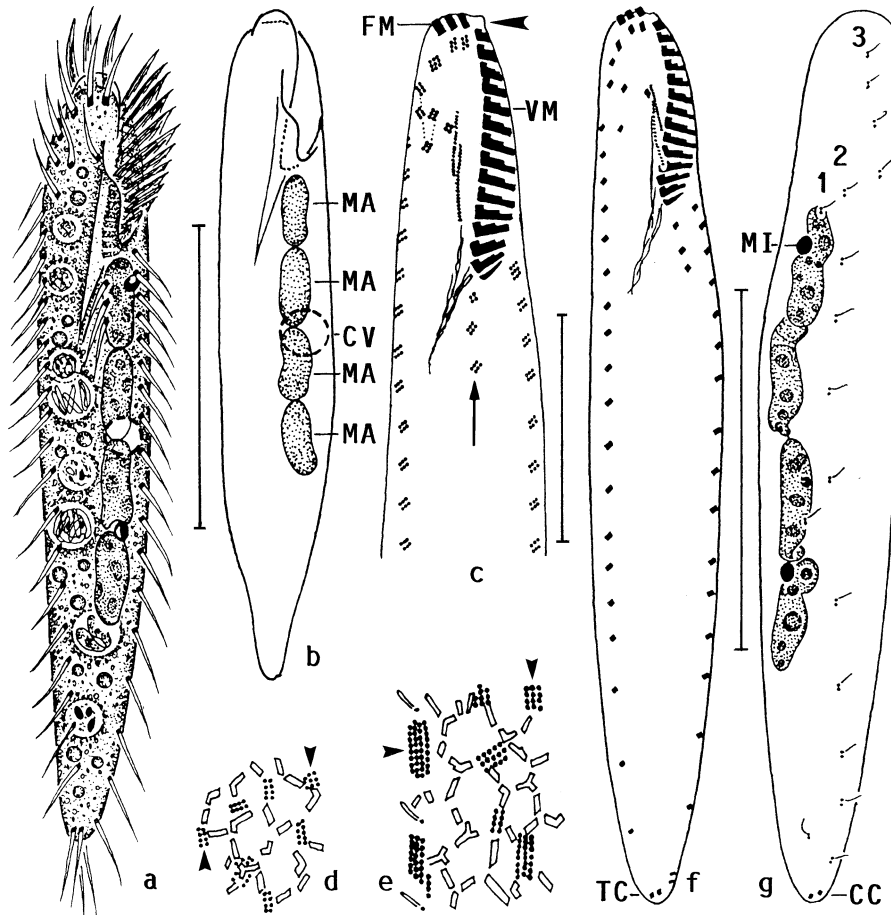
Table 9. (continued)

Characteristics ^a	\bar{x}	<i>M</i>	SD	SE	CV	Min	Max	<i>n</i>
Anterior micronucleus, length	2.7	2.5	0.9	0.2	31.8	2.0	6.0	21
	2.5	2.5	0.4	0.1	16.7	2.0	3.2	19
Anterior micronucleus, width	1.7	1.5	0.3	0.1	14.7	1.5	2.0	21
	1.8	1.9	0.3	0.1	13.6	1.5	2.5	19
Micronuclei, number	2.0	2.0	–	–	–	1.0	2.0	21
	2.0	2.0	–	–	–	1.0	2.0	19
Posterior body end to posteriormost transverse cirrus, distance	≤1 μm							
	≤1 μm							
Posterior body end to right marginal row, distance	8.8	9.0	2.8	0.6	31.4	4.0	13.0	21
	6.0	5.0	2.8	0.6	46.1	3.0	12.0	19
Adoral membranelles, number	14.2	14.0	0.9	0.2	6.5	12.0	16.0	21
	15.8	16.0	1.4	0.3	8.6	12.0	17.0	19
Frontal cirri, number	3.0	3.0	0.0	0.0	0.0	3.0	3.0	21
	3.0	3.0	0.0	0.0	0.0	3.0	3.0	19
Frontoventral cirri, number	4.0	4.0	0.0	0.0	0.0	4.0	4.0	21
	4.0	4.0	0.0	0.0	0.0	4.0	4.0	19
Buccal cirri, number	1.0	1.0	0.0	0.0	0.0	1.0	1.0	21
	1.0	1.0	0.0	0.0	0.0	1.0	1.0	19
Postoral cirri, number	1.7	2.0	–	–	–	1.0	2.0	21
	2.8	3.0	–	–	–	1.0	3.0	19
Transverse cirri, number	2.0	2.0	0.0	0.0	0.0	2.0	2.0	21
(rarely only 1 in <i>E. quadrinucleata</i>)	2.0	2.0	0.0	0.0	0.0	2.0	2.0	19
Right marginal cirri, number	19.0	19.0	1.6	0.4	8.6	16.0	23.0	21
	21.3	21.0	2.1	0.5	10.0	16.0	25.0	19
Left marginal cirri, number	16.6	17.0	1.2	0.3	7.0	13.0	19.0	21
	17.7	18.0	1.4	0.3	7.7	16.0	20.0	19
Caudal cirri, number	2.0	2.0	0.0	0.0	0.0	2.0	2.0	21
	2.0	2.0	0.0	0.0	0.0	2.0	2.0	19
Dorsal kineties, number	3.0	3.0	0.0	0.0	0.0	3.0	3.0	21
	3.0	3.0	0.0	0.0	0.0	3.0	3.0	19
Dorsal kinety 1, number of bristles	3.0	3.0	–	–	–	2.0	4.0	21
	2.5	2.0	1.0	0.2	39.0	1.0	5.0	19
Dorsal kinety 2, number of bristles	9.5	9.0	0.9	0.2	9.2	8.0	11.0	21
	9.4	9.0	1.0	0.2	10.2	8.0	12.0	19
Dorsal kinety 3, number of bristles	3.0	3.0	–	–	–	3.0	4.0	21
	3.6	4.0	0.8	0.2	21.5	2.0	5.0	19

^aData based on mounted, protargol-impregnated (Foissner 1991, protocol A), and randomly selected specimens from a non-flooded Petri dish culture. Measurements in μm. CV – coefficient of variation in %, *M* – median, Max – maximum, Min – minimum, *n* – number of individuals investigated, SD – standard deviation, SE – standard error of arithmetic mean, \bar{x} – arithmetic mean.

***Erimophrya quadrinucleata* nov. spec. (Figures 12a–g, 13b, e; Table 9)**

Diagnosis: Size about 105 μm × 15 μm *in vivo*; slenderly oblongate and slightly twisted about main body axis. On average 4 elongate ellipsoidal macronuclear nodules, 16 adoral membranelles, 21 cirri in right and 18 in left marginal row, 3

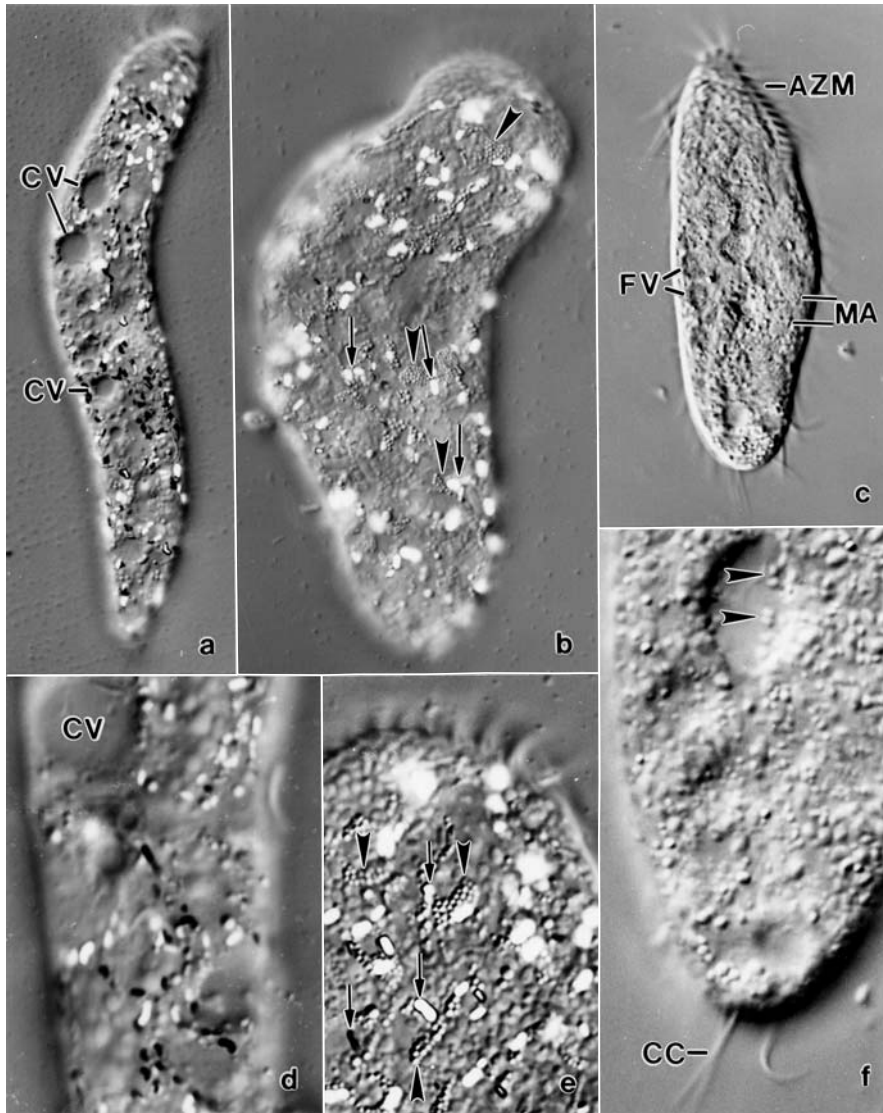


Figures 12a–g. *Erimophrya quadrinucleata* from life (a, b, d, e) and after protargol impregnation (c, f, g). **a**: Ventral view of a representative specimen slightly twisted about main body axis. **b**: Outline of a broad specimen with rather abruptly narrowed posterior body portion. Note the four macronuclear nodules, that is, the main feature of this species. **c**: Infraciliature of oral region at high magnification. Frontoventral cirri connected by dotted line. Note the three postoral cirri (arrow) and the gap (arrowhead) between frontal and ventral adoral membranelles. **d, e**: Surface views showing cortical crystal and plaque (arrowheads) pattern in two specimens. **f, g**: Infraciliature of ventral and dorsal side and nuclear apparatus of holotype specimen. CC – caudal cirri, CV – contractile vacuole, FM – frontal adoral membranelles, MA – macronuclear nodules, MI – micronucleus, TC – transverse cirri, VM – ventral adoral membranelles, 1, 2, 3 – dorsal bristle rows. Scale bars 40 μm (a, f, g) and 20 μm (c).

postoral cirri, 2 transverse cirri, 2 caudal cirri, and 3 dorsal kineties with kinety 1 composed of 2 bristles.

Type location: *Pinus nigra* forest soil in the Stampftal near Vienna, Austria, E16°02'N47°53'.

Type material: One holotype and two paratype slides with protargol-impregnated specimens (Foissner's method) have been deposited in the Biology Center of the



Figures 13a-f. Cortical structures of hypotrichs in vivo. **a, d:** *Erimophrya sylvatica*, dorsal view showing the reticular crystal pattern with sparkling individual crystals (dark or bright depending on light refraction). **b, e:** *E. quadrimucleata*, dorsal views of a squashed specimen showing crystals (arrows) associated with conspicuous plaques of minute granules (arrowheads). **c, f:** *Paragonostomum simplex*, ventral overview and dorsal detail with cortical granules recognizable above the contractile vacuole (arrowheads). AZM – adoral zone, CC – caudal cirri, CV – contractile vacuole, FV – food vacuoles, MA – macronuclear nodules.

Oberösterreichische Landesmuseum in Linz (LI), Austria. The slides contain many specimens, with relevant cells marked by black ink circles on the cover glass.

Etymology: Composite of the Latin numeral *quadri* (four) and the Latin adjective *nucleatus* (with a nucleus), referring to the main feature of the species, viz., the four macronuclear nodules.

Description, Occurrence and ecology, and Comparison with related species: *Erimophrya quadrinucleata* is highly similar to *E. sylvatica* described above, and to the congeners described in Foissner et al. (2002), except of two unique features, viz., the four macronuclear nodules (two in the other species) and the three postoral cirri (one or two in the congeners). Thus, the figures, the morphometric analysis (Table 9), and the following details should suffice: (i) The shape is occasionally distinctly oblongate due to the rather abruptly narrowed posterior body region (Figure 12b); (ii) The rather distinctly wrinkled, abutting macronuclear nodules appear as a rod *in vivo* (Figures 12a, b); (iii) Like in *E. sylvatica*, the cortex contains a crystalline reticulum supplemented by sometimes conspicuous plaques composed of 0.3 µm sized granules, which are possibly precursors of the crystals (Figures 12d, e, 13b, e); (iv) The postoral cirri are arranged one after the other, and thus form a short row (Figures 12c, f); (v) There are no dorsal bristles near to the caudal cirri, which are arranged side by side (Figure 12g); (vi) The species occurred together with *E. sylvatica*, but was less numerous (Table 2).

***Paragonostomum simplex* nov. spec. (Figures 13c, f, 14a–i; Table 10)**

Diagnosis: Size about 85 µm × 25 µm *in vivo*; elongate to indistinctly sigmoidal with narrowly rounded posterior end. On average 10 macronuclear nodules in C-shaped pattern left of midline, 21 right marginal, 16 left marginal, 4 frontoterminal, 8 frontoventral, and 3 caudal cirri; 1 buccal cirrus far above paroral membrane composed of an average of 9 kinetids in continuous row. Adoral zone of membranelles occupies about 37% of body length, composed of 20 membranelles on average.

Type location: *Pinus nigra* forest soil in the Stampftal near Vienna, Austria, E16°02' N47°53'.

Type material: One holotype and four paratype slides with protargol-impregnated specimens (Foissner's method) have been deposited in the Biology Center of the Oberösterreichische Landesmuseum in Linz (LI), Austria. The slides contain many specimens, with relevant cells marked by black ink circles on the cover glass.

Etymology: The Latin adjective *simplex* (simple) refers to the fact that generic classification is easier than in the congeners, where the lack of transverse cirri is difficult to prove due to the tailed posterior end.

Description: This species was studied in three populations, viz., from type location, from a site near type location (Merckenstein), and from a beech forest soil of a suburb of the town of Salzburg. The populations match very well, both *in vivo* and preparations (Table 10), showing that *P. simplex* is a well-defined species. The specimens from Merckenstein and Salzburg have more or less distinct cortical

Table 10. Morphometric data on *Paragonostomum simplex* from type location (upper line) and a beech forest soil from Salzburg (lower line; data kindly supplied by Dr. E. Aeschl).

Characteristics ^a	\bar{x}	<i>M</i>	SD	SE	CV	Min	Max	<i>n</i>
Body, length	76.9	78.0	9.7	2.1	12.6	62.0	92.0	21
	79.9	82.0	8.2	2.1	10.3	60.0	93.0	15
Body, width	25.5	25.0	3.6	0.8	14.2	18.0	32.0	21
	20.8	21.0	1.7	0.4	8.1	18.0	24.0	15
Body length:width, ratio	3.1	3.0	0.5	0.1	17.2	2.3	4.1	21
	3.9	3.9	0.5	0.1	11.9	3.1	4.7	15
Anterior body end to proximal end of adoral zone, distance	28.2	28.0	2.0	0.4	7.1	24.0	32.0	21
	26.3	26.0	2.6	0.7	10.0	23.0	33.0	15
Body length:length of adoral zone, ratio	2.7	2.6	0.4	0.1	14.4	2.2	3.8	21
	3.1	3.2	0.5	0.1	14.3	2.2	3.8	15
Anterior end to last frontoventral cirrus, distance	24.6	25.0	3.8	0.8	15.4	17.0	31.0	21
	23.0	22.0	2.3	0.6	9.9	19.0	27.0	15
Anterior end to buccal cirrus, distance	13.4	13.0	0.8	0.2	6.1	11.0	14.0	21
	11.6	12.0	1.6	0.4	13.8	8.0	14.0	15
Anterior end to right marginal row, distance	3.5	3.0	0.8	0.2	23.2	2.0	6.0	21
	2.9	2.5	1.1	0.3	39.8	1.5	5.0	15
Anterior end to posterior end of right marginal row, distance	74.2	75.0	9.7	2.1	13.1	60.0	90.0	21
	78.0	80.0	8.3	2.1	10.6	58.0	92.0	15
Nuclear figure, length	51.9	51.0	6.0	1.3	11.5	41.0	61.0	21
	51.5	52.0	5.3	1.4	10.2	43.0	59.0	15
Antermost macronuclear nodule, length	6.5	7.0	1.5	0.3	23.7	3.0	10.0	21
	5.0	5.0	0.7	0.2	14.5	4.0	6.0	15
Antermost macronuclear nodule, width	4.4	4.0	0.8	0.2	16.9	3.0	6.0	21
	3.8	4.0	0.7	0.2	18.9	3.0	5.0	15
Macronuclear nodules, number	10.4	11.0	2.5	0.6	24.2	8.0	15.0	21
	10.7	11.0	1.4	0.4	13.4	9.0	14.0	15
Antermost micronucleus, length	2.2	2.0	0.4	0.1	16.4	1.8	3.0	21
	2.0	2.0	–	–	–	1.5	2.5	15
Antermost micronucleus, width	1.9	2.0	0.2	0.1	10.6	1.3	2.2	21
	1.8	2.0	–	–	–	1.5	2.0	15
Micronuclei, number	2.3	2.0	0.9	0.2	39.1	1.0	5.0	21
	2.3	2.0	1.2	0.3	53.8	0.0	4.0	15
Adoral membranelles, number	19.7	20.0	1.0	0.2	4.9	18.0	22.0	21
	19.5	19.0	1.6	0.4	8.4	17.0	23.0	15
Paroral membrane, length	5.2	5.0	0.8	0.2	15.7	4.0	6.0	21
	4.7	5.0	0.7	0.2	14.9	4.0	6.0	15
Paroral kinetids, number	8.4	9.0	1.3	0.3	15.3	6.0	10.0	21
	–	–	–	–	–	–	–	–
Frontal cirri, number	3.0	3.0	0.0	0.0	0.0	3.0	3.0	21
	3.0	3.0	0.0	0.0	0.0	3.0	3.0	15
Frontoterminal cirri, number	3.8	4.0	0.5	0.1	14.3	3.0	5.0	21
	4.1	4.0	1.0	0.3	24.0	3.0	6.0	15
Frontoventral cirri, number	8.3	8.0	1.6	0.4	19.1	6.0	13.0	21
	7.7	8.0	1.6	0.4	21.1	5.0	10.0	15
Buccal cirri, number	1.0	1.0	0.0	0.0	0.0	1.0	1.0	21
	1.0	1.0	0.0	0.0	0.0	1.0	1.0	15
Right marginal cirri, number	21.2	21.0	3.0	0.7	14.1	15.0	29.0	21
	22.4	22.0	2.4	0.6	10.8	19.0	28.0	15

Table 10. (continued)

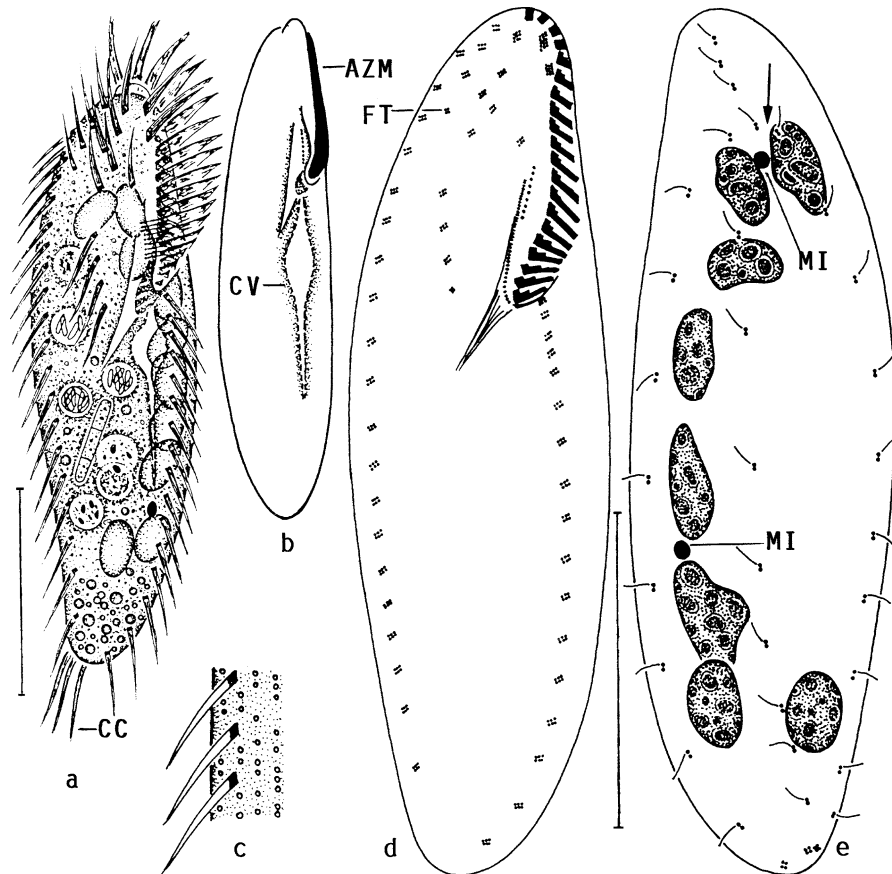
Characteristics ^a	\bar{x}	<i>M</i>	SD	SE	CV	Min	Max	<i>n</i>
Left marginal cirri, number	16.4	16.0	2.7	0.6	16.5	12.0	23.0	21
	16.7	17.0	1.2	0.3	7.0	15.0	19.0	15
Caudal cirri, number	2.9	3.0	–	–	–	2.0	3.0	21
	3.0	3.0	0.0	0.0	0.0	3.0	3.0	15
Dorsal kineties, number	3.1	3.0	–	–	–	3.0	4.0	21
	3.0	3.0	0.0	0.0	0.0	3.0	3.0	15
Kinetids in middle dorsal kinety, number	9.6	9.0	1.5	0.3	15.2	7.0	13.0	21
	9.3	9.0	1.3	0.3	14.4	7.0	11.0	15

^aData based on mounted, protargol-impregnated (Foissner 1991, protocol A), and randomly selected specimens from non-flooded Petri dish cultures. Measurements in μm . CV – coefficient of variation in %, *M* – median, Max – maximum, Min – minimum, *n* – number of individuals investigated, SD – standard deviation, SE – standard error of arithmetic mean, \bar{x} – arithmetic mean.

granules, likely overlooked in the type population. The diagnosis contains only data from the type population.

Size 70–110 $\mu\text{m} \times 20$ –30 μm *in vivo*, usually near 90 $\mu\text{m} \times 25 \mu\text{m}$, length:width ratio about 3.3–5:1 *in vivo*, while 3:1 in protargol preparations, where specimens tend to become inflated in mid-body. Slender with both ends narrowly rounded, never tailed, usually slightly fusiform and sigmoidal, dorsal margin often more distinctly convex than ventral; up to 2:1 flattened laterally; non-contractile (Figures 13c, 14a, b, d; Table 10). Macronuclear nodules in roughly C-shaped pattern along left body margin; individual nodules separated by minute gaps, occasionally out of series, globular to ellipsoidal, on average 7 $\mu\text{m} \times 4 \mu\text{m}$ both *in vivo* and in protargol preparations; contain many small and large nucleoli. Usually a globular micronucleus each near ends of macronuclear series (Figures 13c, 14a, e; Table 10). Contractile vacuole in mid-body region left of midline, with two long, thin collecting canals. Cortex very flexible, does not contain special granules in specimens from type location, while loosely to densely arranged, colourless, minute ($\leq 0.5 \mu\text{m} \times 0.25 \mu\text{m}$) cortical granules, which elongate to 3 μm long, pink rods when methyl green-pyronin is added, occur in the Merckenstein and Salzburg populations (Figures 13f, 14c). Cytoplasm colourless, densely granulated, usually packed with small food vacuoles about 5–10 μm across and up to 4 μm sized lipid droplets mainly in rear end. Feeds preferably on bacteria, rarely some fungal spores and/or green algae are recognizable in the food vacuoles up to 6 μm across. Glides moderately rapidly on microscope slide and soil particles showing great flexibility.

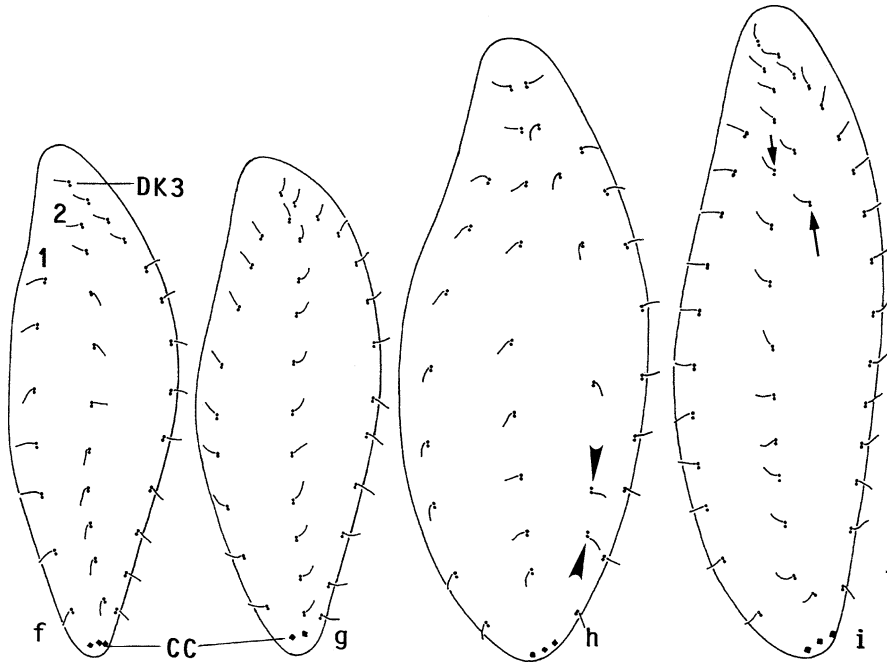
Cirral pattern stable, number of frontoventral cirri rather variable; all cirri about 10 μm long *in vivo* and usually composed of six cilia in 2 min rows, except for the slightly enlarged, 13 μm long frontal cirri (Figures 14a, d; Table 10). Marginal cirri arranged in two rows, left row extends to body midline posteriorly, right inconspicuously shortened at both ends extending slightly obliquely to near dorsal side anteriorly. On average 16 cirri in frontal (oral) area: 3 frontal, 1 buccal, 4 fronto-terminal, and 8 frontoventral cirri. Frontal cirri slightly enlarged, especially cirrus 1 and/or 2 close to the adoral zone and frequently somewhat disorganized, that is,



Figures 14a–e. *Paragonostomum simplex* from life (a–c) and after protargol impregnation (d, e). **a:** Ventral view of a representative, slightly sigmoidal specimen. **b:** Outline and some main organelles of a slender specimen. **c:** Surface view showing cortical granulation of a specimen from Merckenstein. **d, e:** Infaciliature of ventral and dorsal side and nuclear apparatus of holotype specimen. Note lack of transverse cirri (main genus character) and break in dorsal bristle row 3 (arrow). AZM – adoral zone of membranelles, CC – caudal cirri, CV – contractile vacuole, FT – frontoterminal cirri, MI – micronuclei. Scale bars 30 μm .

lacks one to three cilia in variable position; buccal cirrus invariably above paroral membrane; frontoterminal cirri in short, but distinct row near dorsolateral margin of right anterior quadrant of cell; frontoventral cirri in two groups, viz., an anterior cluster of two to three oblique pairs and a posterior group forming a short row extending in body midline to, rarely slightly above level of buccal vertex; lack of transverse cirri checked in over 100 specimens.

Dorsal bristles about 3 μm long *in vivo*, basically arranged in three rows, frequently, however, with rather conspicuous irregularities, such as anterior kinetids of row 3 slightly out of line or a more or less complete fourth row, with kinetids



Figures 14f–i. *Paragonostomum simplex*, variability of dorsal ciliary pattern after protargol impregnation. **f**: A typical specimen with each three dorsal bristle rows and caudal cirri. **g**: A specimen with ordinary dorsal bristle rows, but only two caudal cirri. **h**: A specimen with a fourth bristle row between rows 2 and 3. Arrowheads mark kinetids with reversed polarity. **i**: A specimen with break in bristle row 2 (arrows). CC – caudal cirri, DK1–3 – dorsal kineties. Drawn to scale, bar 30 μ m.

partially turned upside down, between rows 2 and 3 (Figures 14e–i; Table 10). Dorsal bristle rows slightly shortened posteriorly, while distinctly shortened anteriorly from left to right; row 3 anteriorly only slightly shortened and curved to cell's midline. Caudal cirri at posterior body end right of midline.

Oral apparatus in *Gonostomum* pattern (Berger 1999). Adoral zone occupies only 37% (50% in most *Gonostomum* species) of body length on average, commences in mid of anterior body end and extends along left body margin, performing abrupt right bend and slight clockwise rotation to plunge into buccal cavity near left margin of second body third; composed of an average of 20 membranelles with bases up to 4 μ m wide *in vivo*. Buccal cavity very narrow and flat, right half and proximal portion of adoral zone covered by curved, hyaline buccal lip bearing paroral membrane composed of an average of nine widely and equidistantly spaced, *in vivo* 6 μ m long cilia. Endoral membrane at right margin of buccal cavity, conspicuous because more than twice as long as paroral and composed of very narrowly spaced cilia. Pharyngeal fibers clearly recognizable *in vivo* and after protargol impregnation, extend obliquely to body midline and backwards (Figures 13c, 14a, b, d; Table 10).

Occurrence and ecology: As yet found in the two Pine forest soils investigated in this study (Stampftal, Merckenstein) and in soil from a beech forest in Salzburg (Table 2). *Paragonostomum simplex* developed soon after rewetting the sample, suggesting that it is more r- than k-selected (Foissner 1987).

Generic allocation and comparison with related species: Foissner et al. (2002) established *Paragonostomum* for *Gonostomum*-like hypotrachs lacking transverse cirri, and emphasized that *Paragonostomum* is the first oxytrichid genus without such cirri (for a review, see Berger 1999). However, Foissner et al. (2002) could not prove unequivocally the lack of transverse cirri because they found only tailed species, where the cirral pattern was difficult to analyze. *Paragonostomum simplex*, which is tailless, shows the existence of oxytrichids without transverse cirri. This is confirmed by some middle and late dividers contained in the slides. Thus, the genus is now well established.

Of the four species described by Foissner et al. (2002), all from soil, only *P. multinucleatum* has, like *P. simplex*, more than the two macronuclear nodules common in the group. *Paragonostomum simplex* differs from *P. multinucleatum* by body shape (posterior end rounded vs. tail-like narrowed), the much higher number of frontoventral cirri (8 vs. 3), the location of the buccal cirrus (far above vs. at anterior end of paroral membrane), and the structure of the paroral membrane (continuous vs. bipartite). These are conspicuous differences showing that *P. simplex* is a well-defined species.

The populations studied differ in the presence/absence of cortical granules, an important difference usually significant at species level. However, the granules are colourless and sometimes loosely arranged. Thus, we cannot exclude to have overlooked them in the type population.

In vivo, *P. simplex* highly resembles *Gonostomum* spp., especially *G. kuehnelti*, which also has many macronuclear nodules (for a review, see Berger 1999). However, all *Gonostomum* species have transverse cirri, especially *G. kuehnelti*, where four cirri form a rather conspicuous, quadrangular pattern. There is no indication in the literature that *P. simplex* has been found previously, but misidentified (for a review, see Berger 1999).

***Periholosticha paucicirrata* nov. spec. (Figures 15a–s; Table 11)**

Diagnosis (averages from four populations): Size about $100\ \mu\text{m} \times 13\ \mu\text{m}$ *in vivo*; very narrowly oblanceolate and slightly twisted about main body axis. Cortical granules mainly around cirri and dorsal bristles, yellowish to yellow-orange, $\leq 0.5\ \mu\text{m}$ across. On average 15–16 macronuclear nodules in series left of midline, 10–15 adoral membranelles, 6–7 cirri with indistinct midventral pattern in frontal row, 2 frontoterminal (?) cirri, 21–23 cirri in right and 18–21 cirri in left marginal row, 1–2 transverse and 2 caudal cirri, and 2 dorsal kineties.

Type location: *Quercus petraea* – *Carpinus betulus* (oak–hornbeam) forest soil from the Kolmberg in Lower Austria near Vienna, E16°41' N47°58'.

Type material: One holotype and four paratype slides with protargol-impregnated specimens (Foissner's method) from type location and 2–4 voucher slides each from the other populations have been deposited in the Biology Center of the

Oberösterreichische Landesmuseum in Linz (LI), Austria. The slides contain many specimens, with relevant cells marked by black ink circles on the cover glass.

Etymology: Composite of the Latin adjectives *pauci* (few) and *cirratus* (having curl of hair), referring to the few cirri comprising the frontal row.

Description: We studied four populations of this species (see occurrence and ecology section). They are so similar to each other that conspecificity is beyond reasonable doubt (Table 11). Thus, the diagnosis includes all populations, while the *in vivo* description is based mainly on specimens from Austria (Kolmberg) and Croatia because the other populations were investigated mainly in protargol slides.

Size and shape moderately variable and very similar in all populations (Table 11). Size 75–120 $\mu\text{m} \times 10\text{--}20\ \mu\text{m}$ *in vivo*, usually about 100 $\mu\text{m} \times 13\ \mu\text{m}$, length:width ratio 6.2–10.8:1, on average approximately 8:1 *in vivo* and protargol preparations; about 2:1 flattened dorsoventrally. Very narrowly oblanceolate and occasionally indistinctly sigmoidal, slightly to distinctly twisted about main body axis; anterior body end narrowly rounded-truncate, posterior gradually narrowed and bluntly pointed to almost tail-like elongated (Figures 15a–c, j, p–r); acontractile but highly flexible. An average of 16 macronuclear nodules in two indistinct series one upon the other along postoral left body margin; individual nodules globular to elongate ellipsoidal, on average 5–6 $\mu\text{m} \times 3\ \mu\text{m}$ in protargol preparations; nucleoli scattered, globular, small. Two to three globular to ellipsoidal micronuclei scattered along macronuclear series, rather distinct *in vivo* because compact and about 1.5 μm in size. Contractile vacuole in mid-body left of midline, with long collecting canals. Cortical granules located around cirri and dorsal bristles in populations from Croatia and the Müllerboden in Austria, while located around cirri and dorsal bristles and distributed in loose rows throughout cortex in type population; provide cells with a yellowish shimmer *in vivo*, never impregnate with the protargol method used. Individual cortical granules distinct, though only 0.2–0.5 μm across, because compact and of a bright citrine to yellow-orange color (Figures 15f, g, m). Cytoplasm hyaline, usually contains only few food vacuoles and some lipid droplets up to 2 μm across. Feeds on bacteria digested in vacuoles 3–5 μm across. Glides and swims moderately rapidly on microscope slide and between soil particles showing pronounced flexibility.

Cirral pattern and number of cirri of usual variability (Table 11). Cirri 7–9 μm long *in vivo*, most composed of four to six cilia, depending on population and specimen, those in posterior body third consist of only two to four cilia. Marginal rows extend slightly obliquely due to body torsion from anterior to posterior end; right row commences subapically at level of paroral membrane. Frontal cirri form slightly oblique row underneath body end, usually indistinctly enlarged, that is, composed of six cilia. Frontal row extends right of midline, on average slightly shorter than adoral zone of membranelles in all populations; cirri arranged in indistinct midventral pattern, usually consist of four cilia, rarely of six or only two. Two (frontoterminal?) cirri right of anterior end of frontal row, sometimes indistinctly separated from right marginal row. Two to four, usually three or four, cirri on pointed posterior end; some well-oriented cells show that these are one or two transverse and two caudal cirri, often difficult to distinguish from posteriormost marginal cirri (Figures 15a, c, e, h–k, n, o, r, s; Table 11).

Table 11. Morphometric data on four populations of *Periholosticha paucicirrata*.

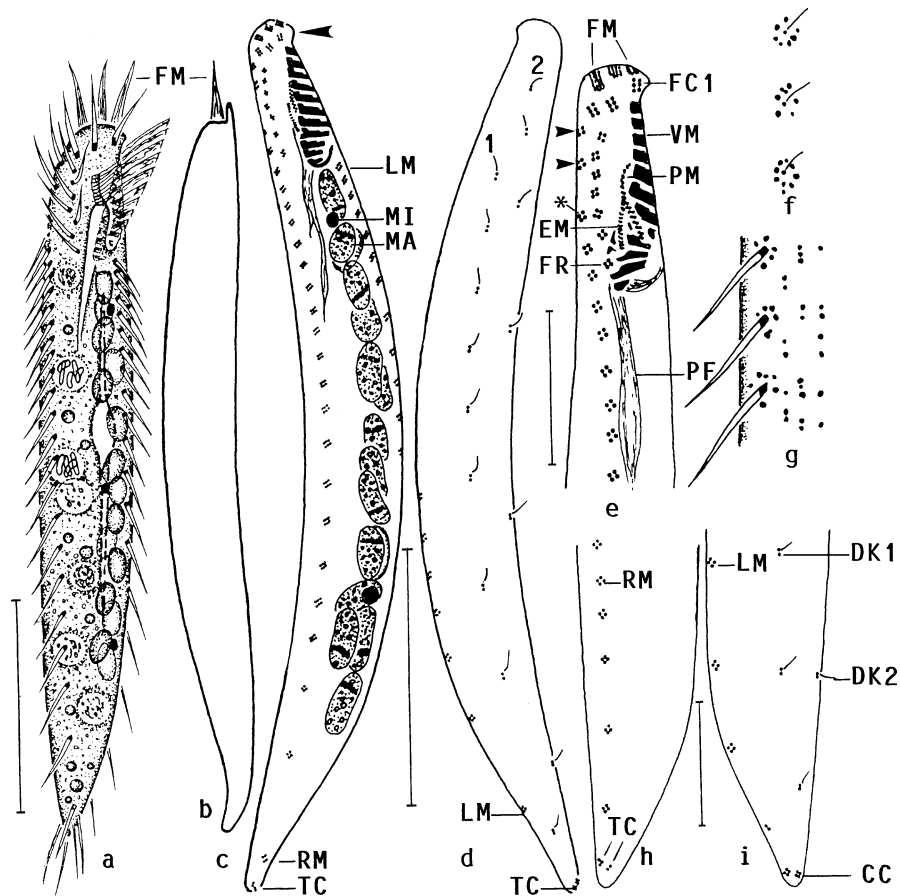
Characteristics ^a	Pop ^b	\bar{x}	<i>M</i>	SD	SE	CV	Min	Max	<i>n</i>
Body, length	K	85.7	85.0	9.0	2.0	10.5	68.0	100.0	21
	ST	85.7	84.0	9.2	2.5	10.7	74.0	100.0	13
	G	88.9	88.0	7.7	2.0	8.7	75.0	102.0	15
	C	87.5	90.0	11.8	3.6	13.5	70.0	103.0	11
Body, width	K	10.7	11.0	1.3	0.3	12.2	8.0	14.0	21
	ST	11.7	12.0	1.3	0.4	11.3	10.0	15.0	13
	G	10.3	10.0	1.1	0.3	10.7	9.0	13.0	15
	C	10.6	10.0	1.3	0.4	12.1	9.0	13.0	11
Body length:width, ratio	K	8.1	7.9	1.2	0.3	14.4	6.3	10.8	21
	ST	7.4	7.4	0.7	0.2	9.8	6.2	8.4	13
	G	8.7	8.8	0.9	0.2	8.9	7.5	10.1	15
	C	8.3	8.2	1.3	0.4	15.2	6.5	10.3	11
Anterior body end to proximal end of adoral zone, distance	K	16.1	16.0	1.1	0.2	6.7	14.0	18.0	21
	ST	17.7	18.0	1.6	0.4	9.1	15.0	20.0	13
	G	17.3	18.0	1.7	0.4	9.6	14.0	20.0	15
	C	15.6	16.0	1.9	0.6	11.9	12.0	20.0	11
Body length:length of adoral zone, ratio	K	5.4	5.4	0.7	0.2	12.6	4.2	6.3	21
	ST	4.9	4.7	0.5	0.2	11.2	3.9	6.2	13
	G	5.0	5.0	0.4	0.1	7.5	4.6	5.9	15
	C	5.7	5.7	0.8	0.3	14.5	4.4	6.9	11
Anterior body end to end of frontal row, distance	K	15.1	15.0	1.1	0.2	7.2	13.0	18.0	21
	ST	17.0	17.0	2.4	0.7	13.8	13.0	22.0	13
	G	16.1	16.0	1.8	0.5	11.4	12.0	20.0	15
	C	14.6	15.0	2.6	0.8	17.8	10.0	18.0	11
Nuclear figure, length	K	50.6	51.0	8.1	1.8	16.0	39.0	65.0	21
	ST	51.9	51.0	6.7	1.9	12.9	43.0	64.0	13
	G	51.5	51.0	6.1	1.6	11.8	42.0	64.0	15
	C	50.2	50.0	11.0	3.3	21.9	37.0	68.0	11
Macronuclear nodules, length	K	5.6	6.0	1.2	0.3	22.1	3.0	8.0	21
	ST	6.2	6.0	1.3	0.4	21.9	5.0	10.0	13
	G	4.8	5.0	1.2	0.3	23.9	3.0	7.0	15
	C	5.2	5.0	0.9	0.3	16.9	4.0	7.0	11
Macronuclear nodules, width	K	2.6	2.7	0.4	0.1	17.2	2.0	3.0	21
	ST	2.9	3.0	0.7	0.2	24.7	2.0	4.0	13
	G	2.9	3.0	0.6	0.2	19.2	2.0	4.0	15
	C	2.9	3.0	0.3	0.1	10.4	2.0	3.0	11
Macronuclear nodules, number	K	16.3	16.0	3.1	0.7	5.4	14.0	29.0	21
	ST	14.7	16.0	2.4	0.7	16.1	8.0	16.0	13
	G	16.3	16.0	1.3	0.3	7.9	14.0	20.0	15
	C	15.4	15.0	1.7	0.5	11.0	12.0	18.0	11
Micronuclei, length	K	1.9	2.0	0.3	0.1	13.7	1.5	2.3	21
	ST	1.9	2.0	–	–	–	1.6	2.0	13
	G	2.2	2.2	0.3	0.1	12.7	2.0	3.0	15
	C	3.1	3.0	0.4	0.1	12.1	2.5	4.0	11
Micronuclei, width	K	1.7	1.6	0.3	0.1	17.1	1.1	2.2	21
	ST	1.8	1.8	–	–	–	1.3	2.0	13
	G	1.9	2.0	0.2	0.1	10.1	1.6	2.2	15
	C	1.9	2.0	0.3	0.1	17.4	1.5	2.5	11

Table 11. (continued)

Characteristics ^a	Pop ^b	\bar{x}	<i>M</i>	SD	SE	CV	Min	Max	<i>n</i>
Micronuclei, number	K	3.1	3.0	1.1	0.2	33.8	1.0	5.0	21
	ST	2.3	2.0	0.5	0.1	20.8	2.0	3.0	13
	G	3.4	3.0	0.9	0.2	26.8	2.0	5.0	15
	C	2.3	2.0	0.8	0.2	34.6	1.0	4.0	11
Adoral membranelles, number	K	13.3	13.0	0.6	0.1	4.3	12.0	14.0	21
	ST	14.1	14.0	0.6	0.2	4.6	13.0	15.0	13
	G	14.9	15.0	1.0	0.3	6.7	12.0	16.0	15
	C	10.6	10.0	1.0	0.3	9.8	9.0	13.0	11
Frontal cirri, number	K	3.0	3.0	0.0	0.0	0.0	3.0	3.0	21
	ST	3.0	3.0	0.0	0.0	0.0	3.0	3.0	13
	G	3.0	3.0	0.0	0.0	0.0	3.0	3.0	15
	C	3.0	3.0	0.0	0.0	0.0	3.0	3.0	11
Frontoterminal cirri, number	K	2.0	2.0	0.0	0.0	0.0	2.0	2.0	21
	ST	2.0	2.0	0.0	0.0	0.0	2.0	2.0	13
	G	2.0	2.0	0.0	0.0	0.0	2.0	2.0	15
	C	2.0	2.0	0.0	0.0	0.0	2.0	2.0	11
Frontal row, number of cirri (without fronto-terminal cirri)	K	7.1	7.0	0.8	0.2	10.8	5.0	9.0	21
	ST	6.9	7.0	0.6	0.2	8.1	5.0	7.0	13
	G	6.9	7.0	0.9	0.2	13.3	5.0	9.0	15
	C	5.6	6.0	1.2	0.4	21.9	4.0	7.0	11
Right marginal cirri, number	K	23.0	23.0	2.0	0.4	8.7	20.0	28.0	21
	ST	20.5	21.0	3.5	1.0	17.0	11.0	26.0	13
	G	21.8	22.0	2.6	0.7	11.9	17.0	27.0	15
	C	23.1	23.0	3.5	1.1	15.2	18.0	28.0	11
Left marginal cirri, number	K	20.2	20.0	2.0	0.4	9.8	17.0	25.0	21
	ST	18.5	18.5	2.8	0.8	15.4	12.0	23.0	12
	G	19.9	19.0	2.6	0.7	13.1	16.0	26.0	15
	C	20.7	21.0	2.7	0.8	13.0	17.0	25.0	11
Cirri (likely transverse and caudal) on posterior body end, number	K	3.2	3.0	0.7	0.2	21.3	2.0	4.0	21
	ST	3.1	3.0	1.2	0.3	38.6	0.0	4.0	13
	G	3.6	4.0	0.6	0.2	17.6	2.0	4.0	15
	C	3.8	4.0	–	–	–	3.0	4.0	11
Dorsal kineties, number	K	2.0	2.0	0.0	0.0	0.0	2.0	2.0	21
	ST	2.0	2.0	0.0	0.0	0.0	2.0	2.0	13
	G	2.0	2.0	0.0	0.0	0.0	2.0	2.0	15
	C	2.0	2.0	0.0	0.0	0.0	2.0	2.0	11
Dorsal kinety 1, number of bristles	K	9.3	9.0	1.0	0.2	10.4	8.0	12.0	21
	ST	9.5	9.0	1.3	0.4	13.3	7.0	12.0	13
	G	9.4	9.0	0.9	0.2	9.7	8.0	11.0	15
	C	8.9	9.0	2.1	0.6	23.8	5.0	12.0	11
Dorsal kinety 2, number of bristles	K	6.5	6.0	0.8	0.2	12.6	6.0	9.0	21
	ST	7.3	7.0	1.6	0.4	21.9	4.0	10.0	13
	G	6.5	6.0	0.7	0.2	11.5	5.0	8.0	15
	C	6.1	6.0	1.0	0.3	17.2	4.0	8.0	11

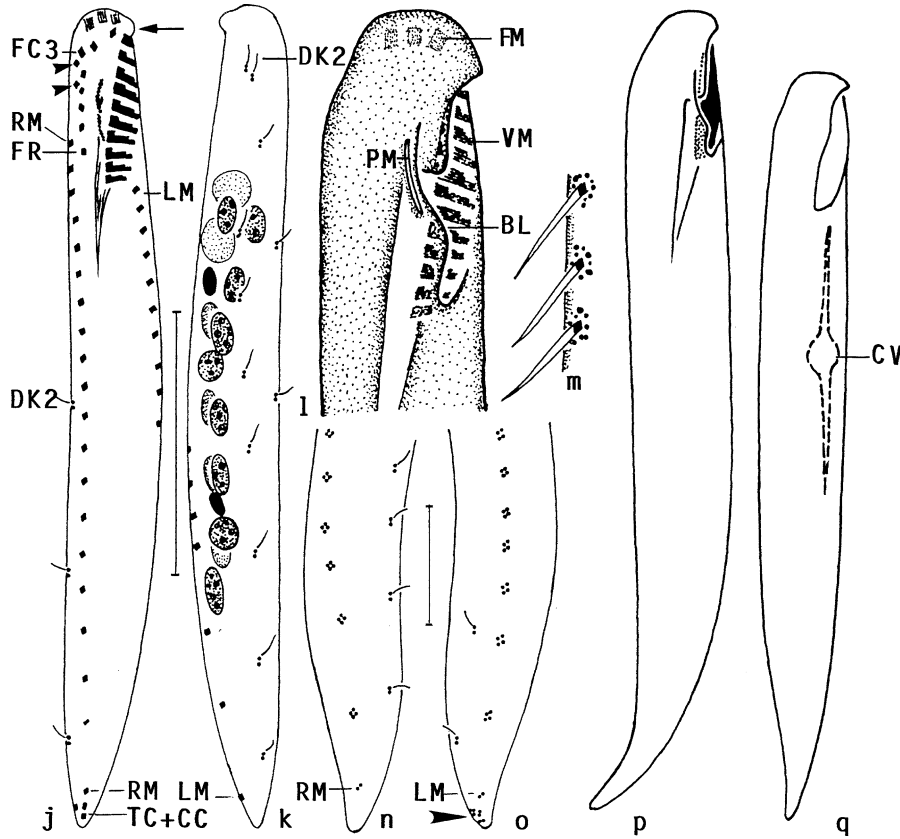
^aData based on mounted, protargol-impregnated (Foissner 1991, protocol A), and randomly selected specimens from non-flooded Petri dish cultures. Measurements in μm . CV – coefficient of variation in %, *M* – median, Max – maximum, Min – minimum, *n* – number of individuals investigated, SD – standard deviation, SE – standard error of arithmetic mean, \bar{x} – arithmetic mean.

^bPopulations: C – Croatia, G – Greece, K – Kolmberg, Austria (type), ST – Stampfital, Austria.



Figures 15a–i. *Periholosticha paucicirrata*, Kolmberg (Austrian) type population from life (a, b, f, g) and after protargol impregnation (c–e, h, i). **a, b:** Ventral and lateral view of a representative specimen slightly twisted about main body axis. **c, d:** Infraciliature of ventral and dorsal side and nuclear apparatus of holotype specimen. Arrowhead marks broad gap between frontal and ventral adoral membranelles. The macronuclear nodules form two rough series one upon the other. **e:** Details in ventral anterior portion. Arrowheads denote supposed frontoterminal cirri, which are indistinctly separated from the first marginal cirrus (asterisk). Note the beak-like projecting left anterior corner bearing frontal cirrus 1 and separating frontal and ventral adoral membranelles. **f, g:** The cortex contains loose rows of minute ($\leq 1 \mu\text{m}$), yellow granules concentrated around dorsal bristles (f) and cirri (g). **h, i:** Infraciliature of ventral and dorsal side in posterior region, where cirri consist of only two to four cilia. Two minute transverse and caudal cirri each are recognizable. CC – caudal cirri, DK(1, 2) – dorsal kineties, EM – endoral membrane, FC1 – first frontal cirrus, FM – frontal adoral membranelles, FR – frontal row, LM – left marginal row, MA – macronuclear nodules, MI – micronucleus, PF – pharyngeal fibres, PM – paroral membrane, RM – right marginal row, TC – transverse cirri, VM – ventral adoral membranelles. Scale bars $30 \mu\text{m}$ (a–d) and $10 \mu\text{m}$ (e, h, i).

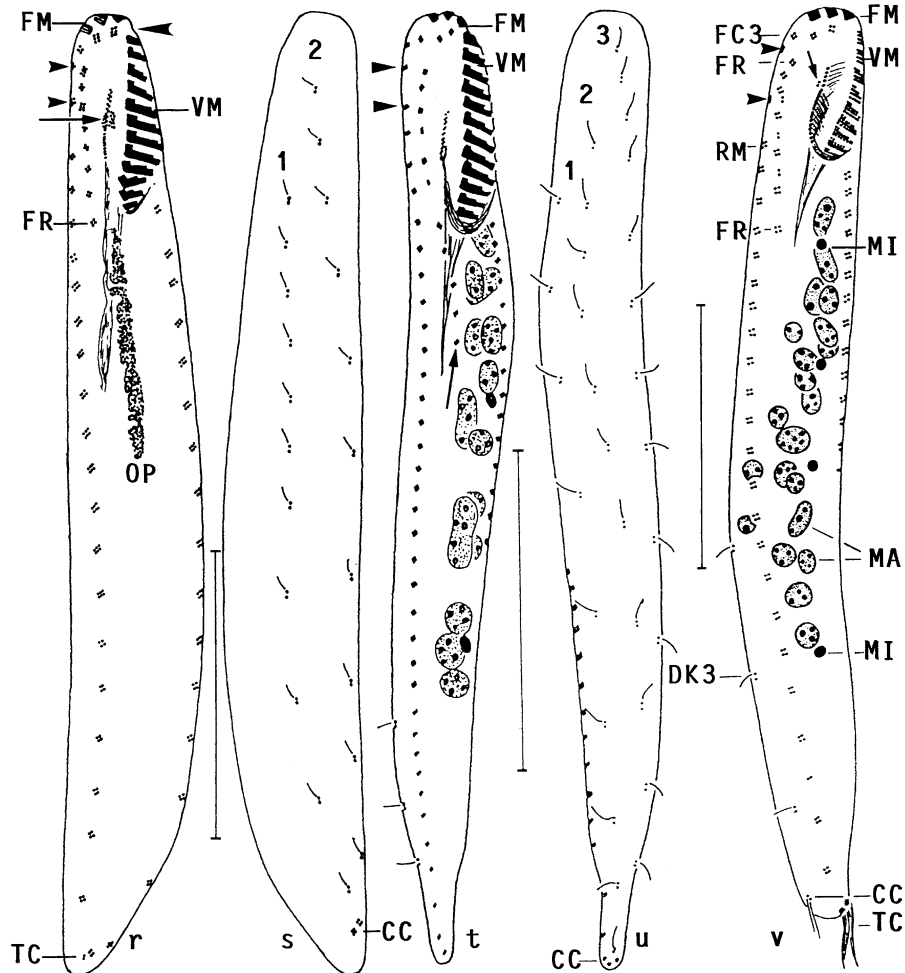
Dorsal bristles $2.5\text{--}3 \mu\text{m}$ long *in vivo*, more closely spaced in row 1 than in row 2, row 1 distinctly shortened anteriorly, that is, commences at level of buccal vertex, both rows slightly shortened posteriorly; invariably arranged in two rows each



Figures 15j–q. *Periholosticha paucicirrata*, Croatian population after protargol impregnation (j, k, n, o) and from life (l, m, p, q). **j, k**: Infraciliature of ventral and dorsal side of main voucher specimen, which is slightly twisted about main body axis. Note macronuclear nodules arranged in two indistinct series one upon the other, and the distinct gap (arrow) between frontal and ventral adoral membranelles. Arrowheads denote supposed frontoterminal cirri, which are almost in line with the right marginal cirri. **l**: Cortex pattern in ventral anterior region. **m**: Cirri and dorsal bristles are surrounded by minute, yellow-orange granules. **n, o**: Infraciliature of ventral and dorsal side in posterior region. Arrowhead marks three minute (transverse and caudal) cirri very near to the posterior end. **p, q**: Shape variants. BL – buccal lip, CC – caudal cirri, CV – contractile vacuole, DK2 – dorsal kinety 2, FC3 – third frontal cirrus, FM – frontal adoral membranelles, FR – frontal row, LM – left marginal row, PM – paroral membrane, RM – right marginal row, TC – transverse cirri, VM – ventral adoral membranelles. Scale bars 30 μm (j, k) and 10 μm (n, o).

composed of very similar numbers of kinetids in all populations (Figures 15d, k, n, o, s; Table 11).

Adoral zone inconspicuous because occupying only 20% of body length, composed of an average of 10–15 membranelles, depending on population; anterior (frontal) three membranelles invariably separated from ventral membranelles by a small, but distinct gap at beak-like left anterior corner of cell. Frontal membranelles insert on anterior body end, proximal portion covered by scutum-like projecting



Figures 15r–v. *Periholosticha paucicirrata* (r, s) and related taxa (t–v), infraciliature and nuclear apparatus after protargol impregnation. r, s: *Periholosticha paucicirrata*, ventral and dorsal view of an early divider from Stampftal population. Primordia develop underneath the undulating membranes (arrow) and posteriorly left of the frontal row. Large arrowhead denotes gap between frontal and ventral adoral membranelles. Small arrowheads mark supposed frontoterminal cirri. This specimen has two clearly recognizable transverse and caudal cirri each. t, u: *Periholosticha lanceolata* (from Foissner et al. 2002) differs from *P. paucicirrata* (r, s) by the number of dorsal kineties (three vs. two) and the much longer frontal row (posterior end marked by arrow). Arrowheads denote supposed frontoterminal cirri. v: *Hemisincirra inquieta* (from Foissner et al. 2002) differs from *P. paucicirrata* (r, s) in having a minute buccal cirrus (arrow) and three (vs. two) dorsal kineties. Arrowheads mark frontoterminal cirri. CC – caudal cirri, DK(1–3) – dorsal kineties, FC3 – third frontal cirrus, FM – frontal adoral membranelles, FR – frontal row, MA – macronuclear nodules, MI – micronuclei, OP – oral primordium, RM – right marginal row, TC – transverse cirri, VM – ventral adoral membranelles. Scale bars 30 μ m.

ventral cell surface. Ventral portion of membranellar zone slightly twisted along main body axis, as described in *P. sylvatica*. Buccal cavity narrow and flat; buccal lip hyaline, projects angularly covering proximal half of adoral zone, anterior half bears paroral membrane in minute cleft. Paroral and endoral membrane appear closely spaced when viewed ventrally, forming a curved line along mid-portion of adoral zone. Paroral membrane 3–6 μm long, slightly curved, composed of zigzagging basal bodies with 5 μm long cilia; anterior, rarely posterior, third occasionally lacking or incompletely impregnated. Endoral membrane of same shape and length as paroral, anterior half appear to overlap posterior half of paroral, composed of narrowly spaced (di?)kinetids. Pharyngeal fibers of ordinary length and structure (Figures 15a–c, e, j, l, r; Table 11).

Occurrence and ecology: *Periholosticha paucicirrata* occurred in 7 out of the 12 sites investigated, both in deciduous and coniferous forests (Table 2), showing that it is a common species with wide ecological range. This is emphasized by the populations from Croatia and Greece, which are highly similar to the Austrian specimens (Table 11). Likely, we rarely separated *P. pauciciliata* from *Hemisincirra inquieta* in our previous investigations because they are difficult to distinguish *in vivo* (see section on species comparison).

In Croatia, *P. paucicirrata* occurred in slightly acidic (pH 6.3 in water) and saline, very sandy coastal soil from Dugi Otok, a small island off the Adriatic Sea coast (sample kindly provided by Dr. W. Petz). In Greece, we found *P. paucicirrata* in a Peloponnese Pine forest between the towns of Katarraklias and Vlasia. The sample (pH 6.3 in water) was a mixture of pine needles, raw humus, and terrestrial mosses. *Periholosticha paucicirrata* was moderately abundant in the non-flooded Petri dish cultures, except of the Greece sample, where it was numerous. It is well adapted to soil life by the slender, flexible body.

Generic allocation and comparison with related species: Classification of this kind of hypotrichs is difficult, as explained in *P. sylvatica*. We assign our populations to *Periholosticha* because they lack a buccal cirrus. On the other hand, the specimens likely have transverse cirri, possibly lacking in the congeners, although this is difficult to ascertain due to the pointed rear body end. This might explain the vague definition by Hemberger (1981, 1985): “no or only inconspicuous transverse cirri”.

Periholosticha paucicirrata differs from the species described by Hemberger (1985), viz., *P. lanceolata* (Figures 15t, u) and *P. acuminata*, mainly by the number of dorsal kineties (2 vs. 3) and cirri comprising the frontal row (6–7 vs. 12–15). *Periholosticha paucicirrata* strongly resembles *P. sylvatica* which, however, is much stouter (length:width ratio 5.9:1 vs. 8.7:1) and has four (vs. three) frontal membranelles. Furthermore, many important morphometrics are significantly different, that is, do not or only slightly overlap, for instance, the number of adoral membranelles (19 vs. 10–15), cirri composing the frontal row (10 vs. 6–7), and macronuclear nodules (19 vs. 15–16).

In vivo, *P. paucicirrata* highly resembles *Hemisincirra inquieta* Hemberger 1985, which, however, has three (vs. two) dorsal kineties and a buccal cirrus (vs. none) recognizable in the specimens studied by Foissner et al. (2002; Figure 15v), and

also in a postdivider of the type population (Hemberger 1981). Nonetheless, *P. paucicirrata* and *H. inquieta* are easily confused *in vivo*, and thus identifications should be checked in protargol preparations.

***Periholosticha sylvatica* nov. spec. (Figures 16a–k; Table 12)**

Diagnosis: Size about $120\ \mu\text{m} \times 20\ \mu\text{m}$ *in vivo*; narrowly oblanceolate and slightly twisted about main body axis. Cortical granules yellowish, rather loosely arranged, $\leq 1\ \mu\text{m}$ across. On average 21 macronuclear nodules in series left of midline, 19 adoral membranelles, 10 cirri with rather distinct midventral pattern in frontal row, 2 frontoterminal (?) cirri, 30 cirri in right and 27 in left marginal row, 4 caudal cirri, and 2 dorsal kineties.

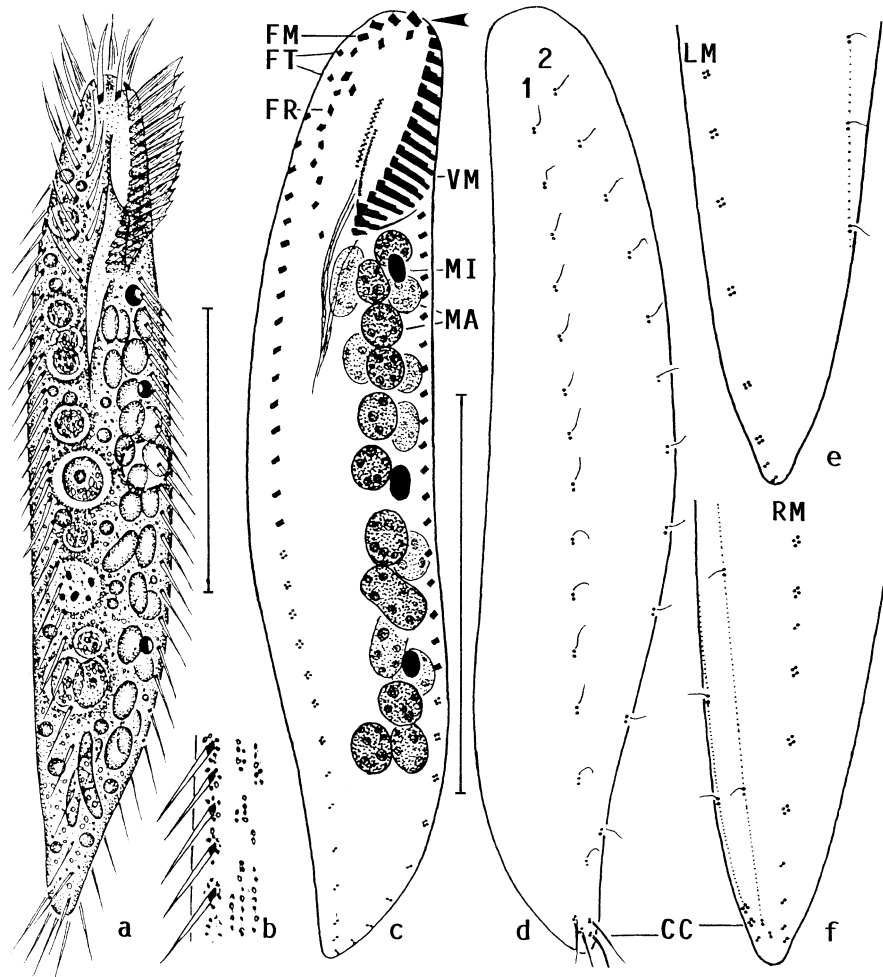
Type location: *Pinus nigra* forest soil in the Stampftal near Vienna, Austria, E16°02' N47°53'.

Type material: One holotype and two paratype slides with protargol-impregnated specimens (Foissner's method) have been deposited in the Biology Center of the Oberösterreichische Landesmuseum in Linz (LI), Austria. The slides contain many specimens, with relevant cells marked by black ink circles on the cover glass.

Etymology: The Latin adjective *sylvatica* (inhabiting forests) refers to the habitat the species was discovered.

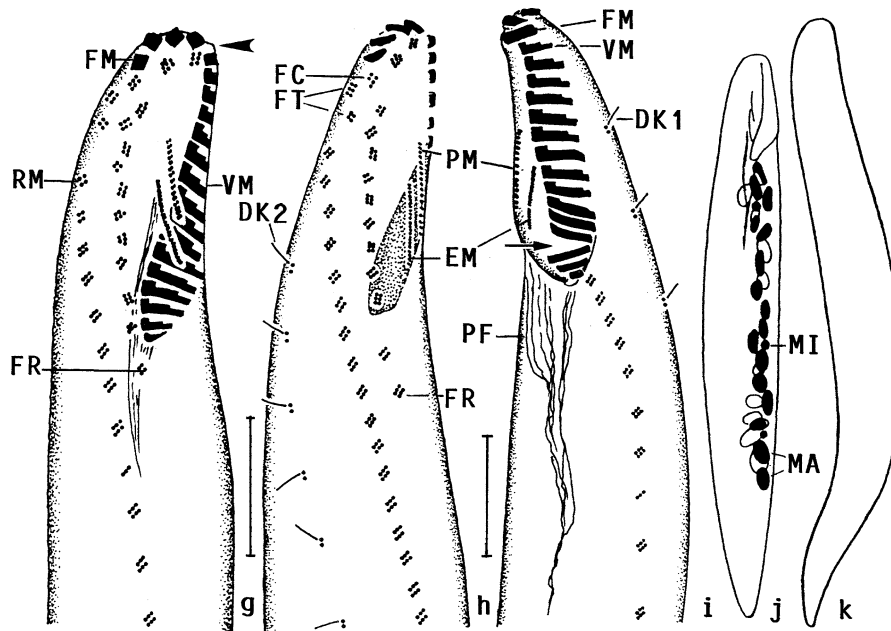
Description: Size $90\text{--}160\ \mu\text{m} \times 15\text{--}25\ \mu\text{m}$ *in vivo*, usually about $120\ \mu\text{m} \times 20\ \mu\text{m}$, length:width ratio highly variable, viz., 4.6–8.1:1, on average 5.9:1 in protargol preparations; slightly to up to 2:1 flattened dorsoventrally. Slenderly oblanceolate to almost vermiform, frequently slightly sigmoidal and twisted about main body axis; anterior body end moderately broadly rounded, posterior third distinctly narrowed and bluntly pointed (Figures 16a, c, j, k; Table 12); acontractile but very flexible. An average of 21 macronuclear nodules in two more or less distinct series one upon the other and/or side by side along postoral left body margin; individual nodules globular to elongate ellipsoidal, on average $7\ \mu\text{m} \times 3\ \mu\text{m}$ in protargol preparations; nucleoli scattered, globular, and of ordinary size. Usually a slightly ellipsoidal micronucleus each in anterior and posterior region of nuclear figure. Contractile vacuole slightly above mid-body at left margin of cell. Cortical granules around cirri and dorsal bristles, and loosely scattered throughout cortex, yellowish to citrine and rather refractive, $0.3\text{--}1\ \mu\text{m}$ in size (Figure 16b); provide cells with a yellowish shimmer in the bright field microscope. Cytoplasm usually packed with food vacuoles $4\text{--}10\ \mu\text{m}$ across and some small lipid droplets. Feeds on bacteria, fungal spores, and heterotrophic flagellates. Glides, swims or winds slowly on microscope slide and between soil particles showing great flexibility.

Cirral pattern and number of cirri of usual variability, except of the highly variable (40%) number of caudal cirri (Figures 16a, c, d, f–i; Table 12). Cirri $10\text{--}12\ \mu\text{m}$ long *in vivo*, most consist of six cilia in two rows, except of posterior third marginal cirri composed of only two to four cilia. Marginal rows extend slightly obliquely due to body torsion and abut on bluntly pointed rear body end; right row commences subapically at level of paroral membrane. Frontal cirri form slightly



Figures 16a-f. *Periholosticha sylvatica* from life (a, b) and after protargol impregnation (c-f). **a**: Ventral view of a representative specimen slightly twisted about main body axis. **b**: Surface view showing citrine cortical granules. **c, d**: Infraciliature of ventral and dorsal side and nuclear apparatus of holotype specimen. The macronuclear nodules form two rough series one upon the other (ventral series dark, dorsal bright). Note distinct size reduction of cirri in posterior portion of marginal rows. Arrowhead marks minute gap between frontal and ventral adoral membranelles. **e, f**: Lateral views of posterior body region of a specimen with five caudal cirri composed of two to four cilia each. Dorsal bristles and their first caudal cirrus connected by dotted lines. CC – caudal cirri, FM – frontal adoral membranelles, FR – frontal row, FT – frontoterminal (?) cirri, LM – left marginal row, MA – macronuclear nodules, MI – micro-nucleus, RM – right marginal row, VM – ventral adoral membranelles. Scale bars 40 μ m.

oblique row subapically, middle cirrus usually slightly enlarged because composed of eight to nine cilia, right cirrus underneath distalmost adoral membranelle. Frontal cirral row extends right of midline to or slightly beyond level of buccal



Figures 16g–k. *Periholosticha sylvatica* after protargol impregnation. g–i: Slightly dorsolateral, strongly dorsolateral, and ventrolateral view of infraciliature in anterior body region showing, inter alia, the supposed frontoterminal cirri and the variability of the frontal cirral row. Arrowhead in (g) marks gap between frontal and ventral adoral membranelles. The ventral membranellar ribbon is rather abruptly twisted proximally, as indicated by the increased distance between the membranelles (arrow). j, k: Shape variability of large specimens, length 142 μm and 135 μm . The macronuclear nodules are arranged in two rough series one upon the other. DK1, 2 – dorsal kineties, EM – endoral membrane, FC – frontal cirrus 3, FM – frontal adoral membranelles, FR – frontal cirral row, FT – frontoterminal (?) cirri, MA – macronuclear nodules, MI – micronucleus, PF – pharyngeal fibres, PM – paroral membrane, RM – first cirrus of right marginal row, VM – ventral adoral membranelles. Scale bars 10 μm .

vertex, cirri arranged in rather distinct midventral pattern, except for one to three cirri at posterior end forming short, oblique tail. Two, rarely three, cirri right of anterior end of frontal row and distinctly separate from right marginal cirri, as in *P. acuminata*, and thus likely frontoterminal cirri, although such cirri are probably lacking in *P. lanceolata*, type of the genus (Foissner et al. 2002; Hemberger 1981). Buccal, postoral, and transverse cirri lacking. Ontogenesis commences with the production of a long, narrow oral primordium left of midline, that is, far away from frontal row, while it begins underneath the last frontal cirrus in *P. lanceolata* (Hemberger 1981).

Dorsal bristles about 3 μm long *in vivo*, more closely spaced in row 1 than in row 2, both rows slightly shortened anteriorly and posteriorly. Caudal cirri fine, that is, composed of only two to four cilia, number highly variable; difficult to distinguish from posteriormost marginal cirri also consisting of only two or four cilia (Figures 16a, c–f; Table 12).

Adoral zone inconspicuous because occupying only 23% of body length, composed of 19 membranelles on average, anterior (frontal) four membranelles invariably set off from ventral membranelles by a small, but distinct gap at left anterior corner of cell; ventral portion of membranelar zone slightly twisted along its main axis, as evident from differently oriented last membranelles (Figure 16i). Buccal cavity narrow and flat; buccal lip hyaline, projects angularly covering proximal portion of adoral zone. Paroral and endoral membrane appear closely spaced when viewed ventrally, forming slightly curved line along posterior half of adoral zone. Paroral membrane short, slightly curved, composed of distinctly zigzagging basal bodies with about 5 μm long cilia. Endoral membrane almost straight, anterior half appear to overlap posterior half of paroral, composed of very narrowly spaced (di?)kinetids. Pharyngeal fibers of ordinary length and structure (Figures 16a, c, g–i; Table 12).

Occurrence and ecology: As yet found only at type location, where it was moderately abundant 2 days after rewetting the sample, suggesting an r-selected life strategy, while most hypotrichs are more k- than r-selected (Foissner 1987a). Likely, we misidentified this species occasionally as *Holostichides terricola*, from which it is difficult to separate *in vivo* (see below).

Generic allocation and comparison with related species: Classification of this kind of hypotrich is difficult (Foissner et al. 2002). Main features are the lack of buccal and transverse cirri, as in *Periholosticha*, *Paragastrostyla*, and some *Holostichides* and *Hemisincirra* species. Our population is most similar to *Periholosticha acuminata* Hemberger 1985. Thus, we allocate it to *Periholosticha*, although ontogenesis does not commence at the last frontoventral cirrus, as in the type species, *P. lanceolata* (Hemberger 1981).

Two *Periholosticha* species have been described, viz., *P. lanceolata* and *P. acuminata* (Foissner et al. 2002; Hemberger 1985). Both have three dorsal kineties and are thus different from *P. sylvatica*, which has only two. The cirral pattern of *P. sylvatica* is very similar to that of *P. acuminata*, but the number of marginal cirri is considerably different: right row 21–37 versus 19–24, left row 19–36 versus 17–22. Likewise, the number of macronuclear nodules is higher in *P. sylvatica* than *P. acuminata*: 12–25 (average 21) versus 11–14 (average not known). *Periholosticha sylvatica* differs from *P. lanceolata*, as redescribed by Foissner et al. (2002) and shown in Figures 15t, u, by the length:width ratio (6:1 vs. 9:1), the length of the frontoventral cirral row (extending to vs. far beyond buccal vertex), the number of frontal membranelles (3 vs. 4), and the number of dorsal kineties (2 vs. 3).

Periholosticha sylvatica also strongly resembles *Holostichides terricola* Foissner 1988. Both have similar size and shape, cortical granulation, two dorsal kineties, and lack buccal and transverse cirri. The main feature separating these taxa is the frontal cirral row, which forms a distinct tail, extending to mid-body, in *H. terricola*. Such a tail is lacking or reduced to one to three cirri in *P. sylvatica*, whose frontal row thus extends only to the buccal vertex. Furthermore, the numbers of frontoterminal cirri (2 vs. 3) and frontal membranelles (4 vs. 3) are slightly different. Altogether, we cannot exclude that our population belongs to *Holostichides*, whose type species, however, has a buccal cirrus (Foissner 1987c), a feature usually

Table 12. Morphometric data on *Periholosticha sylvatica*.

Characteristics ^a	\bar{x}	<i>M</i>	SD	SE	CV	Min	Max	<i>n</i>
Body, length	106.3	102.0	15.8	3.4	14.8	83.0	145.0	21
Body, width	18.1	18.0	1.8	0.4	10.0	15.0	21.0	21
Body length:width, ratio	5.9	5.8	0.9	0.2	14.8	4.6	8.1	21
Anterior end to proximal end of adoral zone, distance	24.3	24.0	2.5	0.5	10.2	19.0	30.0	21
Body length:length of adoral zone, ratio	4.5	4.4	0.6	0.1	13.3	3.5	5.6	21
Anterior body end to end of frontal row, distance	26.0	26.0	3.3	0.7	12.5	20.0	32.0	21
Nuclear figure, length	66.4	67.0	10.9	2.4	16.4	47.0	85.0	21
Macronuclear nodules, length	6.8	7.0	1.3	0.3	19.2	5.0	9.0	21
Macronuclear nodules, width	3.6	3.0	0.8	0.2	21.4	2.5	5.0	21
Macronuclear nodules, number	21.1	22.0	3.5	0.8	16.7	12.0	25.0	21
Micronuclei, length	3.2	3.2	–	–	–	3.0	4.0	21
Micronuclei, width	2.4	2.5	–	–	–	2.0	3.0	21
Micronuclei, number	2.5	2.0	0.4	0.1	15.3	2.0	4.0	21
Adoral membranelles, number	18.9	19.0	1.5	0.3	7.9	14.0	21.0	21
Frontal cirri, number	3.0	3.0	0.0	0.0	0.0	3.0	3.0	21
Frontoterminal cirri, number (rarely occur 3)	2.0	2.0	0.0	0.0	0.0	2.0	2.0	21
Frontal row, number of cirri ^b	9.9	10.0	1.3	0.3	12.7	7.0	12.0	21
Right marginal cirri, number	30.1	30.0	4.9	1.1	16.1	21.0	37.0	21
Left marginal cirri, number	27.2	27.0	4.8	1.0	17.6	19.0	36.0	21
Caudal cirri, number	4.4	4.0	1.8	0.4	40.1	2.0	10.0	21
Dorsal kineties, number	2.0	2.0	0.0	0.0	0.0	2.0	2.0	21
Dorsal kinety 1, number of bristles	15.3	15.0	1.7	0.4	11.2	12.0	19.0	21
Dorsal kinety 2, number of bristles	12.9	13.0	1.7	0.4	12.9	8.0	15.0	21

^aData based on mounted, protargol-impregnated (Foissner 1991, protocol A), and randomly selected specimens from a non-flooded Petri dish culture. Measurements in μm . CV – coefficient of variation in %, *M* – median, Max – maximum, Min – minimum, *n* – number of individuals investigated, SD – standard deviation, SE – standard error of arithmetic mean, \bar{x} – arithmetic mean.

^bWithout frontoterminal cirri.

considered as a generic character. As mentioned above, these and related genera are in need of revision.

***Australocirrus zechmeisterae* nov. spec.**
(Figures 17a–j, 18a–c; Tables 13 and 14)

Diagnosis: Size about $190 \mu\text{m} \times 85 \mu\text{m}$ *in vivo*. Ellipsoidal with both ends broadly rounded. On average 4 macronuclear nodules, 18 fronto–ventral–transverse cirri and 23 cirri each in right and left marginal row. Adoral zone of membranelles occupies about 46% of body length, composed of an average of 39 membranelles with bases up to $22 \mu\text{m}$ long. Undulating membranes intersect underneath mid of buccal cavity. Six ordinary dorsal kineties plus 2–3 shortened, loosely ciliated rows between kineties 3 and 4. Resting cyst with wrinkled wall and fused macronuclear nodules.

Type location: Slightly saline grassland soil from the margin of the Zicklacke, a small soda lake near the town of Illmitz, Burgenland, Austria, E16°48' N47°45'.

Type material: Two holotype (ventral and dorsal view of a specimen each) and two paratype slides with protargol-impregnated specimens (Foissner's method) from type location have been deposited in the Biology Center of the Oberösterreichische Landesmuseum in Linz (LI), Austria. The slides contain few specimens, with relevant cells marked by black ink circles on the cover glass. Impregnation quality is mediocre, that is, the cells are rather opaque because the fixative was amended with aqueous osmium tetroxide to improve preservation.

Dedication: Wilhelm Foissner dedicates this new species to Sophie Zechmeister-Boltenstern, acknowledging her efforts in establishing research in natural forest stands of Austria.

Description: This large and thus conspicuous ciliate has a soft, fragile cortex. Accordingly, it is difficult to preserve, that is, shrunken by about 20% in the protargol preparations.

Size 150–220 μm \times 65–120 μm *in vivo*, usually near 190 μm \times 85 μm ; length: width ratio thus about 2.2:1 both *in vivo* and protargol preparations (Table 13); dorsoventrally flattened up to 2:1 and with distinct dorsal hump in middle third (Figure 17b). Shape ellipsoidal to indistinctly reniform, both ends broadly rounded (Figures 17a, 18a, b). Nuclear apparatus in middle quarters of body near cell's midline, usually comprising four macronuclear nodules and three micronuclei (Figures 17a, j). Macronuclear nodules in line, form two indistinct pairs because the distance between the central nodules is slightly larger than between the marginal nodules (Table 13); individual nodules globular to ellipsoidal, 20–25 μm \times 10–15 μm *in vivo*, contain many minute, scattered nucleoli. Micronuclei attached to far apart from macronuclear nodules, globular to broadly ellipsoidal, about 5 μm across *in vivo*. Contractile vacuole slightly underneath mid-body near left border of cell, with two long canals. Cortex flexible and fragile, does not contain specific granules. Cytoplasm colourless, usually packed with food vacuoles up to 40 μm across and 1–3 μm long crystals with shapes as shown in Figure 17d; many small lipid droplets 2–3 μm across along body margin. Feeds on various fungal conidia, heterotrophic flagellates (*Polytoma* sp.), and small to middle-sized ciliates (*Sathrophilus muscorum*, *Odontochlamys alpestris biciliata*, *Colpoda maupasi*, hypotrichs). Movement without peculiarities.

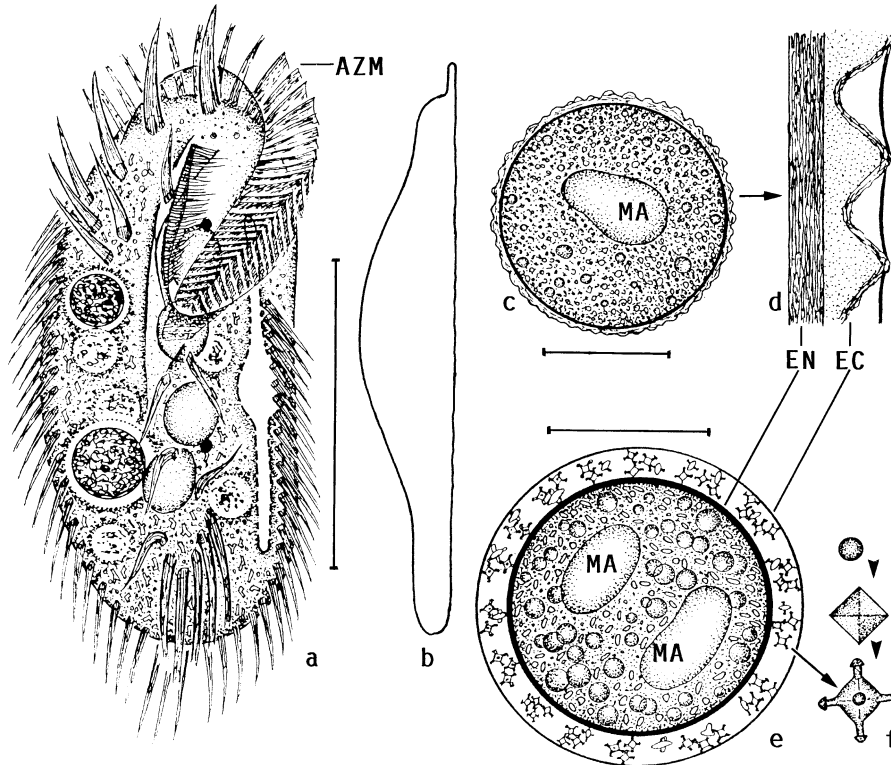
Cirral pattern stable, number of cirri more variable as in other large 18 fronto-ventral-transverse cirri oxytrichids (Table 13). Cirri arranged in typical *Oxytricha* pattern (for a review, see Berger 1999), except for third postoral cirrus distinctly apart from first and second postoral cirrus underneath buccal vertex (Figures 17a, i, 18a; Table 13). Frontal cirri conspicuously enlarged, right (third) cirrus close to distalmost adoral membranelle. Buccal cirrus slightly above mid of paroral membrane. Transverse cirri distinctly subterminal, but project above posterior body margin because 35 μm long *in vivo*; their distal end frayed. Marginal cirri approximately 25 μm long *in vivo*, right row commences underneath level of buccal cirrus, that is, about 25% off anterior body end, likely due to the long adoral zone. Left marginal row extends to body midline posteriorly, where a small gap separates

Table 13. Morphometric data on *Australocirrus zechmeisterae*.

Characteristics ^a	\bar{x}	<i>M</i>	SD	SE	CV	Min	Max	<i>n</i>
Body, length	160.4	165.0	14.8	3.4	9.2	126.0	187.0	19
Body, width	72.3	72.0	9.5	2.2	13.2	56.0	99.0	19
Body length:width, ratio	2.2	2.3	0.2	0.1	9.7	1.7	2.7	19
Anterior end to proximal end of adoral zone, distance	73.3	73.0	6.7	1.5	9.1	61.0	87.0	19
Body length:length of adoral zone, ratio	2.2	2.2	0.2	0.1	7.4	1.9	2.6	19
Anterior end to last frontoventral cirrus, distance	52.0	50.0	6.9	1.6	13.3	42.0	67.0	19
Anterior end to buccal cirrus, distance	28.0	28.0	2.7	0.6	9.6	23.0	33.0	19
Anterior end to right marginal row, distance	40.0	40.0	8.2	1.9	20.6	30.0	62.0	19
Anterior end to paroral membrane, distance	15.4	15.0	2.2	0.5	14.1	13.0	22.0	19
Anterior end to last postoral cirrus, distance	105.1	103.0	10.2	2.3	9.7	83.0	127.0	19
Postoral cirri 2 and 3, distance in between	19.0	19.0	5.2	1.2	27.7	12.0	35.0	19
Posterior end to posterior transverse cirrus, distance	16.2	16.0	3.7	0.9	23.1	10.0	22.0	19
Nuclear figure, length	76.5	79.0	12.4	2.8	16.2	54.0	102.0	19
First two macronuclear nodules, distance in between	2.7	2.0	2.0	0.5	75.6	0.0	7.0	19
Anterior and posterior pair of macronuclear nodules, distance in between	7.5	7.0	3.3	0.8	43.3	3.0	14.0	19
Anterior macronuclear nodule, length	16.6	16.0	2.4	0.5	14.2	13.0	22.0	19
Anterior macronuclear nodule, width	13.1	13.0	1.4	0.3	10.7	10.0	16.0	19
Macronuclear nodules, number	4.3	4.0	0.9	0.2	20.5	3.0	7.0	19
Macronuclear nodules, length	4.2	4.0	–	–	–	4.0	5.0	19
Macronuclear nodules, width	4.0	4.0	–	–	–	3.5	5.0	19
Micronuclei, number	3.5	3.0	1.6	0.4	44.7	2.0	7.0	19
Basis of longest adoral membranelle, length	18.4	18.0	1.3	0.3	6.9	16.0	21.0	19
Adoral membranelles, number	39.3	39.0	4.1	1.0	10.5	30.0	51.0	19
Frontal cirri, number	3.0	3.0	0.0	0.0	0.0	3.0	3.0	19
Frontoventral cirri, number	4.2	4.0	–	–	–	4.0	7.0	19
Buccal cirri, number	1.0	1.0	0.0	0.0	0.0	1.0	1.0	19
Postoral cirri, number	3.1	3.0	–	–	–	3.0	5.0	19
Pretransverse cirri, number	2.0	2.0	–	–	–	1.0	2.0	19
Transverse cirri, number	5.2	5.0	–	–	–	5.0	7.0	19
Right marginal cirri, number	22.5	23.0	1.6	0.4	7.0	20.0	25.0	19
Left marginal cirri, number	23.4	23.0	2.2	0.5	9.4	20.0	28.0	19
Caudal cirri, number	3.0	3.0	0.0	0.0	0.0	3.0	3.0	19
Ordinary dorsal kineties, number ^b	6.1	6.0	–	–	–	6.0	7.0	15
Dorsal kinety 1, number of bristles	41.8	42.0	5.0	1.5	11.9	34.0	49.0	11
Dorsal kinety 5, number of bristles	18.1	17.0	2.4	0.7	13.4	15.0	22.0	11

^aData based on mounted, protargol-impregnated (Foissner 1991, protocol A; fixative strengthened by some ml 2% osmic acid), and randomly selected specimens from a non-flooded Petri dish culture. Measurements in μm . CV – coefficient of variation in %, *M* – median, Max – maximum, Min – minimum, *n* – number of individuals investigated, SD – standard deviation, SE – standard error of arithmetic mean, \bar{x} – arithmetic mean.

^bNumbers without the shortened, loosely ciliated rows between kineties 3 and 4 (cp. Figures 17j, 18b).

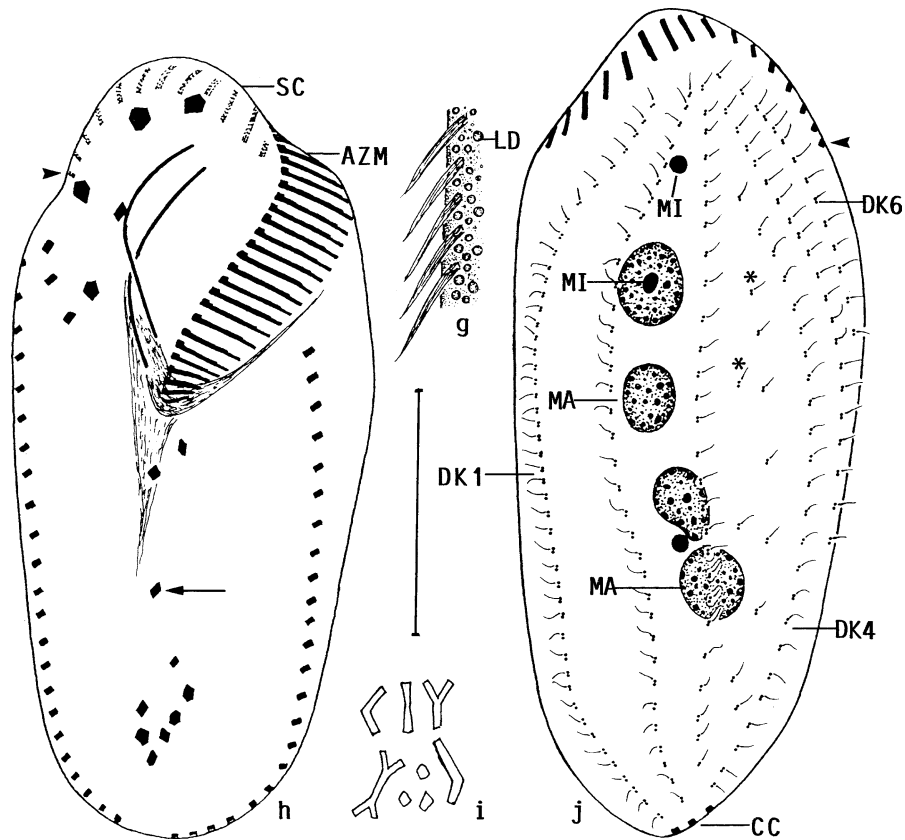


Figures 17a–f. *Australocirrus zechmeisterae* (a–d) and *A. oscitans* (e, f) from life. **a, b**: Ventral and lateral view of a representative specimen. **c, d**: Resting cyst with comparatively inconspicuous wall consisting of an about 1 μm thick, smooth endocyst and a 2 μm thick, wrinkled ectocyst (d). **e, f**: Resting cyst of *A. oscitans*, type of the genus. Ecto- and endocyst are separated by an about 7 μm wide lumen containing stripes of curious, 4–5 μm -sized crystals with six radiating processes; the crystals develop from precursors 1 μm across (f). AZM – adoral zone of membranelles, EC – ectocyst, EN – endocyst, MA – macronuclear nodules. Scale bars 100 μm (a) and 40 μm (c, e).

it from right row; gap right of body midline, on dorsal side occupied by three circa 30 μm long caudal cirri.

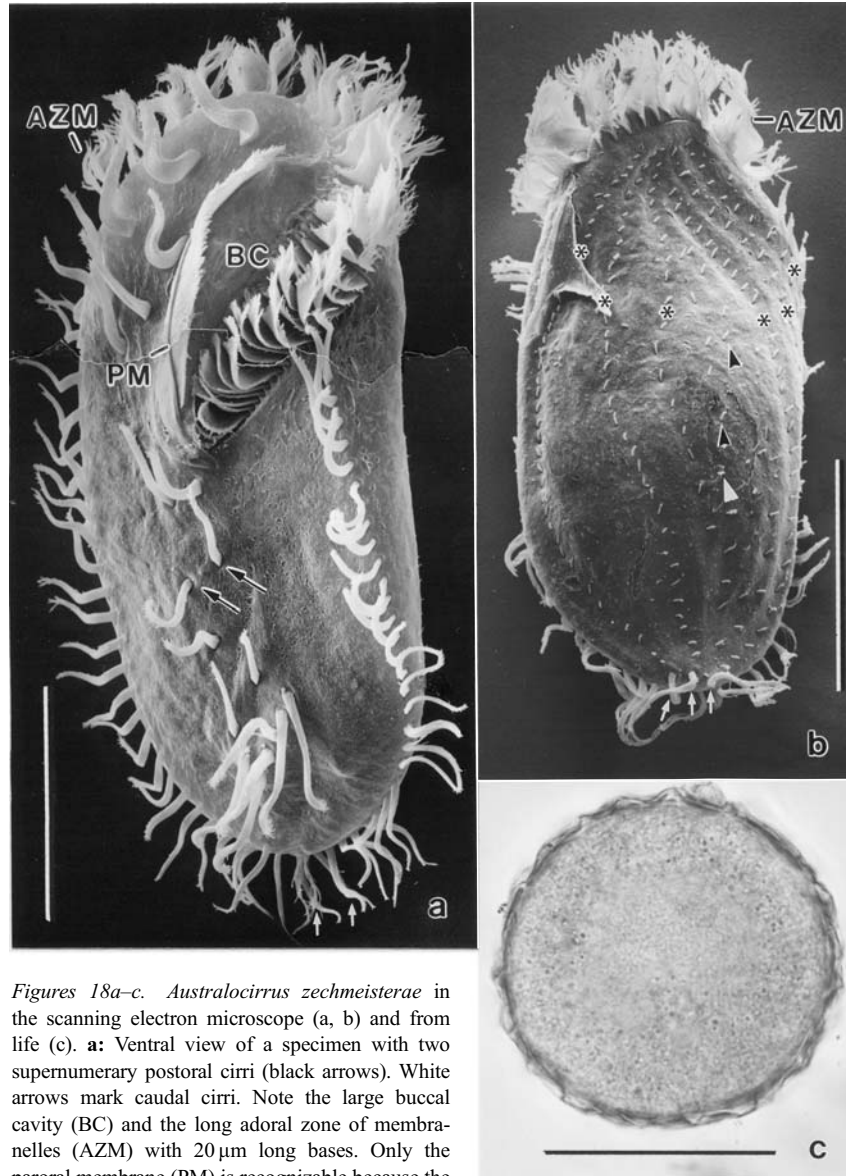
Dorsal bristles 3–4 μm long *in vivo* and thus very short as compared to size of cell, arranged in typical *Australothrix* pattern, viz., three complete rows on left body half; two to three loosely ciliated rows distinctly shortened anteriorly right of midline; and, on right cell margin, two, rarely three, dorsomarginal rows conspicuously shortened posteriorly (Figures 17j, 18b; Table 13).

Adoral zone composed of an average of 39 membranelles of usual structure and with 20 μm long cilia, conspicuous because (i) occupying 39–51%, on average 46% of body length; (ii) extending far (~20%) onto right body margin; (iii) membranelles comparatively widely spaced and membranelar bases up to 22 μm long *in vivo*; and (iv) frontal scutum very high due to the long membranelar bases forming



Figures 17g–j. *Australocirrus zechmeisterae* from life (g, i) and after protargol impregnation (h, j). **g**: Lipid droplets 2–3 μm across occur in the marginal cytoplasm. **h, j**: Infraciliature of ventral and dorsal side and nuclear apparatus of holotype specimens. Note the four macronuclear nodules, that is, the main feature of this species. Asterisks denote two loose bristle rows between dorsal kineties 3 and 4. These loose rows originate by multiple fragmentation of kinety 3 and are the main feature of the genus. Arrow denotes the third postoral cirrus. Arrowheads mark distal end of adoral zone of membranelles, which are comparatively widely spaced; both features are typical for *Australocirrus*. **i**: Cytoplasmic crystals 1–3 μm in size. AZM – adoral zone of membranelles, CC – caudal cirri, DK1, 4, 6 – dorsal bristle rows, LD – lipid droplets, MA – macronuclear nodules, MI – micronucleus, SC – frontal scutum. Scale bar 50 μm (h, j).

a conspicuous corona along anterior margin of dorsal side (Figures 17a, i, 18a, b; Table 13). Buccal cavity conspicuous because large and rather deep, at right partially covered by a convex, up to 7 μm wide, hyaline lip bearing the paroral membrane and covering proximal end of adoral zone of membranelles. Paroral membrane more distinctly curved in protargol preparations than *in vivo*, likely due to the rather pronounced shrinkage of the cells, possibly composed of zigzagging basal bodies having about 15 μm long cilia, intersects curved endoral membrane



Figures 18a–c. *Australocirrus zechmeisterae* in the scanning electron microscope (a, b) and from life (c). **a:** Ventral view of a specimen with two supernumerary postoral cirri (black arrows). White arrows mark caudal cirri. Note the large buccal cavity (BC) and the long adoral zone of membranelles (AZM) with 20 μm long bases. Only the paroral membrane (PM) is recognizable because the the endoral is covered by a thin membrane (cp. Figure 17h). **b:** Dorsal view showing the mighty adoral zone of membranelles (AZM); the six ordinary bristle rows (asterisks); and three shortened, loose bristle rows (arrowheads) between kineties 3 and 4. White arrows mark the three caudal cirri. **c:** Resting cyst, 78 μm across. Scale bars 50 μm .

underneath mid of buccal cavity. Endoral membrane likely composed of dikinetids with long cilia, covered by a thin membrane and thus not recognizable in scanning micrographs (Figure 18a). Pharyngeal fibers of ordinary length and orientation.

Table 14. Morphometric data on resting cysts of *Australocirrus zechmeisterae* (AZ) and a population of *A. oscitans* (AO) from the Republic of South Africa.

Characteristics ^a	Species	\bar{x}	<i>M</i>	SD	SE	CV	Min	Max	<i>n</i>
Length (with wall)	AZ	77.7	78.0	2.4	0.9	3.1	74.0	80.0	7
	AO	79.5	82.0	12.2	3.0	15.4	56.0	96.0	17
Width (with wall)	AZ	76.0	76.0	2.6	1.0	3.4	72.0	80.0	7
	AO	77.2	78.0	11.8	2.9	15.3	56.0	96.0	17
Length (without outer wall)	AZ	–	–	–	–	–	–	–	–
	AO	64.8	68.0	8.6	2.1	13.3	48.0	78.0	17
Width (without outer wall)	AZ	–	–	–	–	–	–	–	–
	AO	64.1	64.0	8.4	2.1	13.2	48.0	78.0	17

^a*In vivo* measurements (μm) on fully developed, five days old cysts. CV – coefficient of variation in %, *M* – median, Max – maximum, Min – minimum, *n* – number of cysts investigated, SD – standard deviation, SE – standard error of arithmetic mean, \bar{x} – arithmetic mean.

Resting cysts spherical to slightly ellipsoidal, 77 μm across on average, colourless. Endocyst an circa 1 μm thick, smooth wall; ectocyst about 2 μm thick and wrinkled. Cyst content granular, macronuclear nodules fused to an ellipsoidal mass (Figures 17c, d, 18c; Table 14).

Occurrence and ecology: To date found at type location and soil from Müllerboden (Table 2). Both sites are flooded from time to time, suggesting that *A. zechmeisterae* is a limnetic species. This is supported by a record from a pond in France (see next section). However, in the quantitative investigations it was found in Klausen-Leopoldsdorf (Table 3), that is, in a typical Woodruff-beach soil.

Generic allocation and comparison with related species: The population described has a flexible cortex (body), widely spaced adoral membranelles, and several loosely ciliated dorsal kineties between rows 3 and 4. Thus, it belongs to *Australocirrus*, as defined by Blatterer and Foissner (1988) and Berger (1999). Two species are known, viz., *A. oscitans* Blatterer and Foissner, 1988 and *A. octonucleatus* Foissner, 1988, which Berger (1999) assigns to a different subfamily and a new genus, *Rigidocortex*, due to its rigid cortex. Unfortunately, this classification is weakened by the resting cysts which have an ordinary structure in *R. octonucleatus* and *A. zechmeisterae* (Figures 17c, d, 18c; Table 14), while those of *A. oscitans*, type of the genus, are unique in having two widely separated walls with the lumen filled by stripes of curious crystals with six radiating processes (Figures 17e, f; Table 14). Further, the nuclear behavior is different: the nodules fuse to a globular mass in *A. zechmeisterae*, while they remain separate in *A. oscitans* and *R. octonucleatus*. Considering these pronounced cyst differences, it might be that each of the species represents, indeed, a distinct genus.

Australocirrus zechmeisterae differs from *A. oscitans* and *A. octonucleatus* mainly by the number of macronuclear nodules (4 vs. 2, respectively, 8). *In vivo*, *A. zechmeisterae* is easily confused with *Sterkiella cavicola* (for a review on that species, see Berger 1999). The best features for separating these species *in vivo* are the cortex (flexible vs. rigid) and the bases of the adoral membranelles which are about 20 μm long in *A. zechmeisterae* and only 10 μm in *S. cavicola*. Further,

S. cavicola has a comparatively flat (vs. deep) buccal cavity. In silver preparations, the different dorsal ciliary pattern unequivocally distinguishes these species.

Likely, *A. zechmeisterae* has been described by Grolière (1970) as *Opisthotricha monspessulana* Chatton and Séguéla. Berger (1999), who thoroughly reviewed all species in discussion, assigned Grolière's ciliate to *Sterkiella cavicola*; however, the large size (220–250 µm × 100–120 µm) and the figures, which show long, widely spaced adoral membranelles, indicate *A. zechmeisterae*.

Acknowledgements

Supported by the Austrian Federal Ministry for Agriculture and Forestry, Environment and Watermanagement and the Austrian Science Foundation (FWF Project 15017 to W.F.). We gratefully acknowledge the technical assistance of Dr. Eva Herzog, Dr. W.-D. Krautgartner, Dr. B. Moser, and A. Zankl.

References

- Aescht E. and Foissner W. 1993. Effects of organically enriched magnesite fertilizers on the soil ciliates of a spruce forest. *Pedobiologia* 37: 321–335.
- Alphei J., Bonkowski M. and Scheu S. 1996. Protozoa, Nematoda and Lumbricidae in the rhizosphere of *Hordelymus europaeus* (Poaceae): faunal interactions, response of microorganisms and effects on plant growth. *Oecologia* 106: 111–126.
- Anderson J.M. and Healey I.N. 1972. Seasonal and inter-specific variation in major components of the gut contents of some woodland Collembola. *Journal of Animal Ecology* 41: 359–368.
- Bamforth S.S. 2001. Proportions of active ciliate taxa in soils. *Biology and Fertility of Soils* 33: 197–203.
- Berger H. 1999. Monograph of the Oxytrichidae (Ciliophora, Hypotrichia). Kluwer Academic Publishers, Dordrecht, The Netherlands.
- Berthold A. and Palzenberger M. 1995. Comparison between direct counts of active soil ciliates (Protozoa) and most probable number estimates obtained by Singh's dilution culture method. *Biology and Fertility of Soils* 19: 348–356.
- Blatterer H. and Foissner W. 1988. Beitrag zur terricolen Ciliatenfauna (Protozoa: Ciliophora) Australiens. *Stapfia*, Linz 17: 1–84.
- Bonkowski M. and Schaefer M. 1997. Interactions between earthworms and soil protozoa: a trophic component in the soil food web. *Soil Biology and Biochemistry* 29: 499–502.
- Buitkamp U. 1979. Vergleichende Untersuchungen zur Temperaturadaptation von Bodenciliaten aus klimatisch verschiedenen Regionen. *Pedobiologia* 19: 221–236.
- Clarke K.R. and Gorley R.N. 2001. PRIMER v 5: User Manual/Tutorial. Primer-E, Plymouth, UK.
- Clarke K.R. and Warwick R.M. 2001. Change in Marine Communities: An Approach to Statistical Analysis and Interpretation. 2nd edn. Primer-E, Plymouth, UK.
- Darbyshire J.F. (ed.) 1994. Soil Protozoa. CAB International, Wallingford, UK.
- Dragesco J. and Dragesco-Kernéis A. 1979. Ciliés muscicoles nouveaux et peu connus. *Acta Protozoologica* 18: 401–416.
- Dragesco J. and Dragesco-Kernéis A. 1986. Ciliés libres de l'Afrique intertropicale. *Faune tropicale* 26: 1–559.
- Dykhuizen D.E. 1998. Santa Rosalia revisited: why are there so many species of bacteria? *Antonie van Leeuwenhoek* 73: 25–33.
- Fierer N. 2003. Variations in microbial community composition through two soil depth profiles. *Soil Biology and Biochemistry* 35: 167–176.

- Finlay B.J. 2001. Protozoa. *Encyclopedia of Biodiversity* 4: 901–915.
- Foissner W. 1981. Morphologie und Taxonomie einiger neuer und wenig bekannter kinetofragminophorer Ciliaten (Protozoa: Ciliophora) aus alpinen Böden. *Zoologisches Jahrbuch Systematik* 108: 264–297.
- Foissner W. 1984. Infraciliatur, Silberliniensystem und Biometrie einiger neuer und wenig bekannter terrestrischer, limnischer und mariner Ciliaten (Protozoa: Ciliophora) aus den Klassen Kinetofragminophora, Colpodea und Polyhymenophora. *Stapfia*, Linz 12: 1–165.
- Foissner W. 1987a. Soil protozoa: fundamental problems, ecological significance, adaptations in ciliates and testaceans, bioindicators, and guide to the literature. *Progress in Protistology* 2: 69–212.
- Foissner W. 1987b. Neue terrestrische und limnische Ciliaten (Protozoa, Ciliophora) aus Österreich und Deutschland. *Sitzungsberichte der österreichischen Akademie der Wissenschaften*, Wien 195: 217–268.
- Foissner W. 1987c. Neue und wenig bekannte hypotriche und colpode Ciliaten (Protozoa: Ciliophora) aus Böden und Moosen. *Zoologischer Beiträge (N.F.)* 31: 187–282.
- Foissner W. 1987d. Faunistische und taxonomische Notizen über die Protozoen des Fuscher Tales (Salzburg, Österreich). *Jahresberichte Haus der Natur*, Salzburg 10: 56–68.
- Foissner W. 1988. Gemeinsame Arten in der terricolen Ciliatenfauna (Protozoa: Ciliophora) von Australien und Afrika. *Stapfia*, Linz 17: 85–133.
- Foissner W. 1991. Basic light and scanning electron microscopic methods for taxonomic studies of ciliated protozoa. *European Journal of Protistology* 27: 313–330.
- Foissner W. 1992. Estimating the species richness of soil protozoa using the “non-flooded petri dish method”. In: Lee J.J. and Soldo A.T. (eds) *Protocols in Protozoology*. Allen Press, Lawrence, Kansas, pp. B–10.1–10.2.
- Foissner W. 1994. Soil protozoa as bioindicators in ecosystems under human influence. In: Darbyshire J.F. (ed) *Soil Protozoa*. CAB International, Wallingford, UK, pp. 147–193.
- Foissner W. 1995. Tropical protozoan diversity: 80 ciliate species (Protozoa, Ciliophora) in a soil sample from a tropical dry forest of Costa Rica, with descriptions of four new genera and seven new species. *Archiv für Protistenkunde* 145: 37–79.
- Foissner W. 1997a. Soil ciliates (Protozoa: Ciliophora) from evergreen rain forests of Australia, South America and Costa Rica: diversity and description of new species. *Biology and Fertility of Soils* 25: 317–339.
- Foissner W. 1997b. Global soil ciliate (Protozoa, Ciliophora) diversity: a probability-based approach using large sample collections from Africa, Australia and Antarctica. *Biodiversity and Conservation* 6: 1627–1638.
- Foissner W. 1997c. Protozoa as bioindicators in agroecosystems, with emphasis on farming practices, biocides, and biodiversity. *Agriculture, Ecosystems and the Environment* 62: 93–103.
- Foissner W. 1998. An updated compilation of world soil ciliates (Protozoa, Ciliophora), with ecological notes, new records, and descriptions of new species. *European Journal of Protistology* 34: 195–235.
- Foissner W. 1999a. Notes on the soil ciliate biota (Protozoa, Ciliophora) from the Shimba Hills in Kenya (Africa): diversity and description of three new genera and ten new species. *Biodiversity and Conservation* 8: 319–389.
- Foissner W. 1999b. Protist diversity: estimates of the near-imponderable. *Protist* 150: 363–368.
- Foissner W. 2000a. Two new terricolous spathidiids (Protozoa, Ciliophora) from tropical Africa: *Arcuospathidium vlassaki* and *Arcuospathidium bulli*. *Biology and Fertility of Soils* 30: 469–477.
- Foissner W. 2000b. A compilation of soil and moss ciliates (Protozoa, Ciliophora) from Germany, with new records and descriptions of new and insufficiently known species. *European Journal of Protistology* 36: 253–283.
- Foissner W. 2000c. Notes on ciliates (Protozoa, Ciliophora) from *Espeletia* trees and *Espeletia* soils of the Andean Páramo, with descriptions of *Sikorops espeletiae* nov. spec. and *Fragmocirrus espeletiae* nov. gen., nov. spec. *Studies on Neotropical Fauna and Environment* 35: 52–79.
- Foissner W. 2003. *Cultellothrix velhoi* gen. n., sp. n., a new spathidiid ciliate (Ciliophora: Haptorida) from a Brazilian floodplain soil. *Acta Protozoologica* 42: 47–54.
- Foissner W. 2004. Soil protozoa. In: Hillel D., Rosenzweig C., Powlson D., Scow K., Singer M. and Sparks D. (eds) *Encyclopedia of Soils in the Environment*. Academic Press, London, pp. 336–347.

- Foissner W., Peer T. and Adam H. 1985. Pedologische und protozoologische Untersuchung einiger Böden des Tullnerfeldes (Niederösterreich). *Mitteilungen der österreichischen bodenkundlichen Gesellschaft* 30: 77–117.
- Foissner W., Agatha S. and Berger H. 2002. Soil ciliates (Protozoa, Ciliophora) from Namibia (Southwest Africa), with emphasis on two contrasting environments, the Etosha region and the Namib Desert. *Denisia* 5: 1–1459.
- Franz H. 1975. Die Bodenfauna der Erde in biozönotischer Betrachtung. Steiner, Wiesbaden, Germany.
- Frostegård Å., Petersen S.O., Bååth E. and Nielsen T.H. 1997. Dynamics of a microbial community associated with manure hot spots as revealed by phospholipid fatty acid analyses. *Applied Environmental Microbiology* 63: 2224–2231.
- Grolière C.-A. 1970. Les premiers stades de la morphogenèse chez *Opisthotricha monspessulana* Ch.et S. 1940, cilié hypotriche Oxytrichidae. *C. r. hebd. Séanc. Acad. Sci., Paris, Série D* 270: 366–368.
- Hill G.T., Mitkowski N.A., Aldrich-Wolfe L., Emele L.R., Jurkonie D.D., Ficke A., Maldonado-Ramirez S., Lynch S.T. and Nelson E.B. 2000. Methods assessing the composition and diversity of soil microbial communities. *Applied Soil Ecology* 15: 25–36.
- Hackl E. 2001. Mikrobieller Stoffumsatz in Böden natürlicher Waldgesellschaften. Ph.D. Thesis, Institute for Ecology and Bioconservation, Universität Wien, Austria.
- Hackl E., Bachmann G. and Zechmeister-Boltenstern S. 2000a. Soil microbial biomass and rhizosphere effects in natural forest stands. *Phyton* 40: 83–90.
- Hackl E., Bachmann G., Pfeffer M., Donat C. and Zechmeister-Boltenstern S. 2000b. Beziehungen zwischen bodenchemischen und bodenbiologischen Parametern in Naturwäldern. *Mitteilungen der österreichischen bodenkundlichen Gesellschaft* 59: 17–20.
- Hackl E., Bachmann G. and Zechmeister-Boltenstern S. 2004. Microbial nitrogen turnover in soils under different types of natural forest. *Forest Ecology and Management* 188: 101–112.
- Hackl E., Pfeffer M., Donat C., Bachmann G. and Zechmeister-Boltenstern S. 2005. Composition of the microbial communities in the mineral soil under different types of natural forest. *Soil Biology and Biochemistry* 37: 661–671.
- Hemberger H. 1981. Revision der Ordnung Hypotrichida Stein (Ciliophora, Protozoa) an Hand von Protargolpräparaten und Morphogenesedarstellungen. Ph.D. Thesis, Bonn University, Germany.
- Hemberger H. 1985. Neue Gattungen und Arten hypotricher Ciliaten. *Archiv für Protistenkunde* 130: 397–417.
- Kahl A. 1930. Urtiere oder Protozoa I: Wimpertiere oder Ciliata (Infusoria) 1. Allgemeiner Teil und Prostomata. *Die Tierwelt Deutschlands* 18: 1–180.
- Kahl A. 1943. Infusorien. Ein Hilfsbuch zum Erkennen, Bestimmen, Sammeln und Präparieren der freilebenden Infusorien des Süßwassers und der Moore. Franck'sche Verlagsbuchhandlung, W. Keller & Co., Stuttgart, Germany, 52 pp. (A forgotten publication containing several new species, two of which were rediscovered during the present study: *Arcuospathidium coemeterii* and *Phialinides muscicola*; a reprint of Kahl's work appeared in *Acta Protozoologica* 43: 1–69).
- Kuntze H., Niemann J., Roeschmann G. and Schwerdtfeger G. 1983. *Bodenkunde*. Ulmer, Stuttgart, Germany.
- Lehle E. 1994. Die Auswirkungen von Düngung und Kalkung auf die Bodenciliaten (Protozoa: Ciliophora) eines Fichtenbestandes im Schwarzwald (Süddeutschland). *Archiv für Protistenkunde* 144: 113–125.
- Lüftenegger G., Foissner W. and Adam H. 1985. r- and k-selection in soil ciliates: a field and experimental approach. *Oecologia (Berlin)* 66: 574–579.
- Mendoza G.A. and Prabhu R. 2001. Prioritizing criteria and indicators for sustainable forest management: a case study on participatory decision making. In: Schmoldt D.L. (ed.) *The Analytic Hierarchy Process in Natural Resource and Environmental Decision Making*. Kluwer, Dordrecht, The Netherlands, pp. 115–129.
- Meyer E., Foissner W. and Aesch E. 1989. Vielfalt und Leistung der Tiere im Waldboden. *Österreichische Forstzeitung* 3: 15–18.
- Müller O.F. 1786. *Animalcula Infusoria Fluvialia et Marina, quae Detexit, Systematice Descripsit et ad Vivum Delineari Curavit*. N. Mölleri, Hauniae.

- Petz W. and Foissner W. 1988. Spatial separation of terrestrial ciliates and testaceans (Protozoa): a contribution to soil ciliatostasis. *Acta Protozoologica* 27: 249–258.
- Petz W. and Foissner W. 1997. Morphology and infraciliature of some soil ciliates (Protozoa, Ciliophora) from continental Antarctica, with notes on the morphogenesis of *Sterkiella histriomuscorum*. *Polar Record* 33: 307–326.
- Stokes A.C. 1885. Some new infusoria from American fresh waters. *Annals and Magazine of Natural History* 15: 437–449.
- Torsvik V., Sørheim R. and Goksøyr J. 1996. Total bacterial diversity in soil and sediment communities – a review. *Journal of Industrial Microbiology* 17: 170–178.
- Townsend C.R., Scarsbrook M.R. and Dolédec S. 1997. The intermediate disturbance hypothesis, refugia, and biodiversity in streams. *Limnology and Oceanography* 42: 938–949.
- Wenzel F. 1953. Die Ciliaten der Moorsrasen trockner Standorte. *Archiv für Protistenkunde* 99: 70–141.
- Zechmeister-Boltenstern S., Bruckner A., Hackl E., Foissner W., Kopeszki H., Sessitsch A. and Waitzbauer W. 2003. Biodiversity in major forest types of Central Europe. Abstract, Conference on Biodiversity in Lancaster.
- Zeide B. 2001. Resolving contradictions in forestry: back to science. *The Forestry Chronicle* 77: 973–981.